Effective Medium Access Control for Underwater Acoustic Sensor Networks

Wael Mohamed Gorma

PhD

University of York
Electronic Engineering

May 2019

Abstract

This work is concerned with the design, analysis and development of effective Medium Access Control (MAC) protocols for Underwater Acoustic Sensor Networks (UASNs). The use of acoustic waves underwater places time-variant channel constraints on the functionality of MAC protocols. The contrast between traffic characteristics of the wide-ranging applications of UASNs makes it hard to design a single MAC protocol that can be adaptive to various applications. This thesis proposes MAC solutions that can meet the environmental and non-environmental challenges posed underwater. Scheduling-based schemes are the most common MAC solutions for UASNs, but scheduling is also challenging in such a dynamic environment. The preferable way of synchronisation underwater is the use of a global scheduler, guard intervals and exchange of timing signals. To this end, single-hop topologies suit UASN applications very well.

The Combined Free and Demand Assignment Multiple Access (CFDAMA) is a centralised, scheduling-based MAC protocol demonstrating simplicity and adaptability to the time-variant channel and traffic characteristics. It is shown to minimise end-to-end delay, maximise channel utilisation and maintain fairness amongst nodes. This thesis primarily introduces two novel robust MAC solutions for UASNs, namely CFDAMA with Systematic Round Robin and CFDAMA without clock synchronisation (CFDAMA-NoClock). The former scheme is more suitable for large-scale and widely-spread UASNs, whereas the latter is a more feasible MAC solution when synchronisation amongst node clocks cannot be attained. Both analytical and comprehensive event-driven Riverbed simulations of underwater scenarios selected based on realistic sensor deployments show that the two protocols make it possible to load the channel up to higher levels of its capacity with controlled delay performance superior to that achievable with the traditional CFDAMA schemes. The new scheduling features make the CFDAMA-NoClock scheme a very feasible networking solution for robust and efficient UASN deployments in the real world.

Table of contents

List of figures

List of tables

Glossary

ACK Acknowledgement
ACMENet Acoustic Communication network for Monitoring of Environment Networks
ALOHA-CA ALOHA with Collision Avoidance
ALOHA-CS ALOHA with Channel Sensing
ALOHA-NA ALOHA with Advanced Notification
ALOHA-Q ALOHA with Q learning
AN Attenuation Noise product
BER Bit Error Rate
BW Bandwidth
CDMA Code Division Multiple Access
CFDAMA Combined Free/Demand Assignment Multiple Access
CFDAMA-CR CFDAMA with Combined Request
CFDAMA-CRAR CFDAMA with Controlled Random Access Requests
CFDAMA-FA CFDAMA with Fixed Assigned requests
CFDAMA-IS CFDAMA with Intermediate Scheduler
CFDAMA-NoClock CFDAMA without synchronised Clock
CFDAMA-PAR CFDAMA with Packet Accompanied Requests
CFDAMA-PB CFDAMA with Piggy-Backed requests
CFDAMA-RA CFDAMA with Random Access requests
CFDAMA-RR CFDAMA with Round Robin strategy
CFDAMA-SRR CFDAMA with Systematic Round Robin
COD-TS Cluster-Based On-Demand Time Sharing
COPE-MAC Contention-based parallel reservation MAC
DACAP Distance-Aware Collision Avoidance Protocol
DTMAC Delay Tolerant MAC protocol
EDETA Energy-Efficient aDaptive hiErarchical and RobusT Architecture
FAMA Floor Acquisition Multiple Access
FDMA Frequency Division Multiple Access

HSR-TDMA Hybrid Spatial Reuse Time Division Multiple Access
MAC Medium access Control
MACA Multiple Access Collision Avoidance
MDS-MAC Multi-Dimensional Scaling MAC
PCAP Propagation-delay-tolerant Collision Avoidance Protocol
R-MAC Reservation-based MAC
RCMAC Reservation Channel Media Access Protocol
RM Riverbed Modeller
SBMAC Smart Blocking MAC
SF-MAC Spatially Fair MAC
SNR Single to Noise Ratio
SSP Sound Speed Profile
ST-MAC Spatial-Temporal MAC
STUMP Staggered TDMA Underwater MAC Protocol
T-Lohi Tone-Lohi
TDA-MAC Transmit Delay Allocation MAC
TDMA Time Division Multiple Access
UASN Underwater Acoustic Sensor Network
UW-MAC Underwater MAC
UWAN-MAC Underwater Acoustic Wireless Sensor Network MAC
UWSN Underwater Wireless Sensor Network

In the name of God, The most merciful, The most gracious. All praise be to God for the strengths and His blessings in completing this thesis. I would like to dedicate this thesis to my loving parents and wife …

Acknowledgements

And I must thank God for having guided me towards one of the most beautiful cities in the world, York, as a whole and particularly towards its outstanding university, the University of York. There, with the assistance, patience, and support of many individuals, I have been able to conduct my PhD studies under the supervision of Paul Mitchell to whom I express my sincerest gratitude for his exceptional guidance and support throughout this journey. I have become an overall more confident person, a qualified researcher linked up with scholars across the world, a successful author/reviewer in leading journals and conferences, and for this, I am truly grateful.

I would additionally like to extend my thanks to the Department of Electronic Engineering for giving me the opportunity to undertake this research as well as allowing me to work as a lab demonstrator. Thanks must also go to all the members of the Underwater Communication Research subgroup in particular and the Communication Technologies Research Group in general whom I owe a lot of the knowledge used for the completion of this thesis, especially Nils Morozs and Yuriy Zakharov. My special thanks to the head of the group David Grace for the motivating discussions during the biannual advisory meetings and for directing towards a vibrant research environment.

I would also like to thank the friends who have made this work easy and enjoyable, especially Kafi and Ali. Finally, a heartfelt word of thanks goes to my entire family whose support was worth more than I can express on paper. Very special thanks to my beloved mother for her endless love and prayers, my wise father for his unwavering support and advice, and my wife without whose love, support and understanding I could never have completed these studies.

Declaration

I declare that this thesis has been composed solely by me and that the work presented in it is my own is so, to the best of my knowledge and belief. References and acknowledgements to other researchers are given as appropriate in the text. I confirm that it contains no material which has been, in whole or in part, accepted or submitted for the award of any other degree. Parts of this work have resulted in the publications and awards listed below.

- (Article) W. Gorma, P. D. Mitchell, N. Morozs and Y. V. Zakharov, "CFDAMA-SRR: A MAC Protocol for Underwater Acoustic Sensor Networks," in IEEE Access, vol. 7, pp. 60721– 60735, (2019)
- (Chapter) W. Gorma, P. Mitchell, and Y. Zakharov, “CFDAMA-IS: MAC protocol for underwater acoustic sensor networks,” Broadband Communications, Networks and Systems. Springer, ISBN: 978-3-030-05194-5, pp. 191–200 (2018).
- (Conference) W. Gorma and P. D. Mitchell, “Performance of the combined free/demand assignment multiple access protocol via underwater net- works,” in Proceedings of the International Conference on Underwater Networks and Systems, ser. WUWNET’17. New York, NY, USA: ACM, pp. 5:1–5:2 (2017).
- (Article) W. Gorma and P. D. Mitchell, "CFDAMA-NoClock: A MAC Protocol for Underwater Acoustic Sensor Networks," to be submitted to Journal of Sensor and Actuator Networks, special issue "underwater networking", (2019).
- (Award) Best Paper Award. The 9th International Conference on Broadband Communications, Networks, and Systems, FARO, PORTUGAL.
- (Poster prize) 2nd Prize Poster Competition. Second Year PhD Poster Competition, Electronic Engineering Department, University of York.

Wael Mohamed Gorma
May 2019

Chapter 1

Introduction

1.1 Overview

The technique of sending and receiving data carried by acoustic waves propagating through water is known as acoustic communication. A number of fixed and/or mobile sensor nodes deployed within the confines of a water body to form a network and carry out tasks collectively by means of an acoustic communication system is known as an Underwater Acoustic Sensor Network (UASN). Low-cost sensing and communication devices are now being developed, which will make the deployment of many underwater sensor nodes (as many as 100 nodes or more) feasible and forthcoming. UASNs are involved in a wide range of applications ranging from scientific to industrial and extending to military and homeland security applications. The applications can be broken down into five main categories, i.e. monitoring, disaster forecasting, security, navigation, and sports.

Networks in general and UASNs in particular require some level of channel sharing. A technique, called multiple access, is typically implemented to achieve channel sharing. Multiple access techniques provide a means of separation amongst multiple transmissions of different terminals to coordinate the utilisation of the available capacity. Classical methods to achieve this separation include separation using time slots, frequency bands, or orthogonal codes. The shared capacity is then accessed based upon a subordinate technique, known as Medium Access Control (MAC) protocol.

The use of acoustic waves underwater places constraints on the functionality of MAC protocols. Time-variant long propagation delays and distance-dependent bandwidth are key channel constraints, which pose the challenge of achieving high network performance, i.e. end-to-end delay, throughput and fairness. On top of the channel-related constraints, are the challenges posed by the statistical behaviour of data traffic of the wide-ranging applications, which make it more challenging to design a single MAC protocol suiting all applications.

A further major underwater constraint is energy consumption; transmission acoustically underwater is the main energy consuming process of battery-powered sensor nodes [3]. Transmission must be rationalised underwater. Unlike multi-hop, single-hop topologies demonstrate low complexity. Most of the intelligence associated with MAC protocols are implemented preferably on a centralised node potentially having access to more on-shore resources. This is a vital factor in future deployments of large scale sensor networks.

Due to the special characteristics of the underwater environment, specially designed underwater MAC protocols are very much in demand. Despite the research undertaken so far, the topic demands more effort in providing guidelines to inform selection amongst MAC alternatives depending on the characteristics and constraints of a given underwater application. Based on the hypothesis stated in the following section, it is believed that Time Division Multiple Access (TDMA) featuring adaptability, adaptive TDMA, with a tolerant scheduling algorithm is a promising baseline towards effective MAC protocols for UASNs. In this thesis, three capacity assignment strategies are investigated in the context of UASNs: Demand Assignment, Free Assignment and the Combined Free and Demand Assignment Multiple Access (CFDAMA) protocols. CFDAMA can provide adaptive TDMA solutions for UASNs. New insights into the implementation of CFDAMA are provided. Significant contributions and advances are made to the effectiveness of the schemes. Novel approaches to the exciting CFDAMA variants are invented to form the basis of the considerable advances.

1.2 Problem Definition

Underwater acoustic channels are known as one of the most complex and time-variant communication media in use today, which makes the coordination of multiple UASN transmissions particularly challenging. The propagation of an acoustic signal through water is characterised with large-scale attenuation that increases with the signal frequency. The background noise also changes with the frequency; i.e. it is not white as it has a decaying power spectral density. The channel capacity is a function of the transmission range and could potentially be extremely limited. Due to these reasons acoustic propagation through water is best supported at low frequencies, making the total available bandwidth typically low. Therefore, scheduling-based MAC protocols are preferred over other capacity sharing techniques. They can enable adaptive channel capacity allocations and allow variable data rates by just changing the number of time slots assigned based on the requirements of each terminal. However, underwater acoustic channel features long time-varying propagation delays, leading to time and space uncertainty. This brings about scheduling difficulties as well as space unfairness among the network terminals. The applications of UASNs are still

evolving, and it can be envisioned that at least two types of data traffic will be generated by such sensing networks: event-driven and periodic sensing. The two types significantly differ in their traffic patterns. Designing a single MAC protocol that can meet the requirements of the two distinct models is also a major challenge.

1.3 Hypothesis

The work presented in this thesis is primarily driven by the following hypothesis:

Medium access control protocols incorporating a hybrid capacity assignment strategy can provide centralised wireless networks featuring time-variant channel and traffic characteristics with the necessary adaptability for excellent delay/utilisation performance.

Designing a single MAC protocol that can meet the requirements of a sensor network featuring time-variant channel and traffic characteristics is difficult, especially if the wireless sensors are connected acoustically and deployed underwater. An efficient underwater MAC protocol requires a special design enabling the network to meet the extraordinary challenges including temporal and spatial uncertainty, the phenomena of space unfairness and momentary connection losses. An adequate underwater MAC design would assure maximum achievable channel utilisation, minimum end-to-end delays, fairness, scalability, adaptiveness to traffic changes, and energy efficiency. The nature of the characteristics presented in the underwater acoustic channel necessitates the demand for novel, efficient, reliable, applicable and straightforward MAC protocols. The performance of a MAC protocol is determined by the ability to adapt to different underwater scenarios (including characteristics with respect to water motion, signal attenuation, background noise, interference etc.) and non-environmental factors such as (the traffic type, network topology, data rate, hop length, network size, packet duration, etc.). The functionality of MAC protocols should be stable despite synchronisation difficulties, space unfairness and bursty short-packet traffic. Due to the inevitable temporal and spatial uncertainty underwater, most scheduling-based protocols require a form of a global scheduler, guard intervals and exchange of relative-timing signals. To this end, single-hop topologies are preferred to minimise the complexity of scheduling algorithms and increase their feasibility.

Given the above facts, it can be assumed that single-hop UASNs that is composed of fixed battery-powered sensor nodes, generating different data traffic types, require scheduling-based MAC solutions featuring simplicity and adaptability. It is then possible to hypothesise that adaptive TDMA-based MAC protocols represent the baseline towards new MAC solutions for such extraordinary scenarios. Combined round-robin free and demand assignment schemes, which fundamentally incorporate a global scheduler, can provide such scenarios

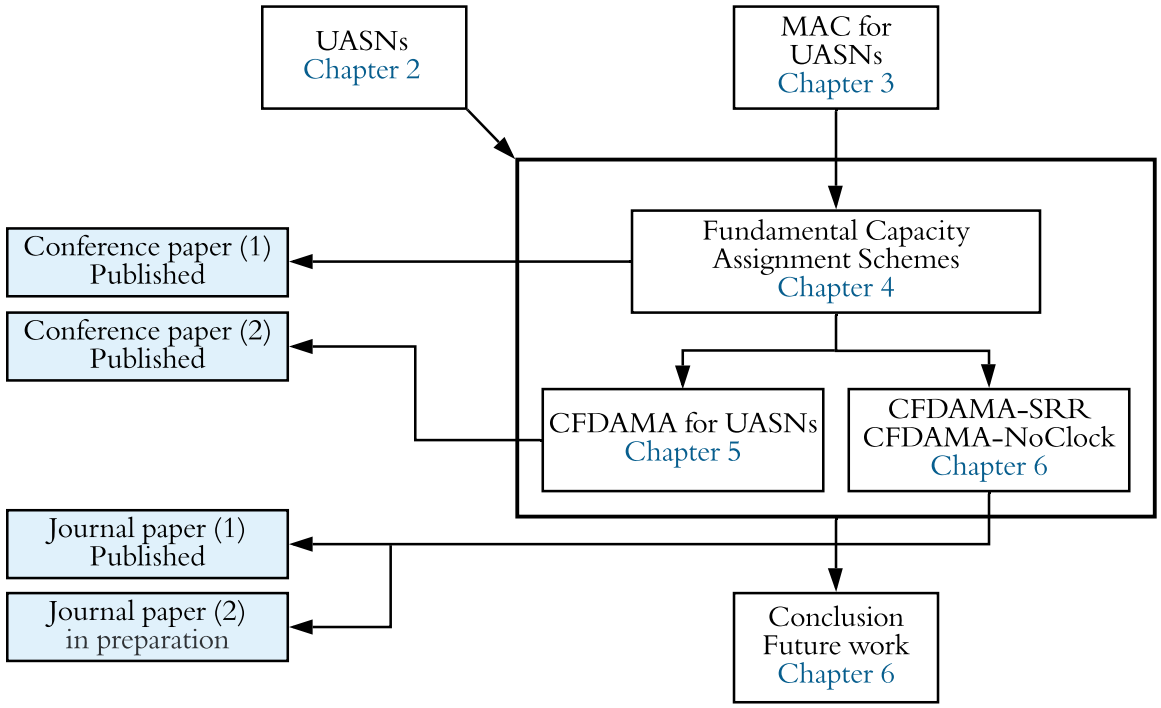

Fig. 1.1 Thesis Structure

with adaptive TDMA-based MAC solutions. Inspired by the excellent delay/utilisation performance of the combined capacity assignment schemes in satellite systems, it is argued that they can help UASNs to alleviate the impact of slow variable propagation speed as well as limited channel capacity, overcome the space unfairness phenomena and adapt to any exponentially random burst or periodic traffic types.

1.4 Thesis Structure

The main body of the thesis is broken down into seven chapters. This section outlines briefly the contents of each chapter. They are graphically represented in Figure 1.1, which identifies the relationship between them and associated completed/undergoing publications. The arrows indicate the information flow between complimentary chapters, and the grouping of boxes indicates intersected chapters where the information of one chapter is required to fully understand the material in the others. Resulted publications are also illustrated aside.

Chapter 2 provides an overview of UASNs. It suggests a conceivable taxonomy of underwater networks to guide the reader down the different classifications to the most relevant one. It sheds light on some challenges and opportunities, and scopes out a number

of applications. It ends with a detailed discussion of the most important acoustic channel characteristics.

Chapter 3 provides detailed background information on essential aspects of underwater medium access control for acoustic systems. It discusses the environmental and non-environmental constraints, limitations and challenging facing the design and functionality of MAC protocols. It reviews the fundamental multiple access techniques and presents a comprehensive literature review of underwater MAC schemes.

Chapter 4 provides new insights by investigating the performance of MAC schemes incorporating a pure capacity assignment strategy. The primary intention of this chapter is to develop the required understanding of the characteristics and the possibly achievable delay/utilisation performance of a number of MAC schemes integrating either random access, free assignment, or demand assignment scheme in the context of a given underwater scenario. This provides useful input to understanding the more complex schemes in Chapter 5 and 6. The results of this chapter enable a deeper understanding of the factors influencing the acoustic channel described in chapter 2 and the factors influencing the medium access control described in chapter 3.

Chapter 5 draws on the findings of the previous chapters and investigates the effectiveness of combined request strategies. It presents a detailed description of the Combined Free/Demand Assignment Multiple Access (CFDAMA) scheme. It describes its scheduling algorithm and frame structures. Throughout a set of simulated underwater scenarios, it investigates a number of underlying request strategies that are capable of adapting to the time-varying channel conditions with two distinct data traffic types. It proposes a new CFDAMA arrangement advancing its effectiveness, namely CFDAMA with Intermediate Scheduler.

Chapter 6 introduces two novel robust MAC protocols we exclusively designed for UASNs based on the principles of CFDAMA. The first scheme employs the round robin request strategy in a systematic manner to exploit the spatial distribution of nodes. It has a bias against long-delay demand assigned slots. The second scheme, namely CFDAMA-NoClock, incorporates a mechanism of relative timing amongst nodes and regular calibration and compensation of propagation delay estimation errors. It is capable of providing Adaptive TDMA to sensor nodes without the need for synchronisation between independent node clocks.

Chapter 7 summarises the work presented in this thesis, concludes its original contributions, and suggests a number of ideas for further work.

Chapter 2

Underwater Acoustic Sensor Networks

2.1 Introduction

This chapter explores key aspects of UASNs. It lays the necessary foundation for development towards the primary focus of this thesis, which is concerned with the design, analysis and development of MAC protocols for acoustic-based underwater sensor networks. It proposes a taxonomy of underwater networks in order to define the problem addressed in this research with respect to the different classifications of underwater networks.

The chapter starts with an overview of UASNs presented in section 2.2. Then, section 2.3 gives a general description of underwater sensors. Section 2.4 lists a number of UASN applications with some examples. Section 2.5 presents the key challenges facing the implementation of UASNs. Section 2.6 introduces the primary factors influencing underwater acoustic networking. Section 2.7 analyses a very important issue for the subsequent chapters, which is the issue of UASN data traffic requirements and proposes suitable traffic models for simulation purposes. Finally, section 2.8 concludes the key facts presented in this chapter.

2.2 Overview of Underwater Acoustic Networks

An Underwater Network is a type of communication network composed of fixed and/or mobile sensor nodes deployed in a marine environment such as the oceans, seas, bays, rivers, lakes, estuaries, or other major water bodies which altogether cover more than 70 % of the Earth's surface. These offshore nodes are either wired together to communicate, or they communicate with one another wirelessly using acoustic, radio or optical signals. Acoustic links are the preferred communication medium; they exhibit superior propagation characteristics compared with the alternatives in the underwater environment. In a typical

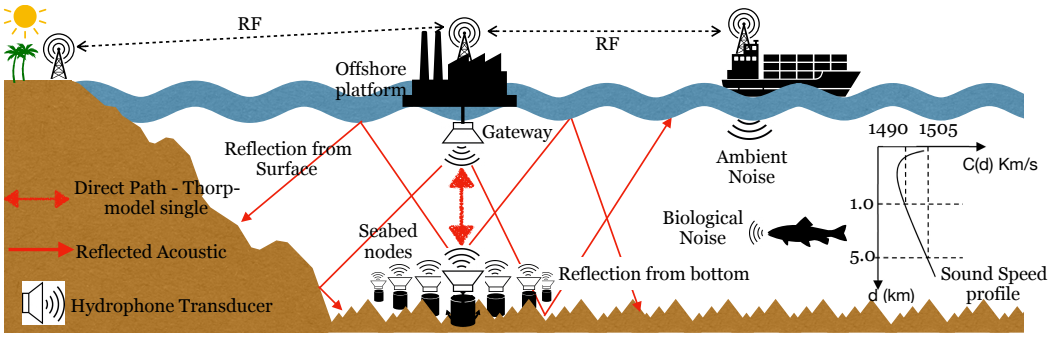

Fig. 2.1 An example of UANs

set-up, a superior node or more, usually named gateway, is equipped with an acoustic underwater communication modem as well as a traditional high-speed radio link. This is to communicate with both underwater sensor nodes and with a network data centre respectively. These network data centres are hosted in ships or other types of onshore installations. For example, a typical implementation would be similar to that shown in Figure 2.1. This is a simple deployment illustration of several sensor nodes collecting and sending their data acoustically to relay nodes, by which the data is forwarded in a hop-by-hop manner to the master node or gateway whose primary task is to receive and resend the same data over a high-speed link (e.g. satellite, Wi-Fi, wire or fibre). Such an implementation is categorised as an Underwater Wireless Sensor Network (UWSN). Since radio waves do not propagate over long distances through conductive underwater medium, and optical waves are extremely constrained by scattering in water, acoustic signals are the common physical layer link used in underwater networks. In other words, radio waves require extremely low frequencies (30–300 Hz), impractically long antennas and high transmission power to propagate through seawater. Optical signals are deflected underwater due to the undissolved particles - the phenomena of turbidity - and require high precision in aiming the narrow laser beams for the intended target to establish a link through water. Therefore, wireless links in underwater networks are often based on acoustic communications. For this reason, such wireless sensor networks are typically called Underwater Acoustic Sensor Networks (UASNs). To provide a context in which the classification of the work described in this thesis comes under, we propose a new taxonomy of underwater networks as depicted in Figure 2.2. In the following sections and chapters, this taxonomy will be referred to and expanded upon through the related literature review, simulation developed and results collected. The red lines show the specific type of underwater network scenario of interest in this thesis.

The taxonomy is divided into three main sections in which underwater networks are classified based on three different communication aspects. The classification is firstly based on the communication technology used, secondly it is based on the communication channel,

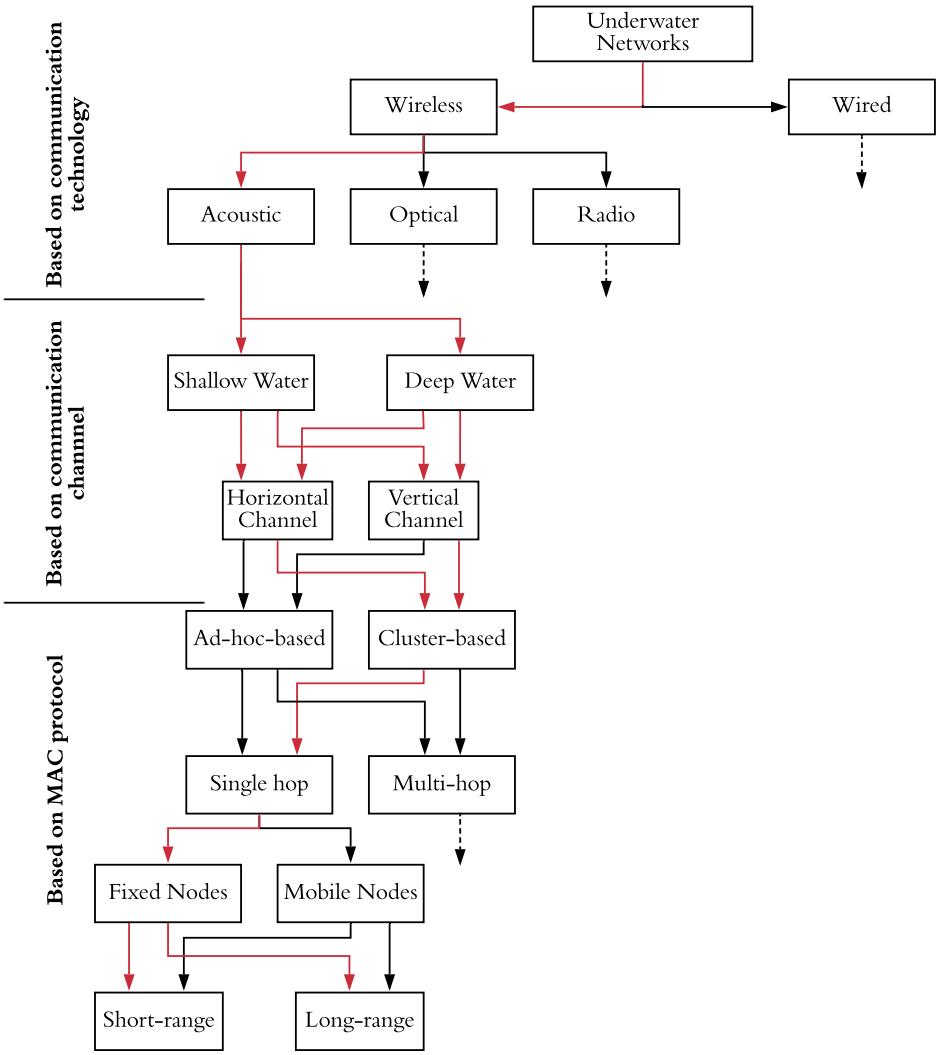

Fig. 2.2 Underwater networks taxonomy

and finally, it is based on the MAC scheme mechanism. Some terms need defining to avoid confusion when using them through this thesis. Underwater acoustic communication links can be classified based on the transmission range/depth to very long, long, medium, short, and very short links. Table 2.1. shows typical bandwidths of the underwater acoustic channel for different ranges. As section 2.6 describes, underwater channel bandwidth is a function of transmission range. The underwater channel is also classified based on the link direction to vertical and horizontal channels, (i.e. the link direction is determined by the direction of the sound ray between the transmitter and the receiver with respect to the water body's bottom and surface). Water bodies are significantly different in their propagation characteristics, particularly in their delay variance and multi-path spreads. Moreover, in this thesis, as usually

Table 2.1 Typical bandwidths of underwater channel

Class	Range (km)	Bandwidth (kHz)
Very long	1000	< 1
Long	10-100	2-5
Medium	1-10	≈ 10
Short	0.1-1	20-50
Very Short	< 0.1	> 100

done in the relevant literature, water with depth lower than 100 m is referred to as shallow water, while deep water refers to depths greater than 100 m.

In 1945, during World War II, an underwater telephone was made in the United States to connect with submarines [4]. Despite the fact that underwater communications have been in existence since then, underwater acoustic networking is a rather immature area. Researchers nowadays are engaged in developing networking solutions for underwater communication via the acoustic channel, yet this field demands more practical and reliable new communication protocols. Major factors that influence the performance of underwater acoustic networks are outlined in this chapter. It is worth mentioning that the most significant changes when moving from conventional radio networks to underwater acoustic networks are the change of the medium and the change of the signal. Water is used in place of air and acoustic waves instead of electromagnetic waves. Therefore, this peculiarity of underwater acoustic networks poses challenges especially to any efforts to design MAC protocols, which are very well established in terrestrial radio networks.

2.3 Underwater Sensors

The primary internal components of an underwater sensor are roughly illustrated in Figure 2.3. It is composed of a central controller/CPU, a sensor interface board that facilitates as an interface platform between the central controller and an underwater instrument or sensor. The controller is the coordinator between the other three main components, which are the sensors, memory and acoustic modem. It receives data acquired by the sensor, stores it in the built-in memory, processes it as appropriate, and sends it to other network terminals via the acoustic modem. The electronic components are well protected against water inside a waterproof housing made typically from PVC. The sensor body is protected as well if required, e.g. using solid frames or PVC grids allowing omnidirectional acoustic communications. This should protect all sensing components and acoustic modems from any potential nearby underwater

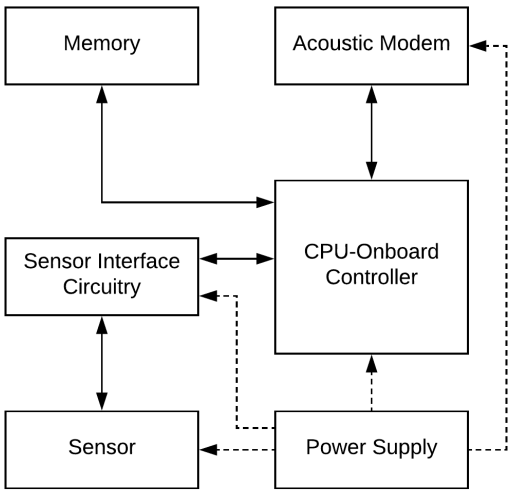

Fig. 2.3 Basic underwater sensor components

activities such as trawling gear in areas where fishing may take place. Underwater sensor types range from simple to more complicated ones. There are sensors that can measure water characteristics such as temperature, density, salinity, acidity, conductivity, oxygen, or hydrogen. Disposable sensors, which are used to detect the highly poisonous protein such that exists in castor beans. DNA microarrays which are used to monitor activity level changes among natural microbial populations. In addition, there are force/torque sensors which useful for underwater applications that require simultaneous measurements of several forces and moments, and quantum sensors which are used to measure light radiation, as well as sensors for measurements of harmful algal blooms [4], [5], [6].

2.4 Application of Underwater Wireless Sensor Networks

UASNs have a wide range of applications ranging from scientific to industrial applications and extending to even military and homeland security applications. Figure 2.4 illustrates a comprehensive classification of some potential applications. This section refers to some examples of each classification. Some of these examples are related to the main topic of this thesis, and hence, will be addressed in detail in chapter 2 as part of the literature review. UASN applications can be broken down into five main categories shown at the top level in the figure, i.e. monitoring, disaster forecasting and management, military, navigation, and sports. Some of these categories can be further classified into relevant subclasses and sub-subclasses as the figure shows.

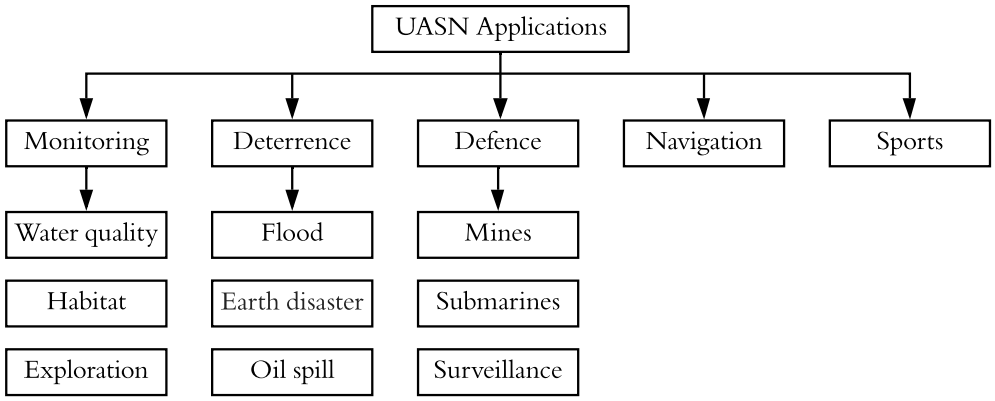

Fig. 2.4 Classification of underwater acoustic sensor network applications

2.4.1 Monitoring Applications

In this kind of application, a number of sensor nodes are deployed underwater to form a network. These nodes can then collectively monitor characteristics, properties, or particular objects of the underwater environment. Monitoring applications can be broken down into (i) water quality monitoring, (ii) habitat monitoring, and (iii) underwater exploration [7].

Water Quality

As an essential component of living bodies, water resources require regular quality checks. Its quality can be monitored using UASNs at its sources varying from canals to oceans. In [8], the authors propose a UASN for water quality monitoring. Their prototype is shown to monitor a number of water properties such as temperature T, dissolved oxygen, pH. The collected data is presented graphically and tabularly via several web platforms.

Habitat

Habitat monitoring is concerned with the study of the natural surroundings of living organisms. Marine habitat monitoring applications include monitoring of marine life, fish farms, and underwater plants/coral reefs. As for marine life, there is a number of proposed systems and prototypes of UASNs used successfully for marine life monitoring applications. ACMENet [9] is a European sponsored project focusing on marine life monitoring such as human or non-human activities within a certain coverage area, in order to be used for geological studies. In [10], a UASN is developed for aquatic monitoring. It is able to provide data that can be used to develop models predicting environmental/underwater climatic changes. Other examples of the applications dealing with the monitoring of various species living through water are proposed in [11], [12] and [13]. Fish farms are another interesting

area where UASNs can help. The fish farming industry has become such an important business, especially for many countries or cities that do not comprise any natural water bodies. Fish farms are very sensitive to environmental quality, and hence, demand a strict non-stop monitoring. Therefore, UASNn can be deployed to monitor the habitat conditions of fish farms to help maintain an ideal environment for fish. In [14], a UASN for monitoring fishes in ponds and lakes is developed and studied. UASNs also have potential in coral reef monitoring applications. Coral reefs are constructed by underwater microorganisms and have various shapes and colours. They are an essential part of marine ecology and marine life. In [15], an intelligent buoy for coral reef monitoring is designed, developed and tested. The buoy is made to be able to exploit the sea-wave energy, and hence, increasing the sensor node lifetime. It has been tested in real time; hence, the authors propose it for potential monitoring applications for coral reefs in particular, and the marine life in general. In [16], a practical and real-time UASN is proposed for monitoring coral reefs. This system is reported to be deployed at seven different coral reef locations in north-eastern Australia and has been functional over the past two years.

Underwater Exploration

There are numerous natural and man-made materials requiring exploration. Whilst 70% of Earth's surface is water which is full of precious resources, the remaining 30% terrestrial counterpart is linked by underwater cables or pipes to mainly transfer data and several forms of energy. UASNs are used to explore the underwater natural resources and also observe the underwater pipeline or cables. Underwater exploration has two key areas: natural resource exploration and cable/pipeline monitoring. In [17], the authors propose a UASN composed of both fixed sensor nodes and mobile (ROVs, AUVs) sensor networks to explore the mineral resources underwater. The proposed system can operate in deep oceans and for large-scale explorations. Oil and gas pipelines laid underseas are numerous, interconnecting the entire world. UASNs have great potential in this sector in terms of providing a remote monitoring platform. A framework for pipeline monitoring using a UASN is prototyped in [18]. The prototype has been examined in a lab environment; thereby, the authors provide recommendations for more reliable networks.

2.4.2 Disaster Deterrence Applications

Typically, natural disasters are unavoidable but may be foreseeable given the existence of appropriate technologies. Water-related natural disasters are particularly life-threatening and a cause of massive destruction. UASNs can enable a wide range of applications for both

before and aftermath management and recovery. More specifically, here are some common types of environmental events in which UASNs can be useful:

Floods

UASNs have helped researchers to design and implement solutions of timely flood alerts. UWANs in this regard allow underwater sensor deployments with an above-water agent facilitating the assessment of aquatic vitals. These vitals are collected and analysed at a remote station reacting to any flood indications. [19] proposes a UASN for flood monitoring caused by rivers. The proposed system is based on the deployment of sensor nodes, an AUV, and a remote station. It has been successfully tested in both a testbed and real time.

Volcano, Earthquake and Tsunami

Underwater earthquakes and volcanoes are amongst the worst natural disasters. They can occur anytime and anywhere driven by seismic and geological variations of the Earth's deeper layers. Monitoring such changes could save lives. [20] proposes a UASN for an early warning system responding to any signs of hazardous events, e.g. earthquakes and tsunamis.

Oil Spills

One of the common consequences associated with overseas transportation is pollution from oil spills. This can be very harmful to marine life and UASNs can contribute to minimising this harm by speeding up the process of finding the affected location. In [21], an ad hoc UASN that detects ocean pollution is discussed. The authors specify different types of sensors, and discuss several aspects of a communication protocol stack, focusing on enhancing the sensor node lifetime and network Quality of Service (QoS).

2.4.3 Defence Applications

Defence and homeland security, in particular, can involve a wide range of applications including monitoring and securing country ports or ships at home or in foreign harbours, as well as mine clearance and communication with submarines and divers. Like in other applications, UASN military applications can eventually lead to more civil applications for human benefits. Applications include the following:

Mines

Although mines are typically hidden, they are still physical objects that can be sensed underwater. They are typically made from metal materials that can be differentiated from other underwater components. Several UASN-based mine detection systems are proposed. In [22], the authors present a system that uses an autonomous vehicle (AUV) with sensors placed on it, in order to detect underwater mines. Based on AUVs, similar work has been done in other studies but with different sensor arrangements to allow multiple views of the scanned area [23], [24], [25].

Submarines

Underwater radars is also another interesting application that can exploit sensor nodes or AUVs to localise submarines. In [26], AUVs are utilised to implement a submarine localisation system. The trial, called the GLINT09, is reported to have successfully experimented the system in a sea trial. In another UASN-based work [27], a system called Particle Swarm Optimization (PSO) is proposed for the estimation of sensor location based on the attenuation, water depth, and transmission range.

Surveillance

UASNs can also be used for surveillance applications where any unwanted interference of undesired entities is discovered. In [28], test trials based on UASNs are implemented to conduct warfare surveillance. A similar implementation is done in [29] as an EU funded project concerned with the protection of offshore and onshore underwater tools and infrastructure.

2.4.4 Assisted Navigation Applications

Most terrestrial and satellite-based navigation systems cannot work underwater due to the peculiarity of the transmission medium. Therefore, to navigate underwater, there is a demand for extraordinary navigation technologies. Several navigation techniques and algorithms are designed and examined in [30], [31] and [32].

2.4.5 Sports Applications

UASNs contribute to aqua leisure and sport-related activities as well. These applications are of special characteristics compared with other UASN applications. They are different with respect to the typical velocity of sensing nodes and sensing parameters, as they have

direct contact with human. In [33] and [34], a UASN is developed as a tool for observing the performance of swimmers.

2.5 Challenges and Opportunities

UASNs are an immature promising field in which there are many challenges and opportunities. This section lists a number of potential challenges with some subsequent opportunities as follows:

- Unpredictable underwater environment: The conditions of the underwater environment are liable to extreme and unpredictable variations. In particular, the differences in pressure and temperature between different water layers and unpredictable water activities make it extremely challenging to design and deploy UASNs.
- Unreliable information: It is almost impossible to keep sensing nodes absolutely stationary underwater. They should be in continuous motion due to waves and deep water currents. Traditional localisation and synchronisation techniques cannot work underwater. Therefore, time and space uncertainty is an inevitable feature of UASNs. This increases the vulnerability of information transmission.
- Demand of novel protocols: The peculiarity of underwater environment necessitates the need for new communication and networking protocols. Long propagation delay and limited bandwidth place constraints to any attempt to employ traditional terrestrial protocols underwater.
- Low data rates - current underwater acoustic modems can provide only low data rates. This is attributable to their low operating frequencies limiting their channel bandwidth. In extreme underwater conditions, traditional technologies with low frequencies are unable to achieve a high number of useful bits per symbol due to the subsequent high bit error rates.
- Physical damage to equipment: Underwater erosion, salt or sand accumulation, algae collection and fish attacks are just examples of many sources of physical damage to the sensors used underwater.
- Cost – Generally terrestrial sensor nodes are relatively low cost and prices are reducing all the time, whereas underwater sensors are currently considered more expensive devices. For large-scale futuristic deployments, lower cost nodes are envisaged which are likely to be characterised by lower data rate capability. This should not come as a

surprise owing to the more complex underwater acoustic transformers and transceivers and also to the hardware protection required in the extreme underwater environment. Moreover, due to the relatively small number of suppliers, underwater sensors have inherently higher production costs.

- Power: The power required for underwater acoustic communications is generally higher than what is required in terrestrial radio communications. This is attributable to a number of factors including the different physical layer technologies, such as the larger transmission ranges, and the more complex signal processing requirements to recover the received signal after being transmitted through the impairments of the channel.

These extraordinary challenges in designing UASNs have made this area of research particularly interesting for researchers. With the continuous development in acoustic modems and underwater sensors, the other big challenge left is the design of practical and efficient protocols for UASNs. This also has attracted a number of researchers to the topic. Nevertheless, the gap is still wide for more research and opportunities.

2.6 Factors Influencing Underwater Networking

This section presents the primary factors of the underwater environment that may affect the performance of UASNs in general. These factors are the primary underwater channel characteristics that must be taken into consideration when modelling an underwater channel.

2.6.1 Acoustic Signal Propagation

The speed of sound through water is a key property of the acoustic channel and is the dominant bottleneck affecting the overall network performance. The sound speed is a function of a number of environmental parameters e.g. the temperature, pressure of the water (sound speed increases with temperature, pressure); therefore, variable in space and time [35]. Figure 2.5 illustrates an approximate general trace of any sound speed profile (SSP) that could be derived from a set of sea trial measurements. The propagation speed of sound underwater near the surface is more or less constant, then it starts to decrease because the temperature decreases rapidly but the pressure remains almost the same. After that, it reaches a point where it is minimal after which the temperature stays constant and the pressure increases causing the sound speed to increase. This means sound signals (rays) will follow curved paths which will be different from the Euclidean distances, and hence, can lead to errors if the propagation speed estimations are made and used.

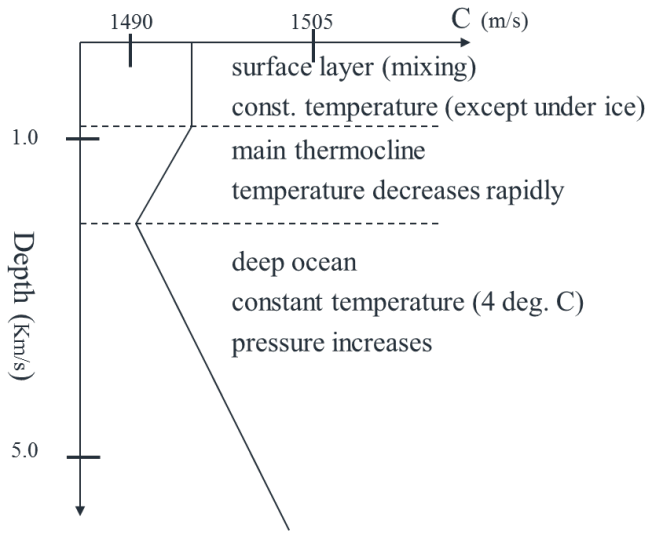

Fig. 2.5 Illustration of an approximated SSP

In simulation-based research, the average speed of sound in water is typically taken to be approximately 1500 m/s. This introduces a substantial propagation delay which is 0.67 ms/m. Looking at Figure 2.5, the above assumption will potentially introduce a margin of error of up to $\pm 0.6\%$. For example, if an acoustic transmission range was 1.5 km, it would take 1 s for the signal to travel over the entire range, according to the assumption of average speed. Whereas in fact, it can take anything between 0.997 s to 1.007 s for the acoustic signal to propagate across. This assumption must be taken into account carefully when designing network protocols for underwater acoustic networks. For a realistic SSP as used in [2], individual cases can be derived with temperature, pressure and salinity data at the desired underwater location. The curved trajectory of acoustic rays caused by real SSPs can then be traced and extracted using the BELLHOP ray tracing program [36]. This allows the actual propagation delays to be estimated, and also the impulse response to be determined (received amplitudes and phases of multi-path arrivals).

Transmission Loss

The underwater transmission loss represents the decline in the acoustic intensity as a result of the propagation of an acoustic pressure wave moving away from its sound source. This decline in the signal strength is named transmission loss or large-scale attenuation. The two major aspects from which this attenuation arises are geometrical spreading and absorption.

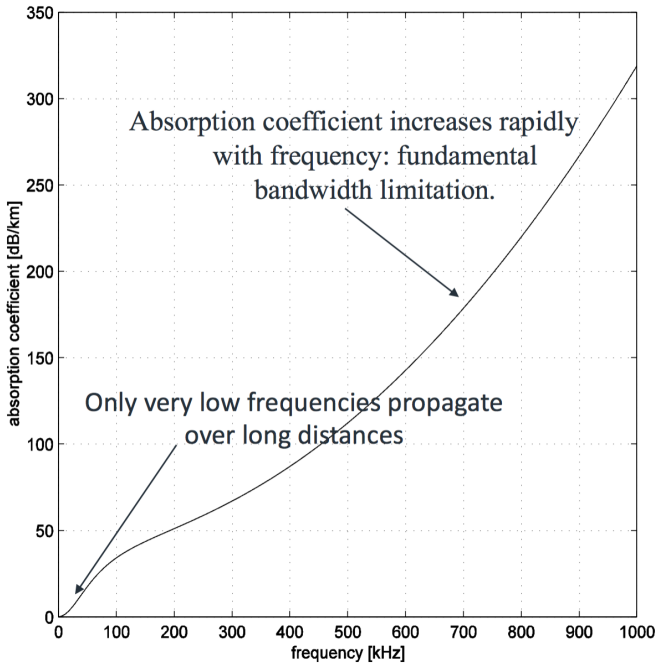

Fig. 2.6 Absorption coefficient vs frequency [1]

The attenuation that occurs over a transmission range l km for a signal with a frequency f kHz can be represented in dB/km by the following [37]:

$$10logA(l,f) = k10logl + l10log\alpha(f) \tag{2.1}$$

The first term represents the loss resulting in from geometric spreading. There are two common types of geometric spreading, and k is used to determine the geometrical spreading type based on the depth of water. It can be substituted with one of the following values: k=1 for cylindrical spreading (horizontal propagation only which is usually the case in shallow water communications), k=2 for spherical spreading (an omnidirectional point source which is usually the case in deep water communications). A significant part of the acoustic energy converts to heat causing signal absorption, which increases at higher frequencies. The second term is the medium absorption coefficient $\alpha(f)$ which can be obtained from one of several available empirical models. The total transmission loss can then be calculated by Equation 2.1.

Absorption Coefficient

Several models can be mathematically used to work out the absorption coefficient $\alpha(f)$ often in dB/km. Each of these models has over time improved the accuracy of estimating the

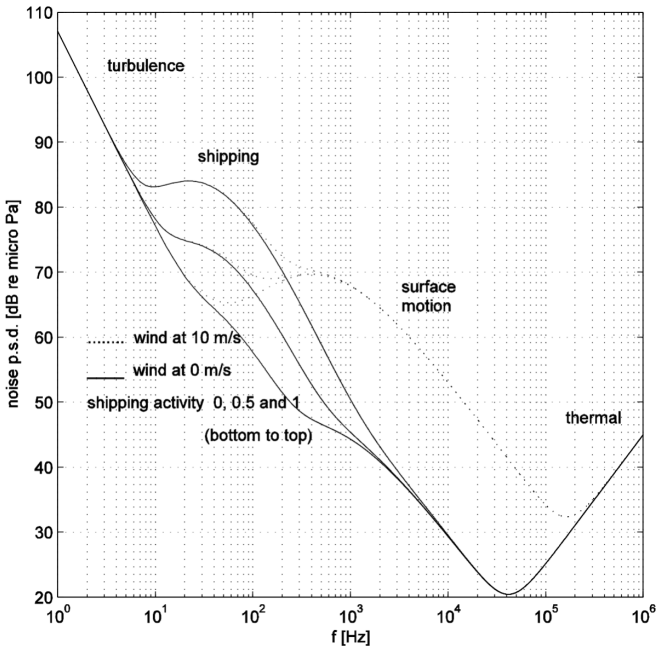

Fig. 2.7 Ambient noise P.S.D vs frequency [1]

degree of absorption. The most popular models include the Thorp [38], Fisher-Simmons [39] and McColm [40] models. The Fisher-Simmons model is the most popular model used in most studies dealing with physical layer issues. However, according to the comparison carried out in [37], the Ainslie-McColm model is relatively more accurate. Nevertheless, at low frequencies of a few hundred Hz, the three models give almost the same outcomes. As the main objective of this thesis is investigating the performance of MAC protocols, and given low frequency of acoustic modems, the Thorp model is the model adopted for the most results represented in this thesis. Chapter 3 gives more details about this.

Received Signal Power

The transmission loss obtained from Equation 2.1 is the degradation in strength that the signal would suffer while travelling across a single propagation path that has no obstacles (free underwater space). Therefore, if a signal travels over distance L km with frequency f kHz and transmission power P_{tx} dB, it will arrive at its destination as P_{rx} dB, which can be calculated as follows:

$$P_{rx} = P_{tx} - 10logA(l, f) \tag{2.2}$$

2.6.2 Ambient Noise Model

In the underwater environment, noise can be categorised based on its source as man-made noise and ambient noise. The former is primarily generated from machinery and shipping activities, while the latter is caused by hydrodynamics (natural movement of water including tides, current, rain, wind), as well as seismic and biological phenomena. The unusual "V" shape of the underwater acoustic noise p.s.d., represented in Figure 2.7 [1], makes the choice of the bandwidth become critical. If the system uses a high central frequency, it can exploit a relatively large bandwidth for communication with less noise (larger Signal-to Noise Ratio SNR). However, due to the reverse relationship between the frequency and the acoustic signal absorption represented in Figure 2.6, [1], either a high transmission power or a smaller transmission range will be necessarily required compensation for the higher attenuation. This means that the higher the central frequency is, the larger bandwidth can be used at the cost of higher attenuation. Attenuation will determine the upper limit of the available channel bandwidth for a given transmission range and power, whereas noise will determine the lower limit of channel bandwidth as noise increases when the frequency decreases.

2.6.3 Other Underwater Channel Aspects

Channel variation over time due to the reflection from the wavering sea surface and bottom as well as due to the variation in sound speed of the underwater acoustic propagation channels and relative (intentional and unintentional) motion of the sender and the receiver can result in the phenomena of multipath as well as Doppler shift. The physical layer signal processing needs to deal with these issues for a given channel. Multipath distortion is relatively negligible in the vertical underwater channel compared to the horizontal channel. This is attributable to that when sound propagates vertically between two points undersea, reflections from the sea surface and bottom cannot geometrically cause different multipath arrivals at the same point. The data transmissions in the scenarios studied in this thesis are mainly between sensor nodes and a gateway, which means data will be exchanged vertically. The Doppler effect is not covered here as the nodes in this study are fixed. Nevertheless, guard intervals can be inserted between transmissions to overcome the issue of propagation delay variance due to potential node drifts.

2.7 UAWSNs Traffic Characteristics

Poisson data traffic is a traditional traffic model that has been for decades the first choice for evaluating communication protocol performance for terrestrial networks [41]. The main

feature of this data traffic is that its inter-arrival times between packets can be modelled as independent exponentially distributed random events at each source. Although the Poisson traffic type is only representative of a subset of applications, such as those naturally occurring events generating exponentially random burst, e.g. [42], [43], it is still widely used for simulation studies as a tool allowing comparison with a tractable theoretical analysis of communication protocol performance. This applies also to UASNs, e.g. [44], [45], [46]. For example, in applications where nodes are hundreds of meters apart and the readings from the nodes are more unlikely to be correlated such as fish detection or security monitoring, the Poisson traffic type can be a good representative.

Wireless sensor network applications, in general, are not always recognised with particular random bursty data traffic, but rather with periodic data traffic, particularly for applications associated with environmental monitoring tasks [2]. In such tasks, the network is configured in a way that every node transmits a packet containing a sensor reading to a base station or a gateway node, e.g. [47]. Therefore, in this case, the inter-arrival times between packets will significantly differ from being exponential. We argue that for a more realistic representation of data traffic generated as a result of underwater monitoring tasks using a high-populated UASNs, data traffic models ought to be produced according to statistically self-similar traffic types. This is because of the periodicity behaviour these tasks can show and the absence of a natural length of a "burst" at any time scale ranging from a few milliseconds to minutes and hours which manifests self-similarity. In self-similar traffic types, there is no natural length for a “burst” but rather there are traffic bursts occurring over a wide range of time scales. In [48], it is found that for wireless sensor scenarios both ON and OFF period distributions (numbers and lengths of periods) are found to obey the Pareto ON/OFF distribution very well.

This study is one of few studies evaluating the performance of its proposed MAC protocols under different data traffic models. More specifically, the MAC schemes proposed in this thesis are designed to deal efficiently with both random bursty traffic conditions (based on Poisson data traffic) and self-similar models of periodic data gathering conditions (based on Pareto ON/OFF) in underwater acoustic sensor networks. The MAC protocols proposed in this thesis are hybrid and can give optimised performance with more tolerance to the changes in the type of data traffic. More details about this in the coming chapters. Hence, in this study, two data generator models have been developed in Riverbed Modeller [49] for MAC protocol performance evaluation, and they are:

- Poisson OFF
- Pareto ON/OFF

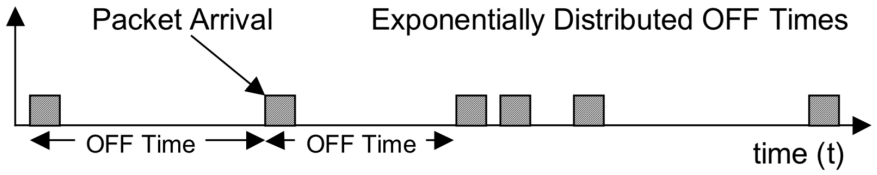

Fig. 2.8 Poisson OFF packet generation

Most of the results presented in this thesis have been obtained with these two data traffic models.

2.7.1 Poisson OFF

The packet generation pattern of the Poisson OFF model is depicted in Figure 2.8. Each packet generation representing an independent random event, and the time between two successive generated packets (the inter-arrival time) is exponentially distributed. The model is recognised as an OFF source with respect to the idle period separating successive packet generations. An equivalent model has been developed in Riverbed Modeller (RM) where each node contributes an equal amount of traffic proportional to the overall offered traffic load. The mean inter-arrival time (OFF period) is derived from the desired overall channel load value specified as a user attribute in the simulation and given by:

$$E_{iat} = \frac{\tau_{frame}}{D}\frac{N}{G} \tag{2.3}$$

where, E_{iat} is the mean inter-arrival time, τ_{frame} is the frame duration, D is the number of data slots in a frame, N is the total number of nodes, and G is the offered channel load in Erlangs.

2.7.2 Pareto ON/OFF

The superposition of multiple ON/OFF data sources switching regularly between ON and OFF periods exhibiting high variability yields combined data traffic that has self-similar nature [50]. The Pareto distribution is the simplest self-similar type that can provide high alteration in ON and OFF periods. A model of Pareto distributed ON/OFF data traffic source has been developed in Riverbed Modeller; a source which has the packet generation pattern depicted in Figure 2.9. The traffic source switches periodically between the two states, ON and OFF, and lasts over the course of each state for a period matching with the Pareto distribution. No data packets are generated throughout the OFF periods, whereas during

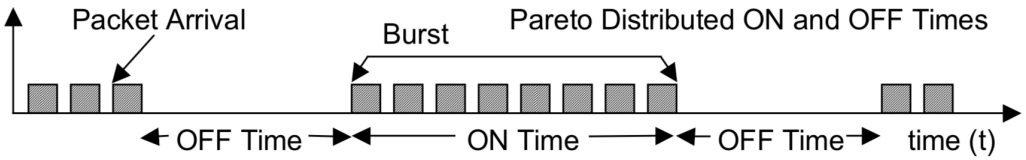

Fig. 2.9 A Pareto distributed ON/OFF packet generation

every ON period data packets are generated at a fixed rate based on the level of overall source activity, with all sources offer an equal amount of data traffic to the channel. The level of overall source activity is determined by the time between generated packets during an ON period. The packet inter-arrival time is given by,

$$E_{iat} = \frac{\tau_{frame}}{D} \frac{E_{on}}{E_{on} + E_{off}} \frac{N}{G} \tag{2.4}$$

where, E_{on} and E_{off} are the mean ON and OFF periods respectively, calculated from the following expression: $E(x) = \frac{k\alpha}{\alpha-1}$ where $E(x)$ is the mean value of the Pareto distribution which has a probability density function: $[f(x) = \alpha k^{\alpha} x^{-\alpha-1}, \quad (x \geq k\ \alpha, k > 0)]$,where, k is the distribution minimum value, and α is the value on which the heaviness of the tail of the distribution is based. The selection of the Pareto distribution parameters k and α determine the degree of self-similarity that the overall traffic will achieve as well as the minimum possible ON and OFF periods. There is a commonly used metric to measure the degree of self-similarity and is known as the Hurst parameter (H) [43]. H is given with regard to the tail parameter α by $H = \frac{3-\alpha}{2}$.

2.8 Conclusion

This chapter presents a brief overview of the fundamentals of underwater acoustic sensor networks. It proposes a general taxonomy of the underwater networks in order to give an idea about with which part this research is concerned with regard to the different classifications of underwater networks. It gives a general description of the underwater sensors hardware and outlines different types of underwater sensors. In this chapter, some UASN applications with many existing and potential examples are reviewed. The chapter describes the primary factors influencing underwater acoustic networking. These factors determine the variability of the challenges posed by the peculiarities of the underwater channel, especially those with regard to monitoring applications for the underwater environment. The ultimate objective of this chapter is to bring together different key parts relevant to the topic of underwater sensor

networks and lay down fundamental bases for the development of the coming chapters of this thesis.

Another important issue this chapter includes is that the traffic requirements of underwater acoustic sensor networks and the potential data traffic models that can be used for simulation leading to a wider representation of real underwater applications. There is not enough information about the statistical characteristics of the traffic typically carried over underwater sensor networks. By exploiting the wealth of knowledge about terrestrial sensor networks, it can be understood from a number of studies that their traffic exhibits an extent of burstiness over a wide range of time scales and is self-similar in nature, especially when the application designed for monitoring purposes. Some other studies addressed application maintaining greater relevance of the Poisson traffic type under certain conditions with regard to the way underwater sensor nodes interact with each other and how much they are correlated. One of the objectives of this thesis is to evaluate the performance of underwater MAC protocols under different data traffic models. The evaluation of MAC protocols performance in this thesis will be carried out with data traffic that is significantly burstier than Poisson such as Pareto ON/OFF, and both scenarios will be compared.

Chapter 3

Underwater Medium Access Control Protocols

3.1 Introduction

Communication networks in general and underwater acoustic sensor networks in particular require some level of channel sharing. A multiple access technique is typically required to achieve this. Multiple access techniques provide a means of separation between multiple transmissions of different terminals to coordinate the utilisation of available capacity. Common methods to achieve this separation include separation using time slots, frequency bands, or orthogonal codes. The shared capacity is then accessed based upon a Medium Access Control (MAC) protocol. MAC is a software-based management technique which corresponds to the lower sub-layer of layer 2 of the International Standards Organisation - Open Systems Interconnection (ISO-OSI) reference model [51].

Accessing a shared communication medium by different terminals requires control techniques that can minimise, or even better, completely stop packet collisions and allow rapid access. Packet collisions are particularly problematic in an environment such as the underwater environment. It features limited bandwidth availability and excessive propagation delay of acoustic signals. A further major concern for channel sharing is energy consumption. Acoustic transmission is a key factor influencing energy consumption of the underwater battery-powered sensor nodes [52]. Transmission must be optimised underwater. Ideally, an effective underwater MAC protocol requires a special design enabling the network to meet extreme challenges such as time and space uncertainty, the phenomena of space unfairness and momentary connection losses. The special design should assure maximum achievable

channel utilisation, minimum end-to-end delays, fairness, scalability, adaptiveness to traffic changes, and energy efficiency.

The chapter reviews some fundamental multiple access techniques and provides a comprehensive literature review of underwater MAC schemes. Section 3.2 describes the multiple access techniques. Section 3.3 and 3.4 discusses the important issues, constraints, and performance criteria of underwater MAC protocol designs. A comprehensive literature review of relevant underwater MAC schemes is given in section 3.5. Section 3.6 discuses the reviewed MAC protocols. The chapter ends with a brief conclusion in section 3.7.

3.2 Multiple Access Techniques

Poor coordination between network transmissions may lead to collisions among transmitted packets and result in degradation in the overall network performance. Hence, one of the primary aims of MAC schemes is to keep collision rates as low as practically possible. A collision happens at the intended receiver whenever two or more packets arrive at the same instant. This will often result in loss of the information but depends on certain factors such as the specific packet structures and the degree of overlap in time. Typical MAC schemes would tackle this kind of concurrent arrivals by slotting the available time or bandwidth and allocate different slots/bands to different transmitters, for instance, or sensing the channel before transmission, etc. On top of arrival time uncertainty, the underwater environment presents space uncertainty as well, owing to the long variable propagation delay and node fluctuation due to water dynamics. Underwater MAC schemes should find a way around this time-space uncertainty to prevent packet collisions [53]. Unfairness among nodes is a particular problem underwater because of the long propagation delay. Long and variable propagation delays bring about a phenomena called space unfairness [54] [55]. i.e., nodes located closer to the receiver will have a location advantage to win access to the channel when they compete with more distant nodes. The two common baselines into which MAC schemes can be split are contention-based and contention free schemes. In contention-free schemes, nodes do not compete to gain access to the communication channel. The idea is to assign distinctive time slots, frequency bands or spreading codes so that transmissions are done via orthogonal (or almost orthogonal) channels. The three main types of this category are Time Division Multiple Access (TDMA), Frequency Division Multiple Access (FDMA) and Code Division Multiple Access (CDMA) as shown below in Figure 3.1. In contention-based MAC protocols, resources are not pre-allocated by any of the three previous means. Instead, nodes are allowed to compete to gain access to a shared medium as required. Thus, the access mechanism in this category usually is a random process, and typically different recovery methods are involved

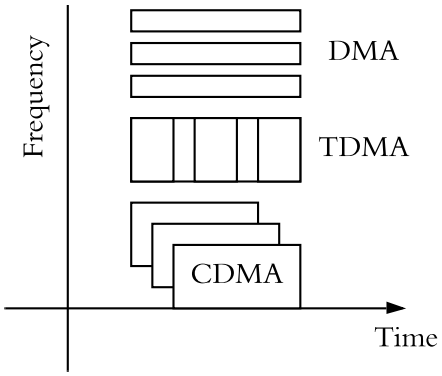

Fig. 3.1 Multiple access techniques

in case of any collisions. Some contention-based schemes employ a kind of time-slotted techniques allowing them to be combined with contention-free TDMA-based schemes. In such cases, random access acts as a MAC protocol to access a TDMA channel rather than a pure multiple access technique. This section details the tree fundamental multiple access schemes FDAMA, CDMA and TDMA, in general, before moving to how they are considered for UASNs.

3.2.1 Frequency Division Multiple Access

Transmitters do not need to compete to obtain a communication channel if they transmit and receive on different frequency bands. Frequency Division Multiple Access (FDMA) divides the available bandwidth into small separated bands allowing transmitters to work simultaneously without contention or collision. However, there is still a potential of collisions within the same small band if each channel is not sufficiently guarded to prevent interference between adjacent channels. This can be mitigated by inserting small guard bands. Figure 3.2 presents the basis of FDMA. In underwater acoustic networks, FDMA was firstly tested in the Seaweb project [56]. In the project, a network with three clusters is deployed, FDMA

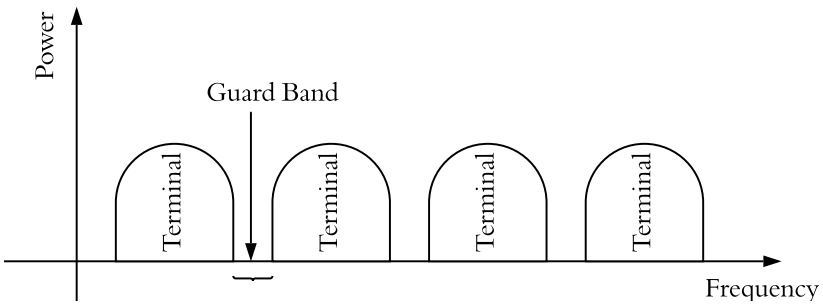

Fig. 3.2 Frequency Division Multiple Access

is selected to be the access strategy for cluster-to-cluster communications and TDMA is implemented within each cluster. The results are not as expected; inefficient utilisation of the bandwidth is reported due to vulnerability to multipath fading. Since then, FDMA in its conventional form has not been the preferred choice for underwater acoustic networks [57]. Using two orthogonal frequencies, the authors in [58] segment the available bandwidth into two channels, i.e. a main channel plus a control channel. The authors called their protocol Reservation Channel Media Access Protocol. This technique is shown to help minimise the probability of packet collisions at the cost of longer delay and lower data rate. This is attributed to the regular exchange of control signals and the partial utilisation of available bandwidth respectively.

3.2.2 Code Division Multiple Access

CDMA uses binary codes to encrypt the bits using a spread-spectrum technique. This allows different nodes to transmit at the same time and through the same frequency bands. In order to differentiate between the transmissions, the scheme relies on the use of various codes that have low cross-correlation. The scheme has some advantages over FDMA, for example, it is not affected by frequency selective fading as each node can use the entire available bandwidth. Another advantage is that, unlike TDMA, nodes can access the shared medium at the same time and at any time. In [59], a combination of CDMA and aloha protocols is proposed. Any node intending to transmit has to work out the required transmission power and the necessary spreading code length and uses pure aloha to deliver these details to the intended destination node. This initial delivery is done without any coding. After that, CDMA takes over and the agreed spreading code, correctly synchronised at the receiver, is used to reproduce the original data.

By striking a balance between the length of spreading code and the effective data rate, it is argued that CDMA could be a suitable choice to use in networks of multiple clusters. The authors in [60] show a proposal for a cluster-based network in which CDMA spreading codes are used in each cluster. It is named UnderWater sensor network MAC protocol (UW-MAC). Handshaking is the access technique between nodes within each cluster by exchanging control packets to reserve the communication channel, whereas TDMA is the medium access scheme for communication between cluster heads and a gateway. Similar work is done in [61], where another cluster-based MAC protocol is proposed, namely Energy-Efficient aDaptive hiErarchical and RobusT Architecture (EDETA). CDMA is again used for intra-cluster communication by assigning a different spreading code for each cluster. Unlike the previous work, nodes within a cluster relied on TDMA in sharing the channel. Another

major difference in this proposal is that allowing the cluster heads to arrange themselves in a tree structure to deliver their collected data packets to the gateway.

3.2.3 Time Division Multiple Access

In Time Division Multiple Access (TDMA), terminals transmit on a common carrier frequency but each of them is allocated a periodic time slot in which their packets are transmitted in a contention-free channel. With its many variants, it is the most popular technique in the literature of underwater networks as it is particularly suitable for periodic and low-data-rate transmissions of monitoring applications. Figure 3.3 illustrates the TDMA concept.

The guard bands in TDMA are usually necessary, and they may result in less efficient channel utilisation as fractions of capacity used for guard bands cannot be used for actual data transmissions. Accurate synchronisation is essential in TDMA to prevent any potential overlap between transmissions from different terminals. A typical way of achieving synchronisation underwater is through a predefined global reference. Typically, a master node, called gateway, facilitates this referencing mechanism owing to the advantages of being provided with a high-speed link to the terrestrial world and timing capabilities. Unlike in FDMA, the full transmitter power is available to every single TDMA carrier during a shorter period of transmission time. This means that terminals operating under a TDMA scheme require sufficient peak power to transmit at a high data rate over the course of a TDMA time slot. On average, the power transmitted will be equivalent to FDMA average transmitted power. FDMA allows for a continuous lower data rate transmission per terminal compared to a discrete high data rate transmission per terminal with TDMA.

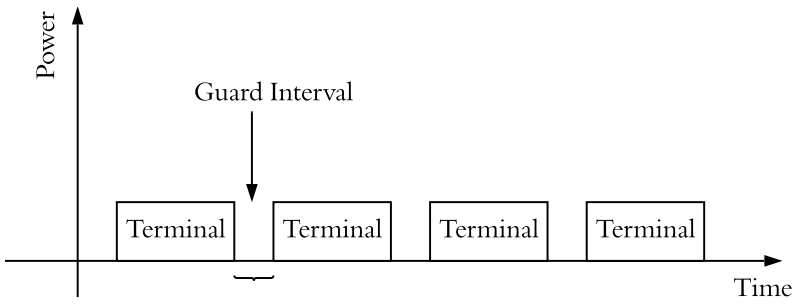

Fig. 3.3 Time Division Multiple Access

3.3 Underwater MAC Protocol Design

MAC protocols are primarily designed to provide channel access coordination mechanisms. This task is particularly problematic in the underwater environment that features limited bandwidth availability and excessive propagation delay of acoustic signals. These features pose extreme challenges to the functionality of MAC protocols; challenges such as time and space uncertainty, the resulting phenomena of space unfairness, and momentary connection losses. For UASNs in particular, the scenario of *burst short-packet traffic* [46] is also an important characteristic for MAC protocol design. An efficient underwater MAC protocol requires a special design to allow the network to meet these challenges. An adequate underwater MAC design would ensure maximum achievable channel utilisation, minimum end-to-end delays, fairness, scalability, adaptiveness, and energy efficiency. The nature of the characteristics presented in an underwater acoustic channel necessitates the demand for novel, efficient, reliable, applicable and straightforward MAC protocols. This section details the difficulties facing underwater MAC protocols design and the kind of design would be desirable under such circumstances.

3.3.1 Underwater Challenges of MAC Protocols

Due to the unique characteristics of acoustic propagation in the underwater environment, the design of MAC protocols for UASNs is a problem with extraordinary complexity. On top of the common challenges of typical sensor networks including hidden and exposed terminals [62], the UASNs have their underwater-specific challenges. The primary underwater-specific MAC challenges are time uncertainty, spatial uncertainty and energy consumption. In this section, the major MAC layer challenges for underwater networking are discussed.

Temporal Uncertainty

UASNs, by definition, have inherent long and location-dependent delays degrading the performance of traditional MAC protocols [63] [64]. Propagation delays need to be estimated in order to maintain synchronisation between nodes, prevent space unfairness phenomena and achieve high network performance [65] [66]. Unknown long and time-variant propagation delays can be dealt with in two primary ways applied in many UASNs:

- First, using a handshake technique between nodes to estimate the propagation delay, as shown in Figure 3.4. For the two neighbouring nodes A and B to estimate the propagation delay between them, node A needs to send a ping and record the departure time of its transmission. Node B then replies with an acknowledgement (ACK) to

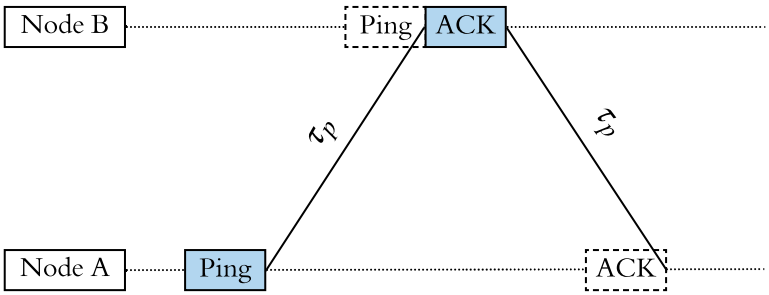

Fig. 3.4 Basic 2-node handshaking algorithm for underwater propagation delay estimation

node A straight after receiving the ping. Then, node A has to record the arrival time of the ACK at its end. Assuming that the round trip between A and B has a symmetric propagation delay, node A will then have enough information to work out an estimated value of the propagation delay. In case node B needs to learn about the propagation delay as well, a three-way handshake can be performed to enable a similar estimation process at node B. Upon receiving the ACK by node A, it immediately returns another ACK back to node B. Node B itself can then estimate the propagation delay in a similar way as node A did. This simple propagation delay estimation technique has variants that are also possible based on the kind of application. For instance, as shown in Figure 3.5, if node B is not yet ready to send back an ACK immediately after receiving the ping from node A and needs some time perhaps to communicate with another terminal, say node C. Node B may then choose to record the arrival time of the ping, as well as the time when it sends out its own ACK. Then, it inserts information in its own ACK showing the time difference between the arrival time of A's ping signal to the departure time of the ACK. Under this estimation scheme, node A first decodes the information in the ACK signal, and then, deduces the appropriate time that is spent at

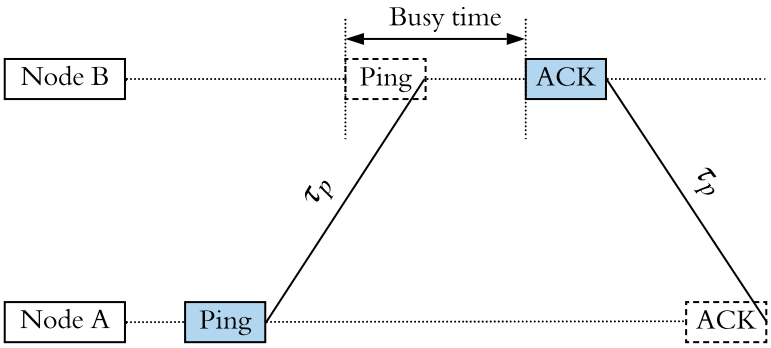

Fig. 3.5 Basic 2-node handshaking with delayed ACK algorithm for underwater propagation delay estimation

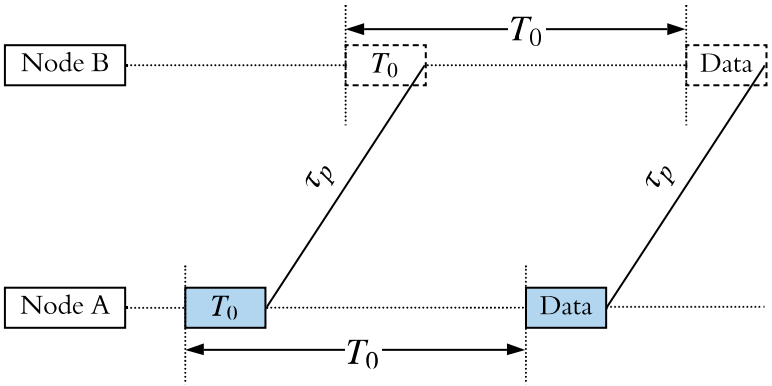

Fig. 3.6 Relative transmission time advertisement

node B before working out the propagation delay. Both references [67] [68] applied this scheme as part of their MAC protocol design.

- Second, a built-in clock at each terminal can be used to get around the uncertainty of underwater propagation delay. This way is to include relative time stamps when exchanging pings, instead of estimating the propagation delay. In this scheme, depicted in Figure 3.6, each node broadcasts a ping advertising to all its neighbouring nodes information about its next transmission time with regard to the current transmission time and based on its own clock as a reference. Let T_0 be the time on the timestamp in the broadcasting ping, i.e, node A informs others that it will send a packet after T_0 seconds. When another node, say node B, receives this information an arbitrary propagation delay time later, it sets its own clock accordingly assuming that it will receive a packet from node A T_0 later. Providing that the propagation delay remains fairly stable within T_0 time and the clock drift between nodes is negligible, node B will actually receive the next transmission from node A as expected and can then adjust its built-in clock accordingly. No further propagation delay estimation is necessary. This method is implemented in some underwater acoustic MAC protocols such as [69] [70]. The regularity of sending an announcement and respecifying a new T_0 is dependent on the statistical behaviour of transmitters and water conditions.

Given the specific characteristics of the underwater environment, there are some drawbacks with both methods. When a propagation delay is estimated directly by a three-way handshake and the knowledge of the propagation delay is gained, there is a time-out during the DATA transmission phase set for the ACK packets based on the estimated propagation delay. In case that an ACK has not been received within a time-out plus twice the propagation delay, then retransmission needs to be made. This brings about an inefficiency in channel utilisation owing to the extra waiting time proportional to the excessive propagation delay. Another

issue associated with the first scheduling method described above is the problem called ”Leader-election”. Without a predetermined leader (the node that triggers the start of the handshaking process), nodes will send at any time to try and establish a leader. However, probable collisions, in this case, increase the likelihood that synchronisation will never be achieved. At present, the most popular approach is the use of "a global scheduler" offering the requirements of a globally scheduled solution. MAC schemes proposed in this thesis use a global scheduler addressed in chapters 5 and 6.

Spatial Uncertainty

Motion is generally an inevitable feature of the underwater medium [63] [71]. In a long-term project, the SeaWeb project [56], a network made up of a number of AUVs is tested. Their MAC layer is based on Collision Avoidance using handshaking [72]. Handshaking is the foundation for other proposed MAC solutions [73] for underwater networks since then. Mobility poses new challenges to the design of underwater MAC protocols. There are at least two conditions have to be fulfilled in order to maintain fairness and provide an appropriate channel access to movable nodes; and they are: (1) One of the nodes must act as a leader in starting a transmission between two or more nodes, (2) the changeable propagation delay must be estimated in a timely manner.

In the physical layer, there is what is known as the coherence time of an impulse response. In analogy with that, [74] defines the "coherence time of propagation delay" at the network layer. The coherent time of the propagating delay is infinite if the two ends of an underwater link are stationary nodes. Providing this condition, the propagation delay does not need to be estimated more than once. Otherwise, the estimation of the propagation delay will be reasonable, only if its coherence time is greater than the time required to complete this estimation. In an analogous scenario with different theorems, this can be thought of as the relationship between the coherence time of the impulse response and the symbol duration; where the former must be much larger than the latter in order for the estimation of a physical layer channel to be useful. However, there is a significant dissimilarity in this analogy which is that the coherence time required to estimate the propagation delay can be significantly greater than the coherence time of the impulse response of the physical layer channel. This means that the underlying physical layer coefficients can change with time without having an immediately noticeable impact on the propagation delay. For instance, considering a case of two nodes located randomly which are free to move around their centres due to water dynamics. Then, the mean propagation delay caused by these small spatial drifts can remain the same as the motion is around a fixed central point, in the meantime, the impulse response coefficients of the physical layer channel can change dramatically. Therefore, the MAC

layer propagation delay coherence time is much larger. However, MAC protocols should incorporate a technique around this kind of potential motion.

In many applications, sensor nodes composing UASNs are stationary. Mobility is out of scope in this thesis, but underwater MAC protocols in general certainly must take nodes motion into account in order to achieve the highest utilisation for each node regardless of its very precise location. Transmission ranges and delay estimation techniques should be carefully designed to ensure that the estimation is done within the coherence time of propagation delay. Guard intervals are an essential design parameter minimising packet collisions due to potential inaccurate delay estimations. For example, in TDMA-based schemes, a 100 ms guard period between data packets can allow tolerance to the changes in node location of up to 150 m before propagation delays require re-estimating. Guard intervals are used in our MAC schemes introduced later in chapter 6.

Energy Consumption

As in other types of wireless sensor networks, sensors in UASNs are often battery-powered and their energy is limited. The limited battery life of the sensor nodes makes it inevitable to design MAC solutions that can enable nodes to survive under underwater long-term operations without a regular need of recharging or replacing their batteries [52], [63]. The most popular MAC solution for this dilemma is the use of sleep/idel schedules, as proposed in S-MAC (Sensor Medium Access Control) [75]. For underwater networks, the same sleep/idel strategy is implemented in multiple MAC protocols [70] with particular consideration to the fact that propagation delays are excessive and usually unknown. Request To Send (RTS) and Clear To Send (CTS) ought to be avoided when the delay is critical, not only to minimise end-to-end delays but also to conserve extra overhead energy. The typical way of keeping the energy wasted via overhead negligible is by making the duration of data packets relatively large. However, in underwater scenarios, the amount of data collected from sensors is potentially small in some applications. Thus, the design of MAC protocols has to be considered differently under the circumstances in which data generation rates are low. Currently, to the best of our knowledge, there is no adaptive UASN-MAC protocol that is capable to act on demand based on the application requirements with respect to the level of their offered loads. If there is, it would be an important contribution towards the design of UASN-MAC protocols. This is one of the features of the MAC schemes proposed in this thesis.

Another issue needs to be considered regarding this is the differences between radio and acoustic modems in terms of sleep, idel, receive and transmit modes. In [3], different specifications for both radio and acoustic modems are investigated, and it is shown to be a

significant difference in power consumption between the two modems with respect to sleep, idle, receive, and transmit states. Protocols are typically designed with certain assumptions about the behaviour of the modem will be used. For example, MAC protocol designers typically assume that the aggregate power required in the sleep mode is significantly lower than that is required in the idle mode. Therefore, there will always be an aim to switch to sleep mode as much as possible. However, the performance of UASN-MAC protocols may become worse, if the conventional sleep/idel concept implemented. Due to the transformation from electrical to acoustic and peculiarity of UASN applications, the worthwhile trade-offs for radio modems may be too costly for acoustic modems [76]. Therefore, what is ideally required for UASNs is the design of an adaptive protocol with low signalling overheads, operating based on a variety of variables including specifications of used modems, application requirements and network size. Hybrid MAC protocols are demanded, where structurally different protocols can be embedded in one protocol mechanism efficiently responding to those variables to find an optimal operating adaptation. The MAC protocols proposed in this thesis are hybrid and can adapt to the aforementioned variables.

3.3.2 Non-Environmental Factors and their Effects

This section briefly describes the non-environmental factors that have a direct impact on MAC protocol performance. Several non-environmental factors may have significant influence over the performance and over the communication quality between sensor nodes in UASNs. However, the impact of these non-environmental factors on performance is rather protocol-specific. In later chapters in this thesis, they will be discussed further under the conditions of our schemes proposed in the thesis.

Network Topology

The actual geometric layout of nodes allows nodes to have a certain arrangement often referred to as the network topology. It shapes the communication architecture and links between nodes to meet the specific needs of an application. Just like terrestrial networks, there are several common network topologies to which a UASN can be arranged including bus, star, ring, mesh, tree or random networks. Certainly, the performance of MAC protocols cannot be independent of the geometric layout of nodes. In [4], authors introduce two efficient communication architectures for underwater networks, which are two and three dimensional (2D and 3D). The study in [4] finds that communication architecture has a significant influence on a set of performance metrics such as energy consumption, throughput and delay. Although there is a wide range of topologies to which UASNs can be set, underwater

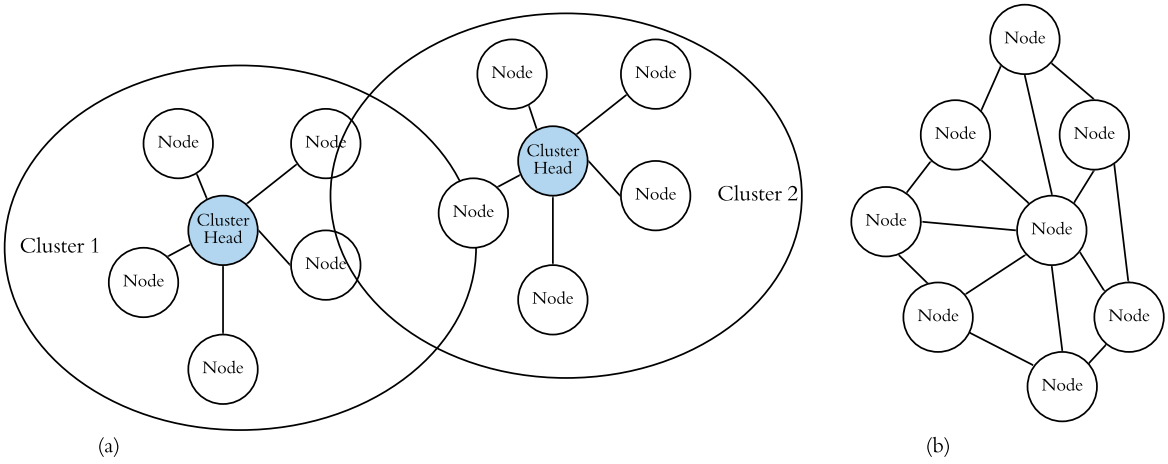

Fig. 3.7 (a) Cluster-based and (b) ad-hoc-based

MAC protocols can be broadly divided into two types according to node deployment. Some protocols are cluster-based and others are ad-hoc-based as Figure 3.7 illustrates. The former type is typically chosen for applications that are delay-tolerant whereas the latter can be a better choice for real-time data transmission [77]. Within a cluster, nodes can be arranged in different kinds of topologies mentioned above. Clusters can comprise a single hop or multi-hop links which can maintain a coverage area larger than the acoustic range of one sensor node. The head of the cluster can be used to achieve some MAC requirements such as synchronisation which would be more feasible with a single hop scenario where all nodes can hear each other directly.

Data Rate

As described in chapter 2, the underwater acoustic channel is characterised with a narrow operating frequency bandwidth which reduces with distance. The current underwater acoustic modems and the current modulation techniques are still not able to achieve high data rates. This is a major issue if the MAC protocol involves packet overheads, owing to the fact data this will reduce the effective data transmission rate. In this case, data packets are associated with a significant proportion of extra bits that must be long enough to achieve the task required from such overheads. Moreover, narrow and noise-dependent bandwidth is a particular constraint if a MAC protocol is supposed to use multiple frequency channels, for example, one for data transitions and another for control packets. In this case, the transmission range will have to be shorter in order to maintain sufficient operating frequencies bandwidth.

Performance of MAC protocols is considerably affected by data rate [78]. For example, a study [78] shows that throughput of a UASN-MAC protocol increases, when the data

rate increases to a certain threshold after which the throughput starts to drop. The data rate also has an impact on energy consumption as shown in [79] which confirms that energy consumption increases as data rate increases. Later in chapters 5 and 6, simulation results show the impact of data rate on the end-to-end delay and achievable channel utilisation of a MAC protocol under multiple specific underwater scenarios.

Hop Length

Due to the long propagation delays and significant signal attenuation, both single-hop and multi-hop communication may be required underwater depending upon the depth of water, to maintain successful delivery of transmitted packets. However, designing MAC protocols for multi-hop communication is more problematic and synchronisation is more complicated. In general, transmission ranges are desired to be short for many applications to maximise channel bandwidth. This means that single-hop communication would be more operational and can be supported with more capable and effective MAC protocol designs. Later in chapters 5 and 6, simulation results show the impact of transmission range/depth on the end-to-end delay and achievable channel utilisation of our MAC schemes under multiple specific underwater scenarios.

Size of Network

This is one of the most signification factors in shaping the performance of a MAC protocol underwater. The size of a network, i.e. number of nodes in the network, is shown in [80] to have an inverse correlation with average energy consumption, throughput, and direct relationship with delay. It is found that an increase in the size of a network causes a direct increase in the end-to-end delay, whereas it causes a decrease in the average energy consumption and throughput.

The impact of network size on throughput is less explicable. The study in [81] finds that increasing the number of nodes while maintaining a constant offered load will cause an increase in throughput owing to a decrease in overhead. However, expanding network size and traffic load may not result in the same change in performance results. This is attributed to the fact that the inclusion of more traffic sources requires more control overhead, whereas raising the transmission rate of a particular source does not necessarily require an increase in control overhead.

Packet Size

The impact of packet size on the performance of MAC protocols is analysed and assessed for an underwater scenario in [82]. It is found that packet size influences MAC performance significantly. Moreover, it is shown that packet size is a central design factor that must be chosen carefully as it can significantly affect energy consumption, delay, and throughput. MAC protocol designers have to choose suitable packet size for the network size and hop length with respect to special application requirements. Later in chapters 5 and 6, simulation results show the impact of packet size on the end-to-end delay and achievable channel utilisation of our MAC schemes under multiple specific underwater scenarios.

3.3.3 Desirable Features of a MAC Protocol

The ultimate goal of designing a MAC protocol is to optimise a number of performance metrics some of which are described in the next section. Before moving to those metrics, this subsection outlines a number of desirable features of underwater MAC protocols. If a protocol has these features, then it can potentially deliver the level of performance required. The desirable features include:

Adaptability to variations in end-to-end delay: Some underwater applications are sensitive to the variation in the end-to-end delay arising not only from variations in the queuing delay at the sensor nodes and gateways but also from variable propagation delays. MAC protocols should be able to get around this constraint.

Adaptability to the changes in channel load: The size of data acquired by most sensors of UASNs such as temperature or pressure sensors, is usually within multiple bytes, and hence, data packets transmitted via UASNs are typically short. The data rates of acoustic modems are also usually low. However, since sensors of many applications are triggered by a sequence of successive events (burst), it may yield heavy data traffic over a short period. Consequently, a number of neighbouring nodes will suddenly generate a short burst of data packets, which require to be transmitted to a gateway fairly and promptly. This scenario is named burst short-packet traffic in UASNs. Load requirements varying from one application to another necessitate the need for MAC protocols to adapt accordingly. This is to accommodate short-term fluctuations in traffic loads as well as any sudden rise in load values as a response to changes in the underwater property under sensing.

Low complexity: It is typically necessary to keep the processing time in any MAC protocol to its minimum by reducing the complexity of its algorithms. It will then consume less power, operate much faster, and will be more reliable and easier to test. This is a critical requirement of low-cost nodes. Also, signalling overheads can be very significant given the small amount of bandwidth available underwater and low data rates. A practical underwater MAC protocol should maintain very low complexity.

Scalability and reconfigurability: It is essential for underwater acoustic networks to have a MAC scheme that can adapt smoothly to any reformation in the number of active sensor nodes that the network may experience, as well as providing the ability to insert and eliminate nodes from the network with flexibility and ease. A good underwater MAC protocol in this respect will have to support a wide range of node population with efficient procedures to handle any new connections or disconnections of nodes due to variation in the underwater environment conditions. The ability of the scheme to continue to provide service in the presence of nodes failures is also an essential factor.

3.4 Performance Measures

Riverbed modeller is the simulator used extensively in the development and performance evaluation of underwater MAC protocols presented in this thesis. The modeller provides a powerful and flexible event-based platform allowing accurate and comfortable collection of performance statistics. Whilst most performance criteria are important, they interact with each other and it is typical that one criterion has an influence over another. In many cases, a reduction in the performance in one criterion is necessary to give a performance improvement to another. Because performance criteria could be interpreted in different ways, especially the way they are modelled, it is important to identify these performance metrics precisely in this thesis. Here are some important performance criteria that are used to evaluate the underwater MAC protocol proposed in this thesis:

3.4.1 Channel Utilisation

Channel utilisation is one of the most significant criteria in the evaluation of MAC protocol performance. It is defined as the amount of data carrying channel capacity that is effectively utilised for useful data throughput. In the light of TDMA-based MAC schemes, for example, it is the actual fraction of time utilised out of the overall allocated transmission slots. The

intention, in this case, must be always to maximise this fraction and minimise overheads in a TDMA frame.

In multiple occasions through this thesis, the terms *channel load* and *offered load* are also used interchangeably. Load refers to the amount of traffic placed on a channel, expressed either as a percentage of the overall data carrying capacity the channel accommodates or in Erlangs. Utilisation refers to the extent at which the channel is used; the extent that is reached by offering an equivalent traffic load into the channel. For example, achieving 80% channel utilisation is attained by a corresponding channel load of 80%, or 0.8 Erlangs. Another relative term used is *channel throughput*, which refers to the proportion of the successfully received data packets that are effectively used to transfer new information. In this thesis, the offered load and throughput formulas used are:

$$Throughput = \frac{Number\ of\ successfully\ received\ packets \times\ Packet\ duration}{Simulation\ duration} \tag{3.1}$$

$$Channel\ load = \frac{Number\ of\ generated\ data\ packets \times\ Packet\ duration}{Simulation\ duration} \tag{3.2}$$

3.4.2 End-to-End Delay

The end-to-end delay of a packet is defined as the time difference between the generation of the packet and the time at which the packet is successfully received by the receiving node. It is composed of several components including queuing delays, transmission duration, and propagation delays.

The end-to-end delay of a network is typically expressed in seconds and as a mean value representing the average delay experienced after transmitting a large number of packets. It is extensively used as a performance metric in this thesis for numerous results showing the mean end-to-end delay performance versus channel load. The resulting graphs obtained for end-to-end delay values can offer a great extent of new insights to the effectiveness of underwater MAC schemes. The end-to-end delay distributions with regard to channel load are also represented on many occasions throughout the thesis as a cumulative distribution function providing specific information on the achievable performance bounds in percentiles.

3.4.3 Fairness of Channel Sharing

MAC schemes differ in the way they are designed with regard to the equality of channel access between all nodes in the network. Some schemes are designed to provide an equal chance of accessing the channel, whereas other schemes provide different levels of priority to nodes based on predefined application requirements. Generally, MAC protocols must be

evaluated in the light of the design criteria, including the level of fairness required between nodes. To this end, MAC protocols must enable the fulfilment of the application requirements whether it is equitable sharing of capacity or effective prioritisation. This is an important performance metric due to the potential resulting phenomena of space unfairness in some UASN applications.

3.5 Underwater MAC Schemes - A Literature Review

Figure 3.8 suggests a graphical representation of UASN MAC protocol classification. Further description of the presented protocols is given in this section. The section reviews the most common MAC solutions in the literature of UASNs. The review is done in two stages: The first stage is this section in which we outline the main features of each reviewed protocol. The second stage is the next section (section 3.6) in which we provide a useful discussion and draw some conclusions. It must be mentioned that protocols that are very relevant to our work will be addressed in later chapters where appropriate. This section also provides a comprehensive tabular representation summarising the main differences between the reviewed protocols to help to provide a detailed discussion at the end of the section. The used classification is broken down into three main roots from which a MAC scheme stems: Time-based, FDMA-based and CDMA-based. It differentiates based on whether the scheme relies on a certain protocol, whether the nodes are clustered, whether handshaking is needed, and lastly whether time synchronisation or receipt acknowledgement is required. It sub-categorises time-based schemes into branches, divisions and subdivisions as follows:

- Scheduled-based: All nodes share the available time interval equally by one of the following techniques:
  - Fixed TDMA: A time slot is assigned permanently to each node to be able to transmit within it.
  - Adaptive TDMA: A time slot is allocated on demand. A coordinator makes the allocation of slots, either dynamically or allowing nodes to compete for them.
- Random-based: Nodes do not need to obey any orders. Transmissions could start or end arbitrarily, and nodes are freely allowed to contend for the channel possession. Protocols based on this scheme can also be subdivided into:
  - Direct: Without any sort of channel reservation, protocols under this section allow their nodes to send their data directly, accepting the risk of collision.

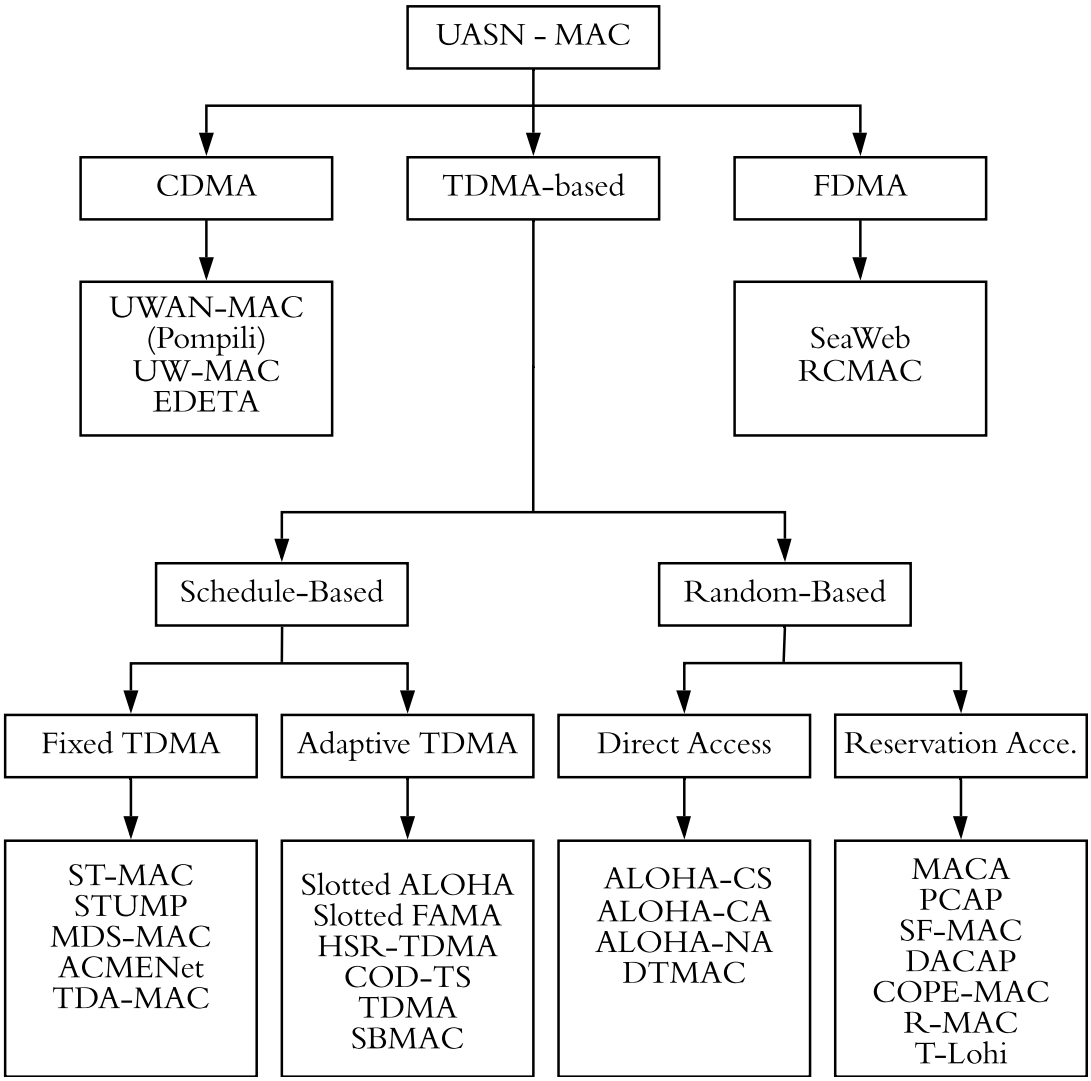

Fig. 3.8 Classification of underwater medium access control protocols

– Reservation: Unlike the previous technique, this group of protocols use control packets to reserve the channel before transmission. Despite channel reservation in this category, sending control packets to reserve the channel is a random process.

3.5.1 Scheduled-Based Schemes

The technique of assigning a time slot to each node to transmit requires synchronisation between all nodes. The synchronisation can be done using one of the synchronisation methods described in section (3.3.1). To guarantee a collision-free transmission, it might be necessary to insert guard intervals between slots as shown in Figure 3.4. The network performance is subject to decline if the duration of the guard interval is too long. The

guard interval duration is dependent on the maximum propagation delay and synchronisation accuracy. Schedule-based schemes can be either fixed TDMA or adaptive TDMA:

Fixed TDMA

The long and variable propagation delay of acoustic waves underwater causes spatial-temporal uncertainty in underwater acoustic networks and makes transmission scheduling particularly challenging. However, some authors used the long propagation delay of acoustic waves through water to their advantages and suggested new scheduling schemes. When the delay is long enough and varies from one node to another, it is possible for far-apart nodes to send their packets simultaneously without collisions, even if their destinations are the same [83]. Based on this fact, several proposals suggest that TDMA-based transmissions could overlap without conflict at the intended destination. The group of authors in [84] proposes a scheduling protocol called spatial-temporal MAC (ST-MAC) to overcome spatial-temporal uncertainty, which considers the TDMA-based scheduling problem as a new vertex colouring problem. These authors firstly constructed the Spatial-Temporal Conflict Graph (ST-CG) to tell apart the different conflict delays associated with transmission links of different nodes, and then, modelled ST-MAC as a new vertex colouring problem of ST-CG. Following that, an optimum solution is determined using a mixed integer linear programming model. Thereby, a new empirical solution is given to solve the vertex colouring problem. The problem of scheduling is also addressed in [85]. The authors call their protocol the staggered TDMA underwater MAC protocol (STUMP). It is a scheduled and collision-free TDMA-based MAC protocol exploiting node location diversity and the slow propagation speed of acoustic signals underwater. The protocol leverages propagation delay information to increase channel utilisation by allowing concurrent data transmission from several nodes. A set of scheduling constraints is derived by firstly determining a certain order of transmissions for the conflicting nodes. Once a sequence of collision-free transmissions is determined, the scheduling constraints are dealt with as a system of difference equations solved using the Bellman-Ford algorithm [86]. To enable finer scheduling, STUMP sets a logical circle surrounding nodes over the covered area as shown in Figure (3.9). Nodes are allowed to transmit only to a particular ring through a certain time slot ensuring that concurrent packets do not collide at their intended receiver. Further improvement follows this proposal in [87] by adding routing capabilities. A more recent alternative is introduced in [88] and is named Multi-Dimensional Scaling MAC (MDS-MAC). In a more complicated version, the protocol combines localisation, synchronisation and communication scheduling for small clusters. The mechanism of the protocol is divided into two phases; coordination and communication phases. The two phases are repeated periodically. In the 1st phase, a

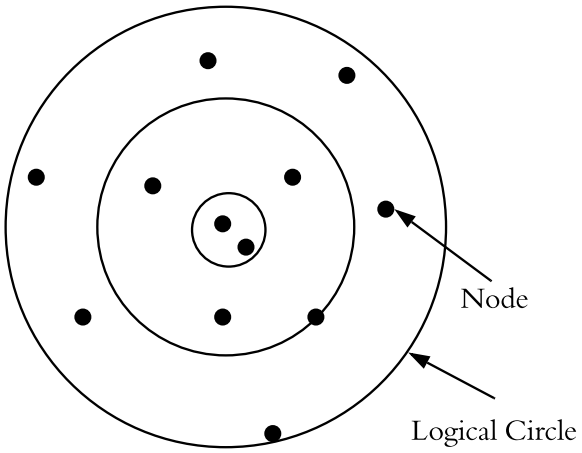

Fig. 3.9 STUMP logical circle to coordinate transmissions

coordination process is done between nodes by performing a set of measurements aiming at estimating the propagation delay to determine a reference time. In the 2nd phase, nodes are made aware of a transmission schedule and routing information that is broadcast by the cluster head. Following that, nodes can normally communicate according to the informed schedule. It is clear that the performance of the aforementioned scheduling-based protocols comes at a high cost in terms of overheads and complexity. This has led the authors in [89] to propose a cluster-based scheduling protocol that reduces the excessive overhead associated with spatial-temporal communication scheduling. The idea is that ST-MAC is used as a MAC protocol internally only within clusters and is coordinated by cluster heads. Every cluster head then informs a central scheduler about its cluster's transmissions schedule. The central scheduler can then assign slots to different clusters based on the schedules received from the cluster heads. The advantage here is that the central scheduler does not need to know the location of every node within the network to ensure a collision-free transmission, because the cluster heads take the responsibility of internal scheduling. Furthermore, the Acoustic Communication network for Monitoring of Environment in coastal areas Networks (ACMENet) protocol [9] is a TDMA-based scheme specifically proposed for small networks that have nodes interacting in a master-slave fashion. Due to the very limited capacity of node batteries that supply power to slave nodes in those networks, it is essential to reduce the energy consumption of the slave nodes. Slave nodes in the ACMENet protocol have a simple design, but the master node is more complex. This method demonstrates that having a master controller that provides transmission opportunities via a polling request process can optimise the utilisation of time slots and increase the efficiency of the typical TDMA protocol. The protocol has been tested in three real sea trials but was not as successful as it is in simulations. The author [9] said, "*The major reason behind the failure of the experiments*

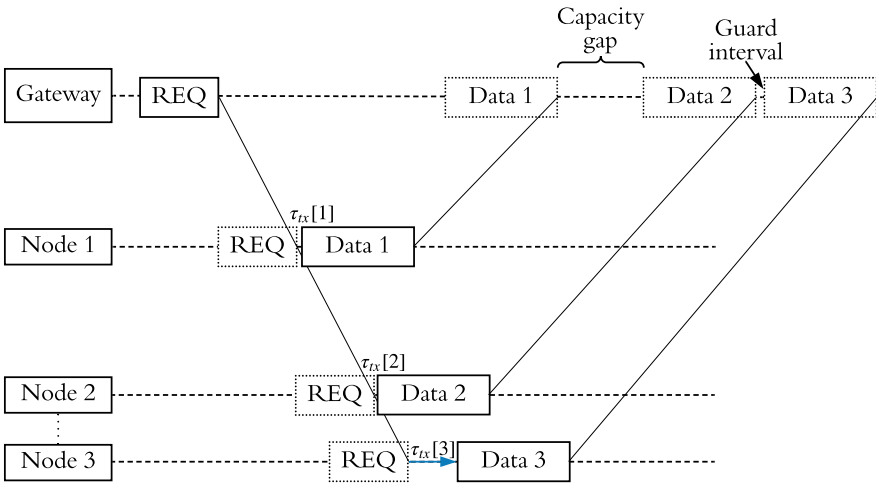

Fig. 3.10 TDA-MAC transmissions timing

was the very harsh conditions that damaged the slave nodes 1 and 3 burying them by sand quickly after the start of the sea trial".

To increase practically, a protocol named Transmit Delay Allocation MAC (TDA-MAC) is proposed in [2] for single-hop UASNs composed of sensor nodes connected to the same gateway. It is shown to provide high throughput performance for up to 100 sensor nodes, without global clock synchronisation. In its data gathering stage, it uses only one packet (REQ in Figure 3.10) per full set of sensor readings for signalling, regardless of the size of the network. Before this stage, it has a set-up stage in which propagation delays between every sensor node and the gateway are estimated and a transmission delay (t_n in Figure 3.10) for each node is allocated accordingly. Each sensor node has to wait for its allocated transmission delay before sending its data packet to the gateway. The advantages of TDA-MAC over previous schedule-based protocols is the simplicity of its synchronisation algorithm, lending it well to large scale sensor network deployments. For full details of the synchronisation algorithm of TDA-MAC, see chapter 6.

Adaptive TDMA

As for adaptive TDMA protocols, nodes are allowed to obtain transmission time slots based on demand. The acquisition of slots can be made via contention and a handshaking procedure or by learning when neighbouring nodes usually transmit. Nodes employing pure ALOHA as well as slotted ALOHA, for example, contend for the channel. However, the difference between the two, which backs the performance of the latter, is that the transmissions in slotted aloha are deferred to the start of different time slots. Hence, each node is required to offset the start of its transmission against the start of a slot. Nevertheless, unlike conventional

TDMA there is still a possibility of collisions if two nodes or more transmit in the same slot. Circumstances are different underwater, due to the spatial-temporal uncertainty in the underwater environment, the performance of slotted ALOHA deteriorates if implemented conventionally. The authors in [90] propose a solution to slotted aloha by adding extra guard intervals among transmission slots. It is claimed that this achieves 17 % enhancement in the throughput over the typical slotted aloha. Another protocol, called Floor Acquisition Multiple Access (FAMA), uses long control packets to avoid collisions between transmitted data [54]. However, using control packets underwater comes at a high cost of energy consumption and throughput decline owing to the long propagation delay. This has motivated the authors in [91] to introduce Slotted FAMA. The protocol reduces the control packet size by using time slots with a length equal to the sum of the maximum propagation delay and the transmission time of a control packet. By doing this, data packets are guaranteed collision-free transmission, but obviously, control packets are still vulnerable to collision. Another work classified as an adaptive-TDMA scheme is done in [92] namely the Hybrid Spatial Reuse Time Division Multiple Access (HSR-TDMA) protocol. Nodes here can be described as “artificially intelligent”. They are given the capability of learning which node among them can transmit at the same time with no collision. To achieve this, nodes determine a list of neighbours and announce it by piggybacking it onto outgoing packets. On receiving an updated list of neighbours, nodes revise their own connectivity matrices on which they rely to decide whether to use the next slot to transmit safely or wait for another. A protocol called Cluster-Based On-Demand Time Sharing (COD-TS) is introduced in [93]. There, nodes are split into clusters, and transmissions are made in rounds. Assigning the slots for each transmission round is done inside each cluster by the cluster head. The Cluster head broadcasts a schedule to be followed by the nodes, and then, each node that has data to send sends its request-to-send at the end of the round. Another task should be supervised by cluster heads is that they need to communicate with one another and work together to prevent collisions with the adjacent clusters. In [94], there is another initiative based on adaptive TDMA for a single hop network. The authors have modified the conventional TDMA protocol by applying lightweight synchronisation. This solution uses a simple superframe to achieve synchronisation between nodes. It uses the expression "defer time" which is the interval from when a node receives the end of the superframe to the beginning of sending its packet. The defer time is used to adjust all transmission times to maintain a sleep strategy to save energy. The protocol also uses a guard time between node transmissions to avoid collisions. Another adaptive TDMA-based protocol is introduced in [95], namely the Smart Blocking MAC (SBMAC) protocol. It is claimed that it works more efficiently in network topologies that have master-slave fashion. The main contribution of this complex protocol is

something called the SBMAC protocol which is the Smart Calculation Block. It is found in the master nodes and accepts a number of inputs (i.e. distance frequency, channel quality, the number of nodes and traffic load), and then sends out the instructions that should be followed by all the slave nodes. The given instructions include decisions on transmission period, data transmission policy (i.e. blocked data or normal), Acknowledgement policy (i.e. No-ACK, Selective-Multiple-ACK, Reduced-Whole-ACK, Multiple-Block-ACK, or Reduced-Block-ACK), etc. The master node then broadcasts a ping message, called the superframe, informing all its slaves the transmission mode, ACK mode, TDMA interval information, gain, and guard time. This smart protocol is claimed to be able to minimise the transmission time by assigning different control packets for different kinds of transmission methods based on the channel conditions.

3.5.2 Random-Based Schemes

Protocols under this subdivision consider complexity and pre-allocation of resources are unnecessary as long as the collision rate is manageable and can be recovered, especially for small networks with a light load of delay-sensitive traffic. Nodes are allowed to compete to obtain access to the channel. The common feature between these protocols is that they perceive the coordination of transmissions as a random process. They also perceive that the time-space uncertainty, the variation of the propagation delay, and nature of sparse networks as enough guarantees to make simultaneous packet arrivals at a node less likely. However, if a collision occurs, there are certain recovery mechanisms on which nodes can rely. These protocols can take one of three forms, which are direct access, handshake access or contention access.

Direct Access

This category does not include protocols that perform any kind of handshaking to reserve the channel. However, there could be some protocols performing carrier sensing before transmission to avoid interrupting ongoing transmissions and retry later when the channel is free. The most basic way to control access to a shared medium is ALOHA, discussed in chapter 4. In pure ALOHA, nodes do not perform any kind of channel assessment or collision detection, nor do they perform retransmission [77]. ALOHA with Carrier Sensing (ALOHA-CS) is an initiative to advance ALOHA and enhance its performance in underwater. To avoid collisions, ALOHA-CS allows nodes to implement a clear channel assessment (CCA). The decision of a node of whether to send a packet or not is dependent on the status of the channel. If an ongoing transmission is detected, nodes delay their transmissions until

the channel is free. A substantial amount of work has been done to study the performance of ALOHA in underwater acoustic networks. [96] is a study to understand the performance of the contention-based protocols by developing an analytical model to implement several forms of ALOHA in a multi-hop network. In spite of the simplifications assumed, the study draws some useful conclusions. The performance of pure ALOHA declines as the number of hops exceeds five hops. However, the throughput performance is found to be higher when using p-persistent ALOHA without dropping packets, and the price for that is increased end-to-end delays. More advanced ideas are introduced in [65], where two new versions of modified ALOHA are implemented. First, ALOHA with Collision Avoidance (Aloha-CA), in which collisions are avoided by estimating the propagation delay between every node pair and overhearing ongoing transmissions. When a node overhears a packet, it can extract information from the packet about the sender and its intended receiver. With knowledge of propagation delays, the node works out the duration of how long the channel will be busy. Second, ALOHA with Advanced Notification (ALOHA-AN), in which collisions are avoided by sending a short alert packet in the vanguard of actual packet transmissions to put out information about a sender and its intended receiver. Another protocol following the rules of this category is CSMA mentioned in [77]. Similar to ALOHA-CS, this protocol performs channel sensing. However, after detecting that the channel is free, the node does not transmit straightaway. Instead, it uses random back-off mechanisms for the sake of collision mitigation. This version is called non-persistent CSMA. In a slightly different version, called p-persistent CSMA, when a node realises the channel is free it transmits with a probability of p. It is worth noting that 1-persistent CSMA is an equivalent protocol to ALOHA-CS. Providing that UASNs are generally large-scale sparse networks with low traffic, the group of researchers in [46] suggests a protocol called Delay Tolerant MAC protocol (DTMAC). The protocol's main idea is that if a node has a packet to send, the packet is repeatedly transmitted m times, with a transmission probability p. The group establishes a probability model determining the throughput of DTMAC and made throughput-optimal values of m and p with the probability of successful transmission as system tuning parameters. The simulation results show that the throughput of DTMAC outperforms some MAC protocols including those which perform reservation techniques to increase throughput.

Reservation Before Access

In this category, channel reservation is the technique nodes use to gain access to a channel. The usual way to achieve this is via handshaking by sending short control packets prior to the transmission of the actual data packets. Reservation of the channel leads to minimising the collision rate and maximising throughput at the cost of longer end-to-end delays. The

additional traffic caused by the control packets is not a very critical issue for some applications, as there are always ways to compensate. To be specific, in this strategy, a node with data to transmit should first send a control packet letting other nodes know about its planned transmission. Once a packet has reached the intended receiver successfully, the receiver replies if the channel is free. Upon reception of the reply, the transmitter has the go-ahead to start a guaranteed transmission. Nevertheless, this time-consuming handshaking mechanism is a random process and still subject to collisions between simultaneous control packets of different nodes.

The first protocol adopting the notion of handshaking is Multiple Access Collision Avoidance (MACA) [97]. The control packet that is sent from the sender to the receiver, RTS, contains the length of the data packet to make neighbouring nodes aware of the time they should wait before they can start their transmissions. The intended receiver should reply by broadcasting a packet, CTS, if it is ready to receive. Although the reply from the receiver, the CTS packet, can extend the alertness of the ongoing transmission to the outermost neighbours, the exposed terminal problem is not entirely overcome, particularly when the propagation delay is very long. [67] proposes a MAC solution called Propagation-delay-tolerant Collision Avoidance Protocol (PCAP). The founder of this protocol believes that while the sender is waiting for the CTS, it can be involved in another transmission with another node before the waited CTS arrives. The protocol defers the transmission of the CTS packet for a maximum of twice the propagation delay. Meanwhile, the sender is free to perform a new transmission with its neighbours, for instance, sending a data packet or setting off a new handshaking process with a different node. The idea of holding on the CTS packet longer is also used by the authors in [45]. The authors call their protocol Spatially Fair MAC (SF-MAC). The CTS packet is deferred for a predefined amount of time during which the receiver is receiving a certain number of RTS packets from different nodes. The receiver evaluates the received RTS packets using an estimation algorithm and determines an optimal order to send a sequence of CTS packets back to the senders as appropriate. Another group selects random access with prior reservation as their baseline and present a scheme called Distance-Aware Collision Avoidance Protocol (DACAP) in [98]. The scheme aims at preventing the probable collisions of RTS packets with data packets in particular. It inserts additional waiting times before sending RTS and starting a data packet transmission. This waiting time can be adjusted according to the appropriate tradeoff between collision probability and throughput. Furthermore, the protocol allows a node to send a warning packet if it overhears another RTS while a CTS is being sent. The group, in [99], discusses the concept of the parallel reservation to improve the channel utilisation. Contention-based parallel reservation MAC (COPE-MAC) is the protocol proposed in the study [99]. Its notion

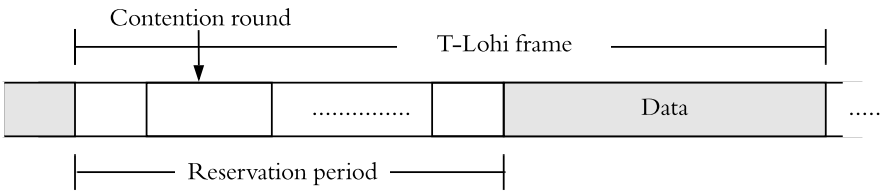

Fig. 3.11 Tone-Lohi frame format

is that one global packet can be broadcast and carry information on multiple reservations to all neighbours. Neighbouring nodes can then learn about the transmissions that are scheduled next and offset their times of channel access accordingly. CTS packets can be marked as high priority packets as the authors do in [68]. For long-term monitoring applications, nodes can follow a random sleep and listen schedule taking into consideration the propagation delay of each node, and then, access the channel in an RTS/CTS manner with a high priority given to CTS. This is called the Reservation-based MAC (R-MAC) protocol. Another work is presented in [100], introducing a different way of handshaking. This time, the receiver is the node that initiates a four-steps handshaking mechanism. As soon as a node is free, it announces that it is ready to receive. Any neighbouring node, with data to transmit to this particular receiver, should inform the receiver the size of their transmission. The receiver then can arrange a transmission order using the initially received information, and the knowledge of the propagation delays. The receiver finally replies to all intended senders to inform them the order they should follow. Thus, data packets from different sources arrive at the receiver in a predefined sequence. Using an adaptive back-off strategy, Tone-Lohi (T-Lohi) in [101] automatically adjusts the contention period based on the number of contented nodes. A short packet, termed tone, is sent out before every data packet to enable the start of a listening state for a duration called the contention round (CR). This distributed MAC protocol uses a frame composed of reservation and date transmission periods as shown in Figure 3.11. A node decides whether to send or to back off for a certain time depending on the number of competing nodes within CR. If there is only one competing node, it wins the channel. When the reservation period ends, the collision-free transmission of data can then start.

3.6 Discussion

Having reviewed the common underwater MAC solutions, a summary can be concluded as shown in Table 3.1. The table presents three main roots from which MAC protocols stem, i.e. Time-based, FDMA-based or CDMA-based. It also specifies whether the protocol relies on a certain scheme (random access scheme, TDMA scheme, CDMA scheme or a combination of

several schemes), whether the nodes are clustered, whether handshaking is needed, and lastly whether time synchronisation or receipt acknowledgement is required. It is clear from this table that the literature of underwater MAC protocols has been dominated by TDMA-based solutions. FDMA and CDMA based solusions are less common compared with TDMA. TDMA-based schemes can easily adjust the number of orthogonal channels, and allocate variable data rates by just changing the number of time slots assigned to a particular node. Contention-based MAC protocols are inefficient underwater. Reservation-based protocols, for example, exhibit poor channel utilisation due to the long waiting time needed to establish an acoustic communication link. Long and variable propagation delays bring about a phenomena of space unfairness. CSMA techniques also have poor delay/utilisation performance in UASNs due to substantial guard intervals required to accurately sense channels with long and variable propagation delays [102]. To improve channel utilisation, end to end delays and fairness by means of a MAC protocol, the regularity of exchanging control packets among nodes should be reduced underwater. Moreover, the time-space uncertainty places a constraint on the functionality of scheduling-based MAC protocols. It has been found that the most feasible and applicable approach for scheduling-based MAC protocols is the use of "a global scheduler". It offers the requirements of a globally scheduled solution by allowing the estimation of approximated propagation delays. Under the scenario of bursty short-packet traffic in UASNs, contention will increase data packet loss rate and decrease throughput. Fixed TDMA also will perform poorly under this scenario as a proportion of slots will still be assigned to nodes that are not involved in this bursty short-packet traffic causing poor delay/utilisation performance. In order to improve the network delay/utilisation performance in bursty short-packet traffic scenarios more adaptive TDMA schemes are required.

Despite the domination of TDMA-based protocols in the literature, there is no absolute winner amongst the reviewed protocols. The type of application in which a network is implemented constitutes the way that the network is deployed. Deployment of nodes plays a vital role in changing the performance of a MAC protocol. Therefore, none of the previous protocols can be considered as the best solution for all applications. Despite the work done focusing on the enhancement of different performance metrics of UASNs for a given application, this area of research demands more effort to find approaches to choosing amongst several underwater MAC solutions based on the constraints of the intended application. Hybrid protocols that combine more than one solution in one scheme adapting itself to the circumstances is the key to a new solution. For example, to improve deterministic schedule-based TDMA methods, contention-based and TDMA-based MAC protocols can be combined. They are classified as adaptive-TDMA where capacity is usually assigned on demand.

Table 3.1 Underwater MAC protocols classification and properties

Category			Protocol	TDMA		CDMA	Random Access	Clustered	Hand-shaking	Requires	
				Fixed	Adaptive					Sync	Prop.Time
FDMA-based			Seaweb [56]	x						x	x
			RCMAC [58]				x		x	x	x
CDMA-based			UWAN-MAC [59]			x	x				
			UW-MAC [60]	x		x	x	x		x	x
			EDETA [61]	x		x		x		x	x
TDMA based	**Scheduled based**	**Fixed TDMA**	ST-MAC [84]	x						x	x
			STUMP [85]	x						x	x
			MDS-MAC [88]	x				x		x	x
			ACMENet [9]	x				x		x	x
			TDA-MAC [2]	x				x	x	x	x
		Adaptive	Slotted Aloha		x		x			x	x
			Slotted FAMA [91]		x		x		x	x	x
			HSR-TDMA [92]		x					x	x
			COD-TS [93]		x	x	x		x	x	
			TDMA-based MAC (SBMAC) [95]		x			x	x	x	x
	Random based	**Direct Access**	Aloha-CA/Aloha-AN [65]				x				
			CSMA [77]				x				
			DTMAC [46]				x	x		x	
		Reservation Access	MACA/MACA-U [97]				x		x		
			PCAP [67]				x		x		x
			SF-MAC [45]				x		x		
			DACAP [98]				x		x		
			FAMA [54]				x		x		
			COPE-MAC [99]				x		x		x
			R-MAC [68]				x		x		x
			T-Lohi [101]				x				

In the next chapter, the following three capacity assignment strategies are investigated in the context of UASNs. Demand Assignment which is shown to have much greater tolerance to increasing channel load and traffic bursts, but with a longer delay. Free Assignment which offers close to the theoretical minimum end-to-end delay, but only at low channel loads. Following that, the Combined Free and Demand Assignment Multiple Access (CFDAMA) protocol combining the two latter protocols is examined in chapter 5.

3.7 Conclusion

There are many reasons that can cause packet collisions in the underwater environment including time-space uncertainty. This environment features limited bandwidth availability and excessive variable propagation delay. This poses challenges to the design of MAC protocols including attempts to achieve low end-to-end delay, high channel utilisation, fairness and low complexity. The functionality of MAC protocols should be stable despite synchronisation difficulties, space unfairness and bursty short-packet traffic. The most common way of synchronisation is the use of a global scheduler, exchange of timing signals and use of guard intervals. To this end, single-hop topologies suit UASN applications very well. The performance of a MAC protocol is determined by the ability to adapt to different underwater scenarios. The underwater scenario means all the surrounding environmental factors such as (water motion, signal attenuation, background noise, interference etc.) and non-environmental factors such as (network topology, data rate, hop length, network size, packet duration, etc.).

The focus on TDMA-based MAC approach in this chapter is primarily attributed to its appropriateness to the sensor networks whose data traffic is rather periodic, especially with monitoring applications. In addition, this approach has more potential for improvement as it can maintain more flexibility by providing dynamic and variable channel allocation and the ability to combine more than scheme together. Despite the work done, the topic demands more efforts in developing guidelines to help to choose amongst several underwater MAC alternatives based on the constraints of the intended application. Ideally, the new solutions must deliver high channel utilisation, low end-to-end delay, and low energy consumption, while guaranteeing fairness amongst the sensor nodes. This can be done by exploiting the advantages of fixed-TDMA, adaptive-TDMA, reservation-based and random access MAC schemes somehow combined in one scheme. Hybrid protocols that combine more than one solution in one protocol adapting itself to the changing circumstances is the key to the new solutions.

Chapter 4

Performance of Capacity Assignment Strategies

4.1 Introduction

By reviewing the common MAC solutions in the literature, chapter 3 leads to the conclusion that there is a demand for adaptive MAC schemes combining more than one assignment strategy in order to meet the special requirements of UASNs. The peculiarity of both the acoustic channel and UASNs, as described in chapter 2 and chapter 3 respectively, necessitates the need for new MAC protocols that can maximise the channel utilisation and minimise the end-to-end delay with fairness and low complexity.

This chapter investigates three capacity assignment schemes in the context of UASNs. They are the demand assignment, the free assignment and the Combined Free and Demand Assignment Multiple Access (CFDAMA) schemes [103] [104]. After it gives details of the developed underwater scenarios, the chapter provides insights into the performance of the MAC schemes that incorporate a single capacity assignment strategy, i.e random access, free assignment, or demand assignment. This has resulted in this publication [105]. The primary purposes of this chapter are:

- To describe the simulated underwater acoustic channel.
- To assess the performance of the single capacity assignment schemes.
- To lay the foundations for more effective and hybrid underwater MAC schemes.

The functionality of random access is assessed and analysed in section 4.2 and section 4.3, the free assignment and the demand assignment strategies are investigated in section 4.4

and section 4.5 respectively. Finally, a summary of the important findings of the chapter is concluded in section 4.6.

4.2 Random Access (the ALOHA Schemes)

The ALOHA schemes were founded at the University of Hawaii for transfer of data between terrestrial sites on different islands [106] [107] and have since been under analysis and development for different kind of networks. The two primary random access techniques are pure and slotted ALOHA. The pure ALOHA scheme does not apply any rules on when nodes can transmit packets. The transmission of each node happens as soon as a packet arrives at its queue. There is no coordination whatsoever between nodes despite the fact that they share the same transmission medium. Therefore, packets may collide and lose their data, if more than one node coincidentally happens to transmit at certain times allowing packets overlap at the intended receiver. A correctly received packet can be followed by an acknowledgement from the receiver to the transmitter. If an acknowledgement has not been received within a certain period of time, a retransmission strategy is triggered to retransmit the lost packet, typically after a randomised back-off. For underwater applications, Pure ALOHA is arguably suitable for certain sparse networks with light traffic loads and diverse terminal locations. It can lead to low end-to-end delay values (minimum bound of 0.5 round trip for centralised single hop networks). On the other hand, if the channel traffic load grows either through an increase in network size or decrease in mean packet arrival rate, the probability of collision will escalate rapidly, and as a result, end-to-end delay values will become longer.

Slotted ALOHA is an advanced variant of the pure ALOHA scheme, a variant which provides twice the maximum channel utilisation but at the cost of increased complexity. In the slotted ALOHA scheme, available time is divided into discrete slots at least equal to the packet length (i.e. duration of a packet transmission plus an appropriate guard interval if required), and the transmission from each transmitting node is deferred to the beginning of a time slot. Collisions, in this case, occur if more than one terminal transmits in the same time slot. The key difference between the two variants of ALOHA schemes is the time span of collision vulnerability; it is two packet durations for pure ALOHA against only one packet duration for slotted ALOHA. This results in the packet collision probability being halved, and therefore, slotted ALOHA introduces a factor of two doubling of throughput. A detailed analysis of the performance of the two ALOHA variants is given in this section.

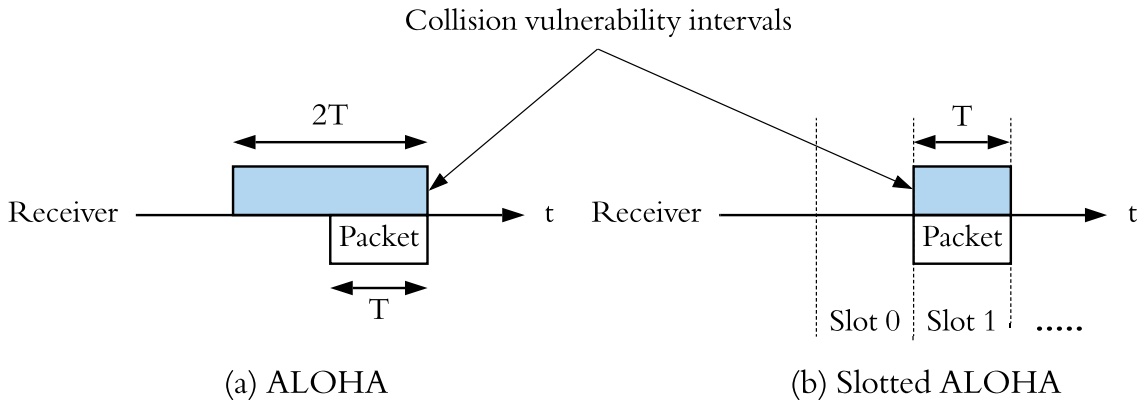

Fig. 4.1 Vulnerability intervals for ALOHA schemes

4.2.1 Theoretical Performance of Random Access Schemes

The derivation of the throughput expressions of the ALOHA schemes is a classic example of mathematical analysis based on the Poisson distribution. The analysis requires some simplifying assumptions but the resulted equations do give a useful theoretical upper bound on the throughput. The simplifying assumptions are as follows:

- The number of transmitters is very large, tending to infinity.
- All packets are of the same size/duration and their generation process obeys the Poisson distribution.
- All packet transmission failures are caused by packet collisions.
- Any partial or full packet overlaps are considered a collision, resulting in complete loss of all involved packets.

Pure ALOHA: Figure 4.1 (a) depicts the potential packet collision situation in pure ALOHA. For example, say a receiver receives a packet at time t. If the same receiver receives at least another packet during the period $[t-T,\ t+T]$, where T is the packet duration, the two transmitted packets will then be involved in a collision causing the reception of both packets to fail.

The probability of k packets occur at the receiver during a period of time t is given by:

$$P_{\mathrm{k}}\{t\} = \frac{\lambda^k e^{-\lambda t}}{k!} \tag{4.1}$$

where λ is the arrival rate (packet/s); hence, $1/\lambda$ (s) is the average packet inter-arrival time as packets are generated in accordance with the Poisson traffic model. The vulnerable

time, during which collisions are probable, is $2T$. Thus, the probability of a successful packet transmission during the vulnerable time can be obtained from Equation (4.1) by setting $t = 2T$ and $k = 0$ as follows:

$$\begin{aligned} P_0\{2T\} &= \frac{\lambda^0 e^{-\lambda 2T}}{0!} \\ &= e^{-2G} \end{aligned} \tag{4.2}$$

where G is the amount of traffic placed on the channel in Erlangs and on average $G = \lambda T$. From the above, the resulting useful throughput S represented in Erlangs can then be calculated as the multiplication of the offered traffic G and probability of success given by Equation (4.2) as follows:

$$S = Ge^{-2G} \tag{4.3}$$

From Equation (4.3), the maximum throughput can be deduced by finding the derivative of the throughput with respect to the offered traffic and setting it to 0. This results in the required offered load for maximum throughput being:

$$G = \frac{1}{2} \tag{4.4}$$

Therefore, the theoretical maximum throughput is 0.1835 Erlangs when the offered traffic is 0.5 Erlangs.

Slotted ALOHA: The throughput analysis of slotted ALOHA is quite similar to pure ALOHA. The only difference is the probability of collision and two additional assumptions:

- The system is perfectly synchronised.
- The length of a slot is set equal to the packet duration.

For a collision to happen, more than one packet must be received within the same time slot at the same receiver. By reconsidering Figure 4.1 (b), it can be seen that the collision interval is reduced to T rather than $2T$ since packets must overlap within the same slot. Therefore, the probability that a packet is successfully received is e^{-GT}, and the throughput for a given offered load becomes:

$$S = Ge^{-GT} \tag{4.5}$$

This gives a theoretical maximum throughput of 0.3679 of the channel capacity (0.3679 Erlangs) when the offered traffic is 1 Erlang. The predicted theoretical throughput characteristic of the two ALOHA Schemes will look like the curves depicted in Figure 4.2

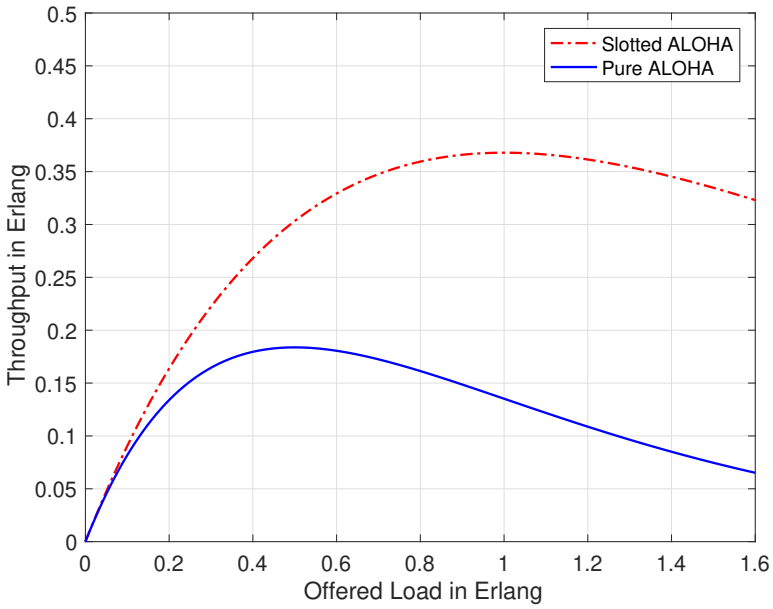

Fig. 4.2 Theoretical throughput characteristics for pure ALOHA and slotted ALOHA

4.3 Performance of Random Access Schemes Underwater

An underwater acoustic channel model has been developed in Riverbed Modeller for this study based on the acoustic channel factors described in section 2.7. It is used in this section to investigate the two ALOHA schemes through simulated underwater scenarios, in order to gain important insights and allow performance comparison with other schemes. In addition, this section enables better understanding of the modeller's pipeline stages by comparing simulation results with the theoretical ALOHA throughput performance derived in the previous section before moving on to consider other underwater scenarios.

4.3.1 Simulation Model of a UASN

Riverbed Modeller (RM) is a network protocol design and simulation tool, which can be used to simulate underwater scenarios. With respect to the underwater channel factors described in chapter 2, a number of the RM pipeline stages require adjusting or modifying to reflect the underwater propagation mechanisms. The fourteen RM pipeline stages, shown in Figure 4.3, are primarily designed for the radio channel, but they can be customised to implement other types of wireless communication links. At least four stages, the shaded blocks in Figure 4.3, must be modified. These pipeline stages are the propagation delay (stage 5), the background noise (stage 9), and the received power (stage 7). Stage 5 is used to set the desired speed of

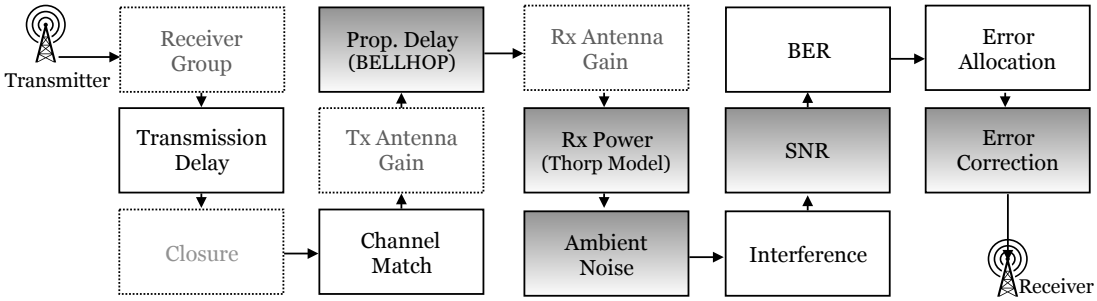

Fig. 4.3 Riverbed-based underwater acoustic channel

sound in water either as a fixed value representing the average speed (1500 m/s) [108] or as a vector containing a set of actual values extracted using the BELLHOP [36] acoustic field computation program based on a realistic underwater sensor deployment. Stage 7 is used to calculate the received power based on an empirical propagation model or also extracted using BELLHOP. Stage 9 is used to represent the level of background noise required. The undersea ambient noise is very often predicted using the set of empirical equations [109]. Some stages, lined with dashed lines in Figure 4.3, have been used with the default RM settings. They are concerned with creating an initial possible receiver group for each transmitter, computing Rx/Tx antenna gains and determining the closure between the transmitter and the receiver (i.e. the ability of physically establishing a link between a transmitter and its intended receiver, which is determined based on the intersections of this link with the earth's surface). Despite the fact that these stages are outside the scope of this study, they must be executed on a per-receiver basis whenever a packet is transmitted.

Based on these modified pipeline stages RM works out the signal to noise ratio (SNR) and Bit Error Rate (BER) values. Depending on these BER values the receiver decides whether to accept or ignore a received packet. The SNR stage computes the instantaneous SNR resulted in by the arrival of a packet at the receiver. This calculation is based on values obtained during the earlier stages including received power, background noise and interference. Due to new interference sources that may become active or inactive multiple times during packet reception, the SNR is re-evaluated for a given packet when the interference level changes. The portion of the packet arriving between two successive SNR updates is called a packet segment. During any given packet segment, the SNR holds a constant value. Following this, the BER stage obtains the probability of bit errors for each packet segment. This is not the empirical rate of bit errors, but rather the expected rate based on a look-up table and the SNR value. Then, the Error Allocation stage counts the number of bit errors in a packet segment over which the bit error probability has been calculated. The RM Kernel runs a bit-error accumulator. Finally, the Error Correction stage determines whether or not

the arriving packet can be accepted at the destination node. This is usually dependent on the result computed in the error allocation stage, but also on whether the packet has experienced a collision as a result of simultaneous packet arrivals from different sources, which should be determined earlier by the Interference stage. The acceptability test at the receiver is based on the number of bit errors occurring in the packet and the error correction threshold of the receiver and is done in this final stage. Moreover, the Interference stage determines any non-zero-length packet overlaps between successive arriving packets. If a non-zero-length overlap is detected, our modified Error Correction stage ensuring that the receiver rejects all packets involved in this overlap. Based on the determination of this final stage, the RM Kernel will either destroy the packet or allow it to proceed into the destination node.

The Simulated Acoustic Channel

As described in section 2.6, the underwater acoustic channel is characterised by a path loss that is dependent on both the transmission distance as well as frequency. Not only does the signal frequency determine the distance-dependent absorption loss, but also the ambient noise (see section 2.6). It can be seen in Figures 2.6 and 2.7 that the noise intensifies as the signal frequency is reduced, whereas the absorption loss rises as the signal frequency is increased for a given transmission range. To realistically model acoustic propagation and noise in our simulation, the Thorp model [38] has been used with a practical spreading value (k = 1.5), a moderate shipping activity (s = 0.5) and a relative wind speed (w = 10m/s) to estimate the noise p.s.d. N (f). Equation (4.6) below shows the Thorp empirical formula, used to estimate the attenuation coefficient $\alpha(f)$:

$$\alpha(f) = \frac{0.1f^2}{1+f^2} + \frac{40f^2}{4100+f^2} + 2.75\times10^{-4}f^2 + 0.003 \tag{4.6}$$

where $\alpha(f)$ is given in dB/km, f is the centre frequency of the transmitted signal, in units of kHz. The ambient noise is mainly made up of four major sources, i.e., turbulence $N_t(f)$, shipping $N_s(f)$, wind driven waves $N_\omega(f)$ and thermal noise $N_{th}(f)$. The p.s.d. is expressed usually in *dB re μPa per Hz* for underwater channels. The approximated empirical models shown below (4.7) - (4.10) are used to represent these sources respectively [1]:

$$10logN_t(f) = 17 - 30logf \tag{4.7}$$

$$10logN_s(f) = 40 + 20(s-0.5) + 26logf - 60log(f+0.03) \tag{4.8}$$

$$10logN_\omega(f) = 50 + 7.5\omega^{0.5} + 20logf - 40log(f+0.4) \tag{4.9}$$

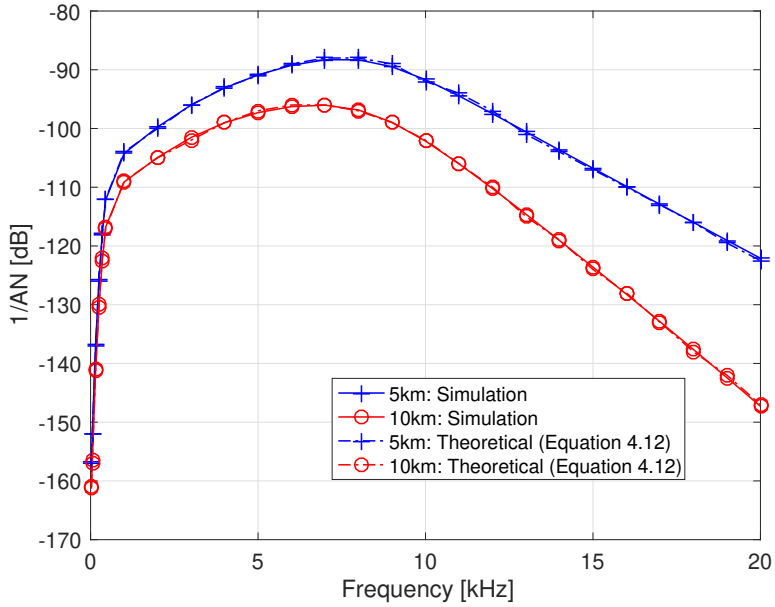

Fig. 4.4 SNR of the acoustic channel with different transmission ranges

$$10logN_{th}(f) = -15 + 20logf \tag{4.10}$$

It is clear from these equations that all these noise sources are frequency-dependent. The aggregate noise is calculated in μPa by:

$$N(f) = N_t(f) + N_s(f) + N_\omega(f) + N_{th}(f) \tag{4.11}$$

Using the absorption model (Equation (2.1) in chapter 2) and the noise p.s.d. N (f) (Equation (4.11)), the SNR experienced by each transmitted packet is evaluated to determine its eligibility for successful reception at its receiver. For simulation validation, the system SNR has been evaluated to observe this special relationship between bandwidth and transmission range. A signal of frequency f and transmission power P is transmitted over a distance l, and its narrow-band SNR can be given by:

$$SNR(l,f) = \frac{P/A(l,f)}{N(f)\Delta f} \tag{4.12}$$

where Δf is the narrow-band receiver noise bandwidth and $A(l,f)$ is the signal path loss given by Equation (2.1). The frequency-dependent part of the SNR, $A(l,f)N(f)$, is usually referred to as the AN product. This important design factor is illustrated in Figure 4.4 for several transmission distances. The figure shows the AN product extracted from the simulated

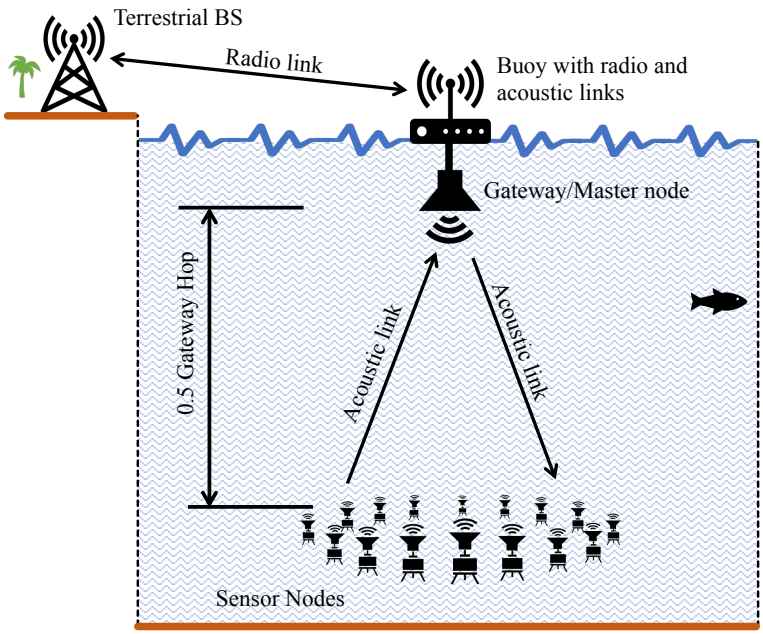

Fig. 4.5 A centralised UASN where a MAC protocol is employed to coordinate data transmissions from the underwater sensor nodes to the gateway that acts as a base station

Table 4.1 Acoustic channel simulation parameters

Attribute	**Description**	**Value**
Sound speed	average speed	1500 m/s
Attenuation	Thorp model - Equation (4.6)	k = 1.5
Noise	N (f) - Equation (4.11)	s = 0.5 & w = 10 m/s
Bandwidth	practical	10 kHz
Data Rate	EvoLogics S2CR	9600bps
Source power	practical	180 dB re 1uPa @ 1m
SINR threshold	practical	10 dB

acoustic channel with excellent agreement with Equation (4.12). More importantly, this figure is useful to help define the system optimal central frequency $f_o(l)$ and the actual channel bandwidth. For a given scenario, once the bandwidth is determined to some range around $f_o(l)$ denoted as $BW(l) = [f_{min}(l), f_{max}(l)]$, the system transmission power can be adjusted to attain the desired SNR value at $f_o(l)$.

Network Topology

With reference to Figure 4.5, different scenarios of 3 different network sizes (20. 50 and 100 nodes) have been studied. Sensor nodes are distributed randomly across a coverage

area of 6×6 *km*, using the simulator RM with a centralised 20 m depth gateway just above the central point of the coverage area. The depths of sensor nodes obey a uniform random distribution and are located between 470 and 490 m. The selection of these parameters corresponds to a typical oil reservoir seismic monitoring scenario, e.g. [110]. They have been chosen to be within the range of operating parameters of current commercial acoustic modems. For example, but not limited to, the EvoLogics S2CR 15/27 modem [111]. These scenarios can provide a range of different test options for performance evaluation of the random access schemes for the sake of new insights or comparison with other approaches in the literature. Table 4.1 summarises our UASN parameters.

ALOHA Scheme Simulation Models

Like any other RM project, both ALOHA models (pure and slotted) involve network, node, and process models. The network model consists of a number of terminals acting as transmitters forming a topology depicted in Figure 4.5, and one central terminal working as a receiver. A traffic generator is placed in each transmitter generating fixed-size packets specified as a simulation attribute. The traffic generators follow exponentially distributed packet interarrival times and operate independently contributing an equal amount of Poisson-distributed data traffic. Unlike the pure ALOHA model, the slotted ALOHA model incorporates transmission time slots. The transmission from each transmitter is deferred to the beginning of a time slot.

Table 4.2 Simulation parameters for ALOHA schemes

Simulation parameter	**Value**
Number of transmitting nodes	100
Number of receiving nodes	1
Transmission range	100m
Duration of simulation	5 hours
Results collected after	30 min
Packet duration	0.032
Packet size distribution	Fixed
Packet Interarival PDF	Exponential
Traffic Load Range	0.1 - 1 Erlangs

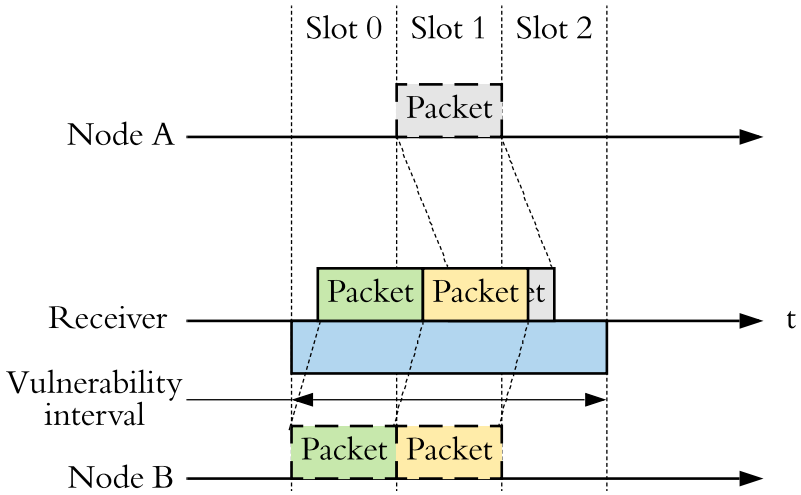

Fig. 4.6 Slotted ALOHA overlap underwater

4.3.2 Random Access Performance Evaluation with UASNs

Several simulations have been conducted to evaluate the performance of each ALOHA scheme, with the parameters defined in Table 4.2. Two interesting features in the throughput performance of the ALOHA schemes have been noticed in the simulated underwater-like environment. It has been found that the throughput of the pure ALOHA scheme is independent of the propagation delay. Despite the slow speed of acoustic wave propagation underwater (1500 m/s) and diversity of node locations, packets inter-arrival time at receiver side remains virtually consistent with the packet arrivals pattern at the corresponding transmitter. No matter how long the propagation delay is, it cannot fundamentally change the statistical distribution governing the inter-arrival time at the receiver. Variations in the propagation delay due to potential node location drifts are not considered at this stage (it is in chapter 6) as this random phenomena still cannot change the throughput performance of a random access scheme. The second interesting result is the dramatic change in slotted ALOHA throughput. It does not outperform the performance of pure ALOHA as it would do in the case of a traditional radio channel. This is attributable to the overlap between synchronised slots at the receiver as depicted in Figure 4.6. Packets transmitted by Node A within slot 1 can possibly collide with any packet transmitted by node B within slot 1, as well as any packet transmitted within slot 2. In the underwater context, pure slotted ALOHA performance is exactly the same as pure ALOHA except if the propagation delay is a multiple of the ALOHA slot interval. To understand this, it is necessary to look at packet arrival instants at the receiving node, instead of looking at packet transmission times at the transmitting node. Despite the fact that slotted ALOHA packets are meant to be sent within pre-defined time slots, there is no guarantee underwater that they will arrive in a timely manner with

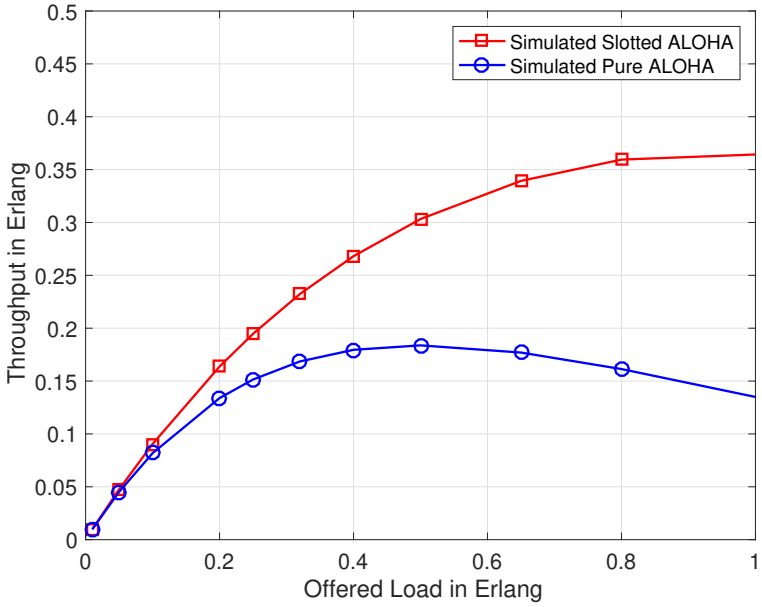

Fig. 4.7 Throughput performance of both ALOHA schemes with UASN

respect to the slots. Therefore, slotted ALOHA becomes equivalent to unsynchronised pure ALOHA except for the case when the division of transmission distance by the underwater sound speed can result in an integer number of time slots. The achievable channel utilisation for slotted ALOHA in underwater is dependent on node locations, propagations delays and slot durations. Practically, slotted ALOHA can be implemented by adding location-based transmission delay offsets long enough to enable arrivals within reception slots. Estimation of propagation delays can be made by one of the techniques described in section 3.3. By guaranteeing arrivals aligned with receiver-based slots in our simulations, Figure 4.7 illustrates the throughput performance of the pure ALOHA and adjusted slotted ALOHA schemes against a range of channel loads.

4.4 Free Assignment

The free assignment strategy is a TDMA-based scheme in which capacity is allocated without any form of request. In this strategy, capacity is not permanently guaranteed to a node, but rather an offered bonus, useful only if nodes happen to have data packets to transmit the instant a free assigned slot occurs. Assigning the available slots to nodes is usually done, one-by-one, based on a particular strategy such as round robin. The fundamental advantage of this strategy is its contention-free nature and the potential minimum delay that can be

coincidentally achieved if a free assigned slot arrives just after the arrival of a packet in an empty node queue. Its delay performance, however, is mainly dependent on the network size. If round robin assignment of slots is used then the larger the number of nodes is, the less regular the free assigned slots are. This will cause an increase in the aggregate end-to-end delay of packets. The efficiency of the scheme in handling variable traffic sources is based on the strategy used. Nonetheless, depending on the type of traffic, it must be more efficient than fixed TDMA in most of the cases as it does not guarantee permanent allocated capacity to each node without consideration for the node's status. With knowledge of propagation delays, nodes must adjust the start of their frames to ensure arrivals in a timely manner based on the free allocated slot.

4.4.1 Simulation Model of Pure Free Assignment

A simulation model of the round-robin-based free assignment scheme has been developed in the RM simulator. More details about the simulated model will be given in chapter 5, as this free assignment model is an underlying part of the versatile RM model of CFDAMA which is described in chapter 5. With respect to the UASN example depicted in Figure 4.5, the scheme has been evaluated with both the Poisson and self-similar (Pareto ON/OFF) data traffic models described in section 2.6. To enable comparisons with other capacity assignment schemes, the free assignment model has been developed with two universal frame formats presented in Figure 5.1. They are the forward frame (from the gateway to the sensor nodes) and return frame (from the sensor nodes to the gateway). Irrelevant frame components such as request and acknowledgement slots have been disabled. Through a suitable selection of simulation parameters that take into consideration underwater acoustic modems and applications, the scheme has been investigated. The parameters are given in Table 4.3 as well as the acoustic channel parameters given in Table 4.1.

Table 4.3 Simulation parameters for the pure round-robin free assignment scheme

Attribute	**Value**
Number of Nodes	20, 50 or 100
Data Slot Size	64 bit
Number of Data Slots in frame	100
Pareto $\alpha_{on}\alpha_{off}$	1.2
Pareto k_{on}/k_{off}	1
Traffic Load Range	0.1 - 1 Erlangs

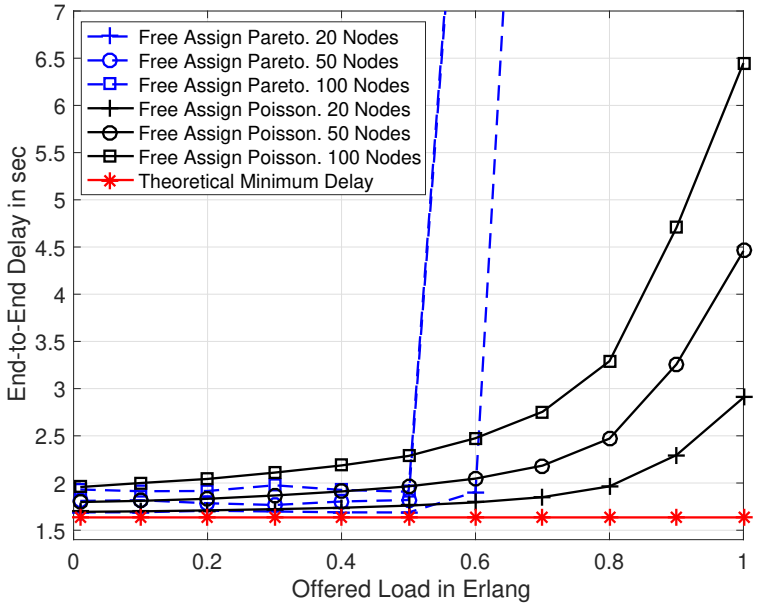

Fig. 4.8 Free assignment delay/utilisation performance

4.4.2 Free Assignment Performance Evaluation

Figure 4.8 shows the mean end-to-end delay values achieved by the free assignment scheme, against a range of channel load levels offered by 20, 50, and 100 nodes with both Poisson and Pareto ON/OFF traffic models described in section 2.7. The results show degradation in delay/utilisation performance as the channel load and/or the number of nodes increase. At low channel loads, the minimum mean end-to-end delay is achieved at low traffic loads with Pareto ON/OFF traffic. The reason is that the packet arrival rate is slower than the rate of assigning free slots in a round-robin fashion under these conditions. This means that the likelihood of transmitting every packet just after its arrival is very high. Whereas with Poisson traffic, the scenario is slightly different at this load level due to the fact that several packets could arrive between successive free slot allocations. Given the fact that the free assigned slots are evenly spread between packet arrivals over the course of simulation time, the delay distribution will be uniform as long as only a single packet arrives between two successive transmission slots. Hence, the mean end-to-end delay value will be proportional to the number of nodes as well as the average propagation delay between sensor nodes and their gateway. Whereas queuing delay is negligible at such low load levels owing to the slow packet arrival rate. The slight difference in performance between the two traffic types is attributable to their statistical behaviour, especially the ON/OFF nature and how often packets arrive within a burst.

When the channel loads exceed 50% of the channel capacity, each node will highly likely be receiving a burst requiring more capacity than that the round robin free assignment mechanism can provide. With Pareto ON/OFF, at this high load level, the free assignment scheme cannot adapt to the individual node requirements. Packets start to build up throughout all node queues in the system during ON periods for a potentially significant period of time. Hence, the mean end-to-end delay increases sharply becoming totally dependent on the statistical behaviour of the offered traffic. Despite that, the scheme is incapable of handling the increased burstiness of the Pareto ON/OFF traffic. It can also be seen that the scheme effectively supports Poisson data traffic, especially with small node population sizes, where the free assignment of slots on a round robin basis is more regular.

4.5 Demand Assignment

In the demand assignment strategy, nodes are allocated capacity in the form of slots responding to individual requests. The scheme allows a minimum bound on the end-to-end delay of 1.5 round trips, (a round trip for a capacity request and its corresponding acknowledgement plus at least 0.5 round trip for data packet transmission). There are two types of demand assignment, i.e. fixed rate and variable rate, based on how regular the capacity allocation is updated.

With the fixed rate demand assignment, whenever a connection is required by a node, it makes a request. If the request is successful then the node starts to receive a frequent allocation of time slots for exclusive use over the duration of the connection. When the connection ends, the scheduler must be notified by the node, allowing the capacity to be released for use in other connections. Figure 4.9 illustrates the operation of the fixed rate demand assignment. Despite its suitability to discrete-connection-based applications, this variant is inefficient for variable bit rate traffic due to the fixed allocation of capacity which cannot accommodate varying node demands. With variable rate demand assignment, allocation of capacity is more dynamic. This variant is commonly employed to accommodate all types of traffic in which the capacity requirement rapidly varies over time. An illustration of the mechanism of this variant is shown in Figure 4.10. As the figure shows, nodes regularly make requests for capacity based on their instantaneous requirements. The requests are made for a specific number of slots sufficient to serve all packets waiting in their queue at the time. The ability to handle instantaneous node requirements allow this strategy to achieve high channel utilisation. However, the long propagation delays associated with underwater acoustic links limits the achievable end-to-end delay. By the time capacity requests reach the scheduler, the status of node queues could become different, restricting the ability of the

scheme to accurately respond to instantaneous capacity requirements. It can be concluded that both demand assignment variants require a request mechanism. The available time in this strategy is divided into frames, and a proportion of every frame is reserved for request slots as shown in Figure 4.9 and Figure 4.10. A suitable access strategy is required to enable fair access to the request slots. This brings about a secondary medium access issue. Typically, they are assigned to nodes on a fixed, round robin or random access basis. Again, for the same reasons of slotted ALOHA, all frames must be deferred according to nodes locations to allow packet arrivals in a timely manner at the receiver. chapter 6 address the issue of frame timings in detail.

4.5.1 Simulation Model of Pure Demand Assignment

A model of the pure variable rate demand assignment scheme has been developed to form the second underlying part of the RM versatile model of CFDAMA model. Details of the whole model are provided in section 5.1. Through a selection of the parameters suitable for underwater communication modems and applications, the model has been utilised to investigate the performance of demand assignment. The two frame formats (return and forward frames) are similar to those used with the pure free assignment scheme. The only additional regions in the frames is a round-robin request slots region at the beginning of the return frame and its corresponding acknowledgement region in the forward frame (see Figure 5.1 showing the standard CFDAMA frame structure). The model has been simulated to work in accordance with the UASN scenario presented in Figure 4.5 with both Poisson and Pareto ON/OFF data traffic types. Simulation parameters can be seen in Table 4.3, with

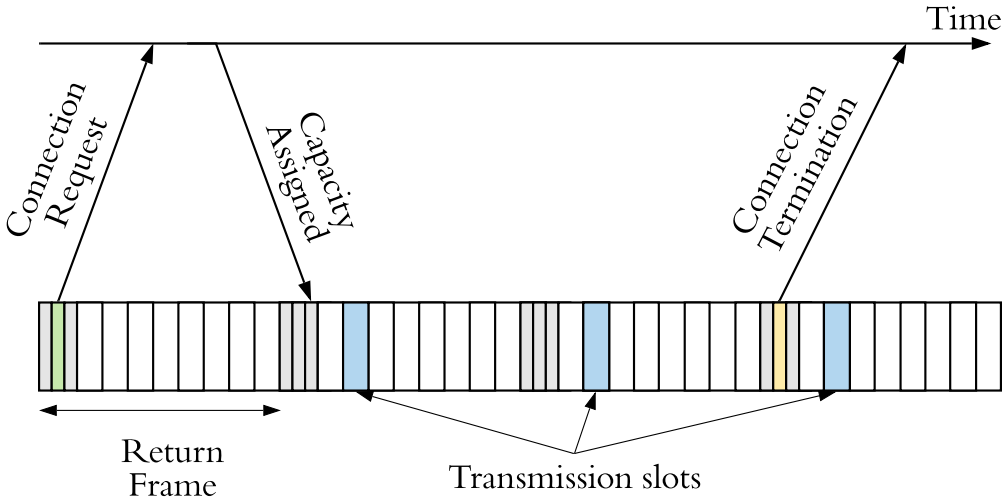

Fig. 4.9 Fixed rate demand assignment

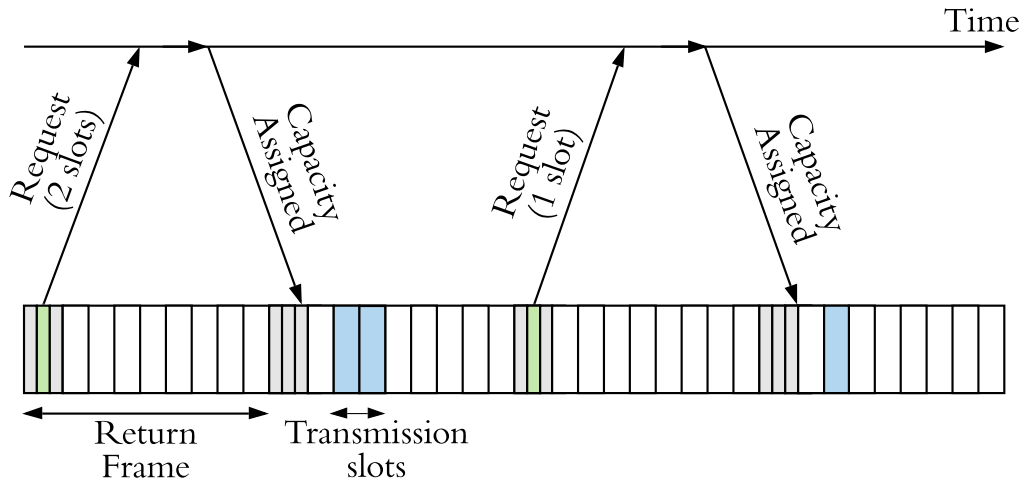

Fig. 4.10 Variable rate demand assignment

Table 4.4 Simulation parameters for the pure round-robin demand assignment scheme

Attribute	**Value**
Request Slot Size	8 bit
Number of Request Slots in Frame	10, 25, 50

some additional parameters given in Table 4.4 as these are not required in the case of pure free assignment.

4.5.2 Demand Assignment Performance Evaluation

The mean end-to-end delay values achieved by the pure demand assignment scheme is shown in Fig. 4.11 against a range of channel load levels offered by 20, 50, and 100 nodes with both Poisson then Pareto ON/OFF traffic types.

The results show that the delay/utilisation performance of the strategy is heavily dominated by the inevitable lower delay bound of 1.5 round trips. The scheme exhibits an advantage of stability and generally low variation in the mean end-to-end delay regardless of the channel load level. This can be understood by considering the scheme mechanism. Each node is consistently provided with regular and periodic opportunities to make requests if needed. This maintains a quite frequent and smooth slot allocation process owing to the direct mapping of requests to slot assignments at the scheduler. The observed linearity is attributable to this consistent behaviour of slot allocation based on individual node requirements. When the channel load rises, the packets start to build up at node queues and the size

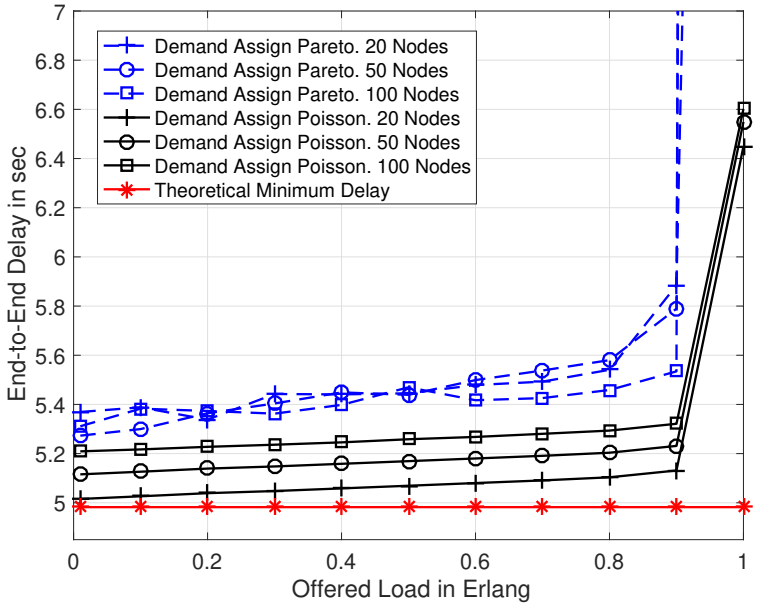

Fig. 4.11 Demand assignment delay/utilisation performance

of requests increases. This will also extend the length of consecutive slot allocations to each node increasing the mean end-to-end delay by a small amount at very high loads.

The performance of the demand assignment scheme is virtually independent of the data traffic characteristics whether it is periodic or exponential. Mainly because of the provision of regular and guaranteed request opportunities no matter how short the packet inter-arrival times are or how long the burst is. The ability of demand assignment to maintain a high channel utilisation level is guaranteed by the dynamic allocation of capacity in response to instantaneous requirements. The results show a dramatic rise in delay for the 100-node scenario of Pareto ON/OFF traffic at 85% channel load. This is because of the statistics of Pareto ON/OFF data traffic which produce a longer period of time during which the number of nodes generating bursts exceeds a certain sustainable number. If a long burst of packets is generated from a Pareto ON/OFF source, the request opportunities will be infrequent, and therefore, a substantial number of packets would start to build up at the node's queue. This will then result in a significant demand by this node and subsequent slot allocations, which means the node will dominate the return frame for a significant period of time, blocking other nodes from making their requests. All this will eventually cause a dramatic increase in the mean end-to-end delay at very high channel loads. The scheme achieves operational end-to-end delay performance constrained by the minimum end-to-end delay boundary of 5.1s.

4.6 Conclusions

This chapter assesses the performance of MAC schemes integrating one of the fundamental capacity assignment strategies (i.e. random access, free assignment, or demand assignment) through simulated underwater scenarios. Simulation results enable some useful insights into the functionality of each assignment method and assist the development of new underwater schemes. It provides the necessary understanding of the capability of each scheme in achieving adequate delay/utilisation performance under the conditions of both Poisson and Pareto ON/OFF traffic types over a simulated underwater acoustic link.

The free assignment scheme is a simple and very reliable technique that is capable of providing end-to-end delay values just above 0.5 round trip time at low channel loads and with a moderate number of nodes. This excellent performance is shown to degrade as the number of nodes increases due to the increased time between successive allocated slots. With Poisson traffic, the scheme maintains good delay performance over almost the entire range of channel loads, but with Pareto ON/OFF data traffic, the scheme is much less capable to effectively cope with high channel load levels. This is attributable to the increased burstiness of the traffic source and the incapacity of the scheme to support varying allocation mechanism in response to different nodes short-term requirements.

The demand assignment scheme is shown to be able to provide a very high channel utilisation level for both channel traffic models Poisson and Pareto ON/OFF. The reason behind that is the adaptive way of allocating capacity effectively in response to fluctuations in demand. With guaranteed and regular request opportunities the scheme's delay performance remains similar over almost the entire channel load range irrespective of the source traffic characteristics. The disadvantage, however, is a low end-to-end delay boundary of 1.5 round trips.

CFDAMA, which is introduced in the next chapter, combines all these schemes together in order to optimise their complementary advantages. With demand assignment achieving a high maximum channel utilisation level, and free assignment maintaining practical delay performance, channel traffic conditions permitting, combined schemes can strike a balance between the mean end-to-end delay and channel utilisation. Slotted ALOHA, on the other hand, is capable of providing rapid channel access with poor throughput performance. This drawback suggests that the slotted ALOHA scheme can be the choice for packets that are less important than data packets. It can be used for request packet transmissions to act as a random-access request strategy. More details about different request strategies will be provided in chapter 5.

Chapter 5

CFDAMA Schemes for UASNs

5.1 Introduction

This chapter gives a detailed description of the Combined Free/Demand Assignment Multiple Access (CFDAMA) scheme. It describes its scheduling algorithm and frame structures. For a range of simulated underwater scenarios, it investigates a number of underlying request strategies. The primary purposes of this chapter are:

- To evaluate the performance of CFDAMA in the context of UASNs.
- To provide guidelines to help to choose amongst several CFDAMA variants.
- To propose a new CFDAMA arrangement advancing its effectiveness.
- To lay the foundations for new underwater-specific CFDAMA variants.

To the best of the author's knowledge, this is the first study to propose and describe the implementation of CFDAMA as a MAC protocol for UASNs. The work presented in this chapter has led to new insights and further enhancement to the performance of CFDAMA underwater, which has resulted in a number of publications [105] and [112].

CFDAMA was originally proposed by Le-Ngoc for satellite systems [113]. The scheme combines two fundamental capacity assignment schemes, i.e. free assignment and demand assignment addressed in chapter 4. CFDAMA has several fundamental variants introduced by Le-Ngoc and other enhanced variants introduced by Mitchell in [114] and [115]. It must be highlighted that all those CFDAMA variants have been proposed for satellite systems that are composed of relatively powerful terminals, e.g. satellite and base stations. Implementing an existing CFDAMA variant in a network that is composed of battery-powered sensors communicating acoustically in a harsh environment with severe constraints, requires careful

examination and adaptation. The use of acoustic waves to communicate underwater places constraints on the functionality of MAC protocols (described in detail in chapter 3). We are motivated by the excellent ability that CFDAMA shows in meeting similar challenges in satellite systems.

The CFDAMA frame formats and other simulation model details are provided in section 5.2. The CFDAMA scheduling algorithm that is common across the CFDAMA variants is described in section 5.3. A discussion of the fundamental behaviour and properties of CFDAMA variants follows in section 5.4. Sections 5.5 and 5.6 introduce detailed investigation and performance evaluation of individual request strategy and combined request strategy schemes respectively. Section 5.7 introduces a new CFDAMA arrangement suited to UASNs. Section 5.8 summaries the chapter and provides a conclusion.

5.2 Simulation Model Implementation Details

An integrated set of simulated models are developed in the Riverbed Modeller for this study, enabling the implementation of all CFDAMA variants involved in this study as well as their two underlying capacity assignment schemes. This approach of using a versatile simulation platform allows more convenient performance comparison between the different capacity assignment schemes and enables switching between several request strategies as required. The general return and forward CFDAMA frame structures are depicted in Figure 6.3. These are generic formats, and the relevant frame components are activated based on the desired variant and request strategy. With respect to the UASN scenario illustrated in Figure 5.3, the return frame is for transmissions from sensor nodes to the master node (gateway) on the multiple access return channel. The forward frame is for the opposite transmissions from the gateway to the sensor nodes. Both frames are made up of two segments: a data slot segment plus a segment of request slots in the case of the return frame. Whereas, the forward frame comprises a segment of acknowledgement slots plus an optional data slot segment if required. The utilisation of data slots is a common feature in all CFDAMA variants, whereas the utilisation of request slot regions depends on the requirements of the request strategy. Capacity is allocated to nodes either as free assigned slots (F) or demand assigned slots (D). Request packets are transmitted in the request slots on the return frame and are subsequently acknowledged in the acknowledgement slots of the forward frame. The forward frame is delayed with respect to the return frame by a period long enough to allow the request packets that are received in the return frame to be immediately processed and acknowledged with assignments in the forward frame. The exact frame formats and the number of requested slots depend on which request strategy is used. Each node is responsible for aligning the

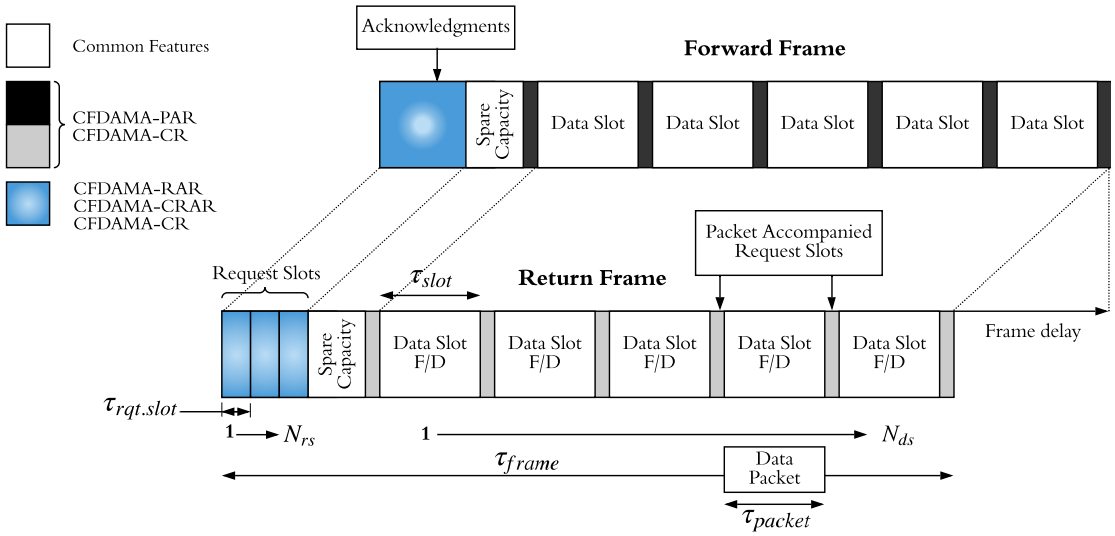

Fig. 5.1 The general format return and forward CFDAMA frames

arrival of its packet with the beginning of its allocated slot by adding an appropriate time offset to its transmissions. Nodes must synchronise their built-in clocks with the master node's clock. In practice, propagation delays need to be estimated in order to attain this synchronisation. Typically, this estimation of the long and time-variant propagation delay of acoustic waves is dealt with using a handshake technique [2] as described in section 3.3. Spare capacity is inserted in both frames to make their lengths equal for simplicity. Guard intervals between slots can also be added to prevent any potential packet collisions caused by inaccurate synchronisation.

5.3 CDAMA Scheduling Algorithm

As described in chapter 3, the constraint that long and time-variant underwater acoustic propagation delays place on the functionality of MAC protocols supports the argument that the most feasible and applicable approach for scheduling-based MAC protocols is the use of "a global scheduler". With reference to Figure 5.3, the CFDAMA scheme by default relies on a centralised scheduler. The gateway as a master node can use its location advantage and extra processing capabilities to facilitate scheduling requirements. CFDAMA scheduling is performed using two serving tables operating at the gateway. They are known as the free assignment table and the reservation request table. The function of the reservation request table is to maintain a first-input-first-served queue of capacity requests made by sensor nodes. As requests are made, this table is updated to keep track of the identity (ID) of the requesting node and the corresponding number of slots needed. In the meantime, the other table keeps a

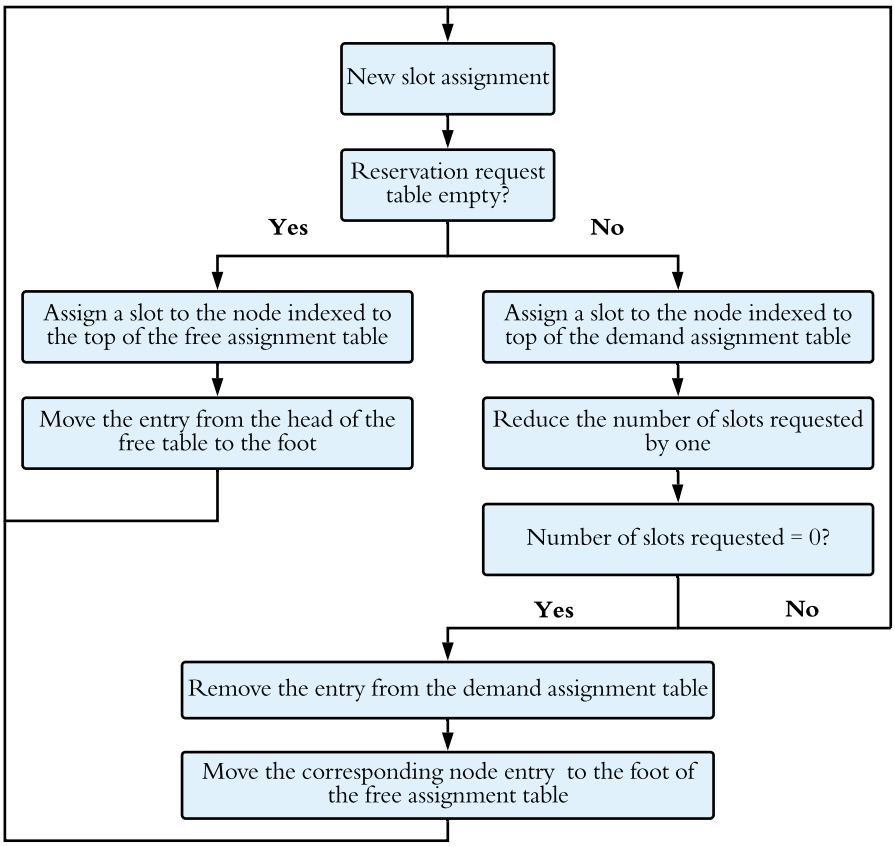

Fig. 5.2 CFDAMA scheduling algorithm

list of the IDs of all active sensor nodes in the network. The scheduler switches between the two tables according to the algorithm depicted in Figure 5.2. On a frame-by-frame basis, the central gateway exchanges information with its peripheral sensor nodes about the allocations and scheduling information as appropriate. The cycle starts when a request is made. The scheduler informs the sensor nodes of their allocations in a Time Division Multiplex (TDM) fashion on the forward frame. Slots are initially assigned using the demand assigned mode, according to the entries in the reservation request table. Once all requests waiting in the queue have been dealt with, the scheduler then switches to free assignment mode and starts freely assigning remaining slots to nodes in a round robin fashion. This is made by assigning a set of successive slots, one after another, to the nodes whose IDs are, at that moment, waiting at the top of the free assignment table. Following each slot allocation, each served node-ID is dropped to the bottom of the table. This approach maintains fairness between nodes. Likewise, each time a node is allocated demand assigned slots and is omitted from the reservation request table, its ID is also moved to the tail of the free assignment table.

5.4 Fundamental CFDAMA Characteristics

By combining two capacity assignment strategies, the CFDAMA scheme is seen as a means of providing a low end-to-end delay for packet transmissions and a high channel utilisation capability. The scheme combines the free assignment and demand assignment strategies. In the free assignment, capacity is assigned without any form of request and is essentially bonus capacity granted to nodes, which will be used only if they coincidentally have data packets ready for transmission at the instants when free assigned slots occur. This strategy has mainly two fundamental advantages: its contention-free nature plus the minimum end-to-end delay. It can be achieved when the packet to be transmitted arrives at the instant of an empty node queue ahead of it. The delay performance, however, is mainly a function of the network population size. A large number of nodes will make it less regular for slots to be freely assigned, due to the fact that the free slot assignment is made using a round robin method, and therefore, this increases the average end-to-end delay. In the demand assignment strategy, nodes can make requests for capacity as needed. Capacity is allocated in the form of slots, according to individual requests which helps achieve a high maximum of channel utilisation. The price for this will be a minimum end-to-end delay of 1.5 round-trip even at low channel loads (a round-trip for a capacity request and the following slot assignment plus half a round-trip for the data packet transmission). An appropriate request segment is inserted into a frame to enable this access strategy. This requires a consequent MAC solution, which is another advantage as CFDAMA can adapt to different network requirements with different request strategies. Later in chapter 6, an analytical model is developed for our proposed CFDAMA variant. However, this section develops a model that incorporates the dominant factors which contribute significantly in determining the average end-to-end delay of packets. The delay caused by queuing is not included, not only because of the fact that with Poisson traffic and long propagation delays, queuing is not very significant but also for simplicity. Each successfully received packet must have gone through one of three possible scenarios:

- Scenario 1, in which packets get through by the use of free assigned slots.
- Scenario 2, in which a packet succeeds via a slot requested for a previous packet from the same node.
- Scenario 3 in which a packet succeeds via a slot requested and granted for itself.

The end-to-end delay of a packet will depend on the scenario it experiences. With respect to Figure 6.3 and Figure 5.3, and considering a packet's behaviour in Scenario 1, the mean end-to-end delay $E[D_{eted}]$ experienced by a packet arriving at an empty sensor node's queue

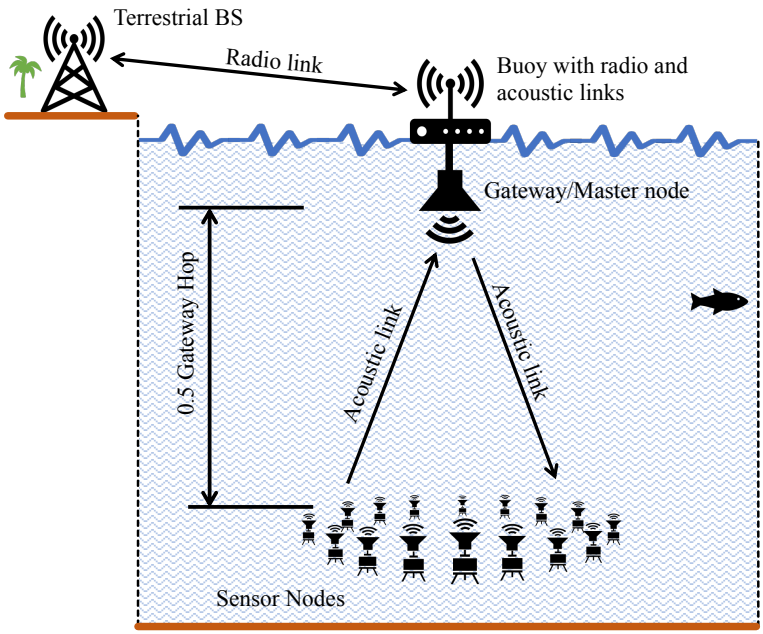

Fig. 5.3 En example of node deployment conceived for the simulated UASN scenarios

is the combination of three terms:

$$E[D_{eted}] \approx \frac{N\tau_{slot}}{2} + 2\tau_{packet} + \tau_p \tag{5.1}$$

The first term represents the average time a packet needs to wait until the next transmission slot, where N is the number of sensor nodes and τ_{slot} is the data slot duration. The second term is related to the time needed for the packet transmission at the sensor node and the consequent reception at the master node which is dependent on the packet duration τ_{packet}. The third term accounts for the aggregate propagation delay which is τ_p (the propagation time needed for a packet to travel to/from the gateway). At high channel load levels, nodes demand more capacity and therefore have to make a larger number of capacity requests more frequently. The protocol then will run with a much higher proportion of demand assigned slots (Scenario 3) causing an increase in the delay for packet transmissions. Incorporating the frame duration τ_{frame}, the mean end-to-end delay of Scenario 3 can be expressed as follows:

$$\begin{aligned} E[D_{eted}] &\approx \frac{\tau_{frame}}{2} + 3\tau_{packet} + 3\tau_p \\ where \quad \tau_{frame} &= N_{ds}\tau_{slot} + N_{rs}\tau_{rqt.slot} \end{aligned} \tag{5.2}$$

Based on the state of the sensor node queues, the average end-to-end delay will be gradually moving between its two extremes, i.e. the low extreme, which is experienced during Sce-

nario 1 and its mean given by Equation 5.1 and the high extreme, which experienced during Scenario 3 and its mean given by Equation 5.2. Scenario 2 will dominate over the other two extreme scenarios when the traffic load is moderate.

5.5 CFDAMA Variants Suitable for UASNs

The key idea in CFDAMA is that in every terminal, a sufficient number of slots must be requested upon the arrival of a request slot, taking into account two factors: the number of outstanding requests (slots that have been requested and have yet to be assigned) and the number of packets waiting currently in the node's queue. The number of slots requested each time must be sufficient to take the current queue size down to zero. A number of CFDAMA schemes have been proposed over the years; and each scheme implements a certain request strategy to form a specific CFDAMA variant. The original CFDAMA variants which are introduced by Le-Ngoc for satellite systems [113], [116] include:

- CFDAMA with Fixed Assigned requests (CFDAMA-FA).
- CFDAMA with Piggy-Backed requests (CFDAMA-PB).
- CFDAMA with Random Access requests (CFDAMA-RA).

Following that Mitchell in [114], [115] introduces some new and modified variants from Le-Ngoc's schemes for further performance improvement for geostationary satellite systems. The newer CFDAMA variants include:

- CFDAMA with Controlled Random Access Requests (CFDAMA-CRAR).
- CFDAMA with Packet Accompanied Requests (CFDAMA-PAR).
- CFDAMA with Round Robin strategy (CFDAMA-RR).
- Combined Request strategy scheme (CFDAMA-CR), combining both PAR and CRAR.

It is desirable to run MAC schemes at levels of channel utilisation close to the channel capacity, maintaining the highest quality of service. Hence, the traditional key factor when comparing the performance of CFDAMA request strategies is their achievable channel utilisation. To this end, the combined request strategy is shown to outperform the alternative request strategies in satellite systems. In the context of underwater systems, there are other factors which are not less important than channel utilisation when making a distinction between the request strategies. Complexity and fairness amongst nodes are key factors. The peculiarity

of the underwater environment narrows down the list of feasible CFDAMA variants. For reasons described in this section, we argue that the single CFDAMA request strategies are more practical and suitable for UASNs, especially CFDAMA-PAR and CFDAMA-RR. The combined request strategy may be overly complex for battery-powered sensor nodes communicating acoustically in the harsh underwater environment with all the constraints described in section 3.3.1. However, based on the affordable level of system complexity, CFDAMA-CR can enable further development and improvement of the fundamental request strategy performance.

The section provides guidelines to help to choose amongst the CFDAMA request strategies. It investigates and evaluates the performance of those CFDAMA variants for a number of underwater scenarios, with different sensor node population sizes and data packet durations. It presents a comparative performance evaluation based on end-to-end delays and channel utilisation. End-to-end delay performance is presented in term of both its mean values and cumulative distribution functions (CDF) of all packet delay values. The section underlines the suitability of the alternative variants to two traffic types (Poisson and Pareto ON/OFF). It also points out their fundamental limitations for UASNs, with thoughts and mechanisms to improving and stabilise their performance for a wide range of underwater scenarios.

5.5.1 CFDAMA with Packet Accompanied Requests (CFDAMA-PAR) strategy

CFDAMA with Packet Accompanied Requests (CFDAMA-PAR) is introduced in [114] as a slightly adjusted version of the CFDAMA-PB scheme which is introduced in [117]. Both versions are proposed for satellite systems. The slight difference between the two versions is in their treatment of data packets. Whilst CFDAMA-PB piggy-backs requests for capacity onto data packet themselves, CFDAMA-PAR adjoins request slots with data slots in the return frame. The CFDAMA-PAR return frame format is depicted in Figure 5.4. Piggy-backed requests may require the utilisation of variable sized data packets, which is not the case with CFDAMA-PAR where data packets are not changed. In CFDAMA-PAR, capacity requests accompany their data packet transmissions and the access to a particular request slot is limited to only the node that transmits in the adjacent data slot. Thus, if a node happens to make a request, its request packet will be adjoined with its data packet transmission in two adjacent slots. The number of slots requested is given by:

$$N_{rs} = [N_{PQ} - 1] - N_{OR} \tag{5.3}$$

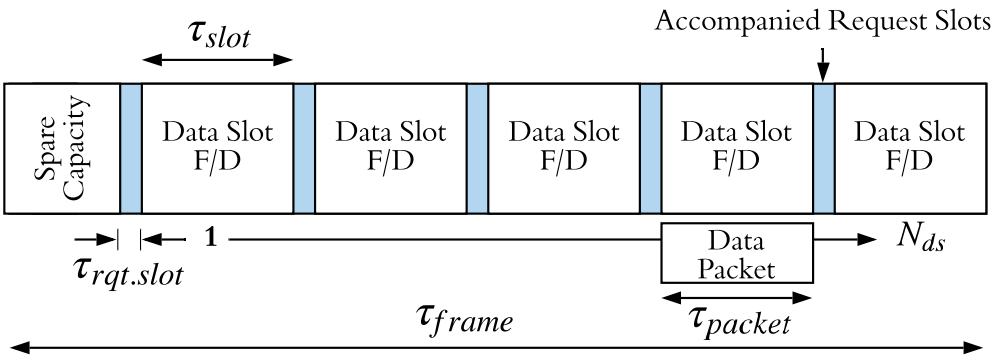

Fig. 5.4 CFDAMA-PAR return frame

This kind of strategy will let one of the queued packets be transmitted in the allocated slot, and therefore, the number of remaining packets in the queue should be dropped by one: $N_{PQ} - 1$.

The foremost advantage of this strategy is that it enables a contention-free request mechanism with a bounded delay to receive requests. In the context of underwater systems, we argue that this strategy can smoothly work with the existing underwater TDMA protocols such as TDA-MAC and STUMP. In order to achieve this combination, capacity requests need to be piggy-backed or accompany the data packets, while transmissions can be coordinated based on the underwater TDMA protocol adopted. Chapter 6 shows the performance of CFDAMA-PB with TDA-MAC, enabling a new CFDAMA variant operating without a global clock synchronisation. This increases the practicality of this strategy underwater.

The key limitation of the strategy is the possibility for a few nodes to dominate the return channel by repeatedly requesting capacity, which will potentially inhibit other nodes from accessing the channel for either data packet or request packet transmissions. This issue might become even worse under certain underwater conditions when the channel is busy with heavy and frequent access demand. This potential limitation suggests that CFDAMA-PAR may be suitable for certain underwater scenarios in which traffic levels are moderate. The next section evaluates the performance of this variant for different underwater scenarios.

Performance investigation of CFDAMA-PAR

The versatile simulated CFDAMA model outlined in the introduction of this chapter is configured to operate in accordance with the CFDAMA-PAR scheme functionality. With respect to the underwater scenario of uniformly distributed sensor nodes forming a ring topology as illustrated in Figure 5.3. Table 4.3 lists the parameters of the simulated acoustic channel. With respect to the return frame depicted in Figure 5.4, Table 5.1 lists all the remaining parameters.

Table 5.1 Simulation parameters for the CFDAMA-PAR assignment scheme

Attribute	**Value**
Transmission Range	$6 \times 6\ km$
Number of nodes	20, 50 or 100
Topology	see Figure 5.3
Number of data slots (N_{ds})	650
Request slot size	8 bit
Data slot size	64 bit
Packet size	64 bit
Pareto $\alpha_{on}\alpha_{off}$	1.2
Pareto k_{on}/k_{off}	1
Traffic load range	0.1 - 1 Erlangs

Figure 5.5 shows the mean end-to-end delay performance in seconds against a full range of channel loads in Erlangs, with three different network population sizes (i.e. 20, 50, and 100 nodes) and two data traffic types (i.e. Poison and Pareto ON/OFF). At low channel load levels and with both traffic types, the scheme has a steady mean end-to-end delay developing gradually just above the minimum possible bound of 0.5 gateway hop (that is the round trip from sensor nodes to the gateway - see Figure 5.3). When the offered load is within 50% of channel capacity, the scheme can comfortably operate with only the fundamental free assignment scheme. The reason behind that is the average rate at which the free assigned slots arrive outweighs the average rate at which data packets arrive. Under these conditions, every sensor node's queue is cleared regularly as each packet can be transmitted in the first free assigned slot following its arrival. Hence, requests for demand assigned slots are very infrequent. The stability of mean end-to-end delay is attributable to the consistent successive slot allocations in coexistence with the packet arrivals alongside the increase in channel load level from 0.1% to 50% of channel capacity. However, it can be seen that the mean end-to-end delay is slightly greater with Poisson than with Pareto ON/OFF at such low channel levels. This is attributable to the periodic ON/OFF nature of the traffic source and how often the packet arrivals within a burst are. In this instance, the uniform regularity of a low periodic traffic ON/OFF source leads to that every packet will have a higher chance to be transmitted in the first free allocated slot just after its arrival. Whereas, with Poisson traffic, the scenario is different where several packets could arrive between successive free slot allocations in some cases leading to a longer waiting time until the next free assigned slot arrives; meanwhile, a request for demand assigned slots will potentially be made. For the same aforementioned reasons, the increase in the number of nodes has a low impact on

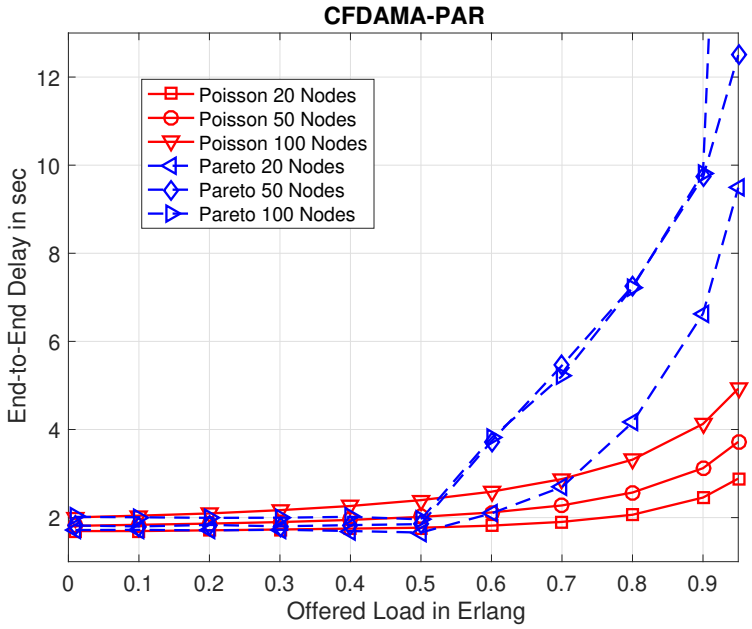

Fig. 5.5 Mean end-to-end delay as a function of channel load for CFDAMA-PAR with Poisson and Pareto ON/OFF traffic sources, 64-bit packets, and several numbers of nodes

the mean end-to-end delay when the channel load levels are less than 50% of the channel capacity.

As channel load level exceeds 50% of the channel capacity, the scheme starts to gradually switch to the demand assignment scheme, which eventually dominants over the free assignment scheme at high channel load levels, and this domination becomes even clearer with a greater number of nodes. As a result, over the course of channel load levels from 50% to 100% of the channel capacity, the scheme performance is influenced by an increasing proportion of demand assignment. Hence, the mean end-to-end delay increases rapidly and at some point overshoots the minimum traditional DAMA delay bound of 1.5 gateway hops (see section 4.5). It can also be seen that the end-to-end delay is much higher with Pareto ON-OFF traffic because of the greater burstiness of the ON-OFF data traffic. This is because of the statistics of the Pareto ON/OFF data traffic which produce a longer period of time during which the number of nodes generating bursts exceeds a certain sustainable number. When a long burst of packets is generated from a Pareto ON/OFF source, a substantial number of packets will start to build up in the node's queue. This results in significant demand by this node and subsequent slots allocation. It means that a node may dominate the return frame for a significant period of time. All this eventually causes a dramatic increase in the mean end-to-end delay at very high channel loads.

The results show that CFDAMA-PAR in general exhibits high delay/utilisation performance. It can enable a high channel utilisation level with a practical mean end-to-end delay at up to 95% channel load. Beyond this limit, the performance is unstable due to the inability of the scheme to cope with any more instantaneous traffic changes above the average. The performance, however, becomes poorer at both the high channel load levels of Pareto ON/OFF and a high number of nodes. In the next section, the performance of the scheme will be put side by side with the performance of CFDAMA-RR to investigate this drop in the performance in more detail.

Figure 5.6 shows the Cumulative Distribution Function (CDF) of the end-to-end delay of packet transmissions at two channel load levels (30% and 70%) offered by 100 nodes and with both traffic models (Poison and Pareto ON/OFF). At 30% channel load and with both traffic types, the end-to-end delay has gradually increasing values. This is attributable to the fact that packets are transmitted through free assigned slots promptly following their arrivals which happens uniformly between successive free assigned slots. It can be seen that at this level of channel load, 100% of the packets experience minimum end-to-end delays just above a 0.5 round trip delay.

At 70% channel load, the free assigned slots are unable to accommodate the increasing number of packet arrivals, causing the scheme operation to be dominated by demand assigned

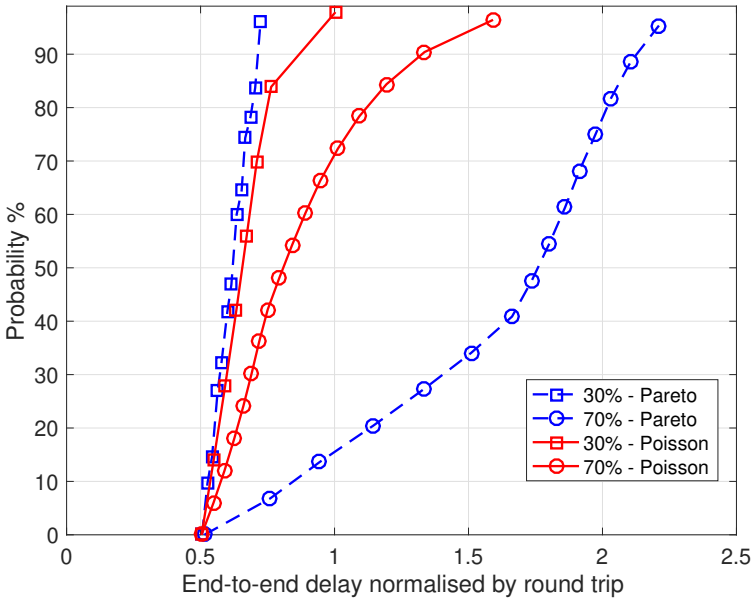

Fig. 5.6 Cumulative distribution function of end-to-end delay for CFDAMA-PAR with Poisson and Pareto ON/OFF traffic sources, 64-bit packets, and 100 nodes at 30% and 70% channel loads

slots, especially with Pareto ON/OFF traffic. Therefore, 65% of packet transmissions of Pareto ON/OFF have an inevitable minimum end-to-end delay of 1.5 gateway hops due to the excessive use of demand slots. In spite of the fact that under this condition the scheme operates with a predominately demand assignment, it can be seen that the free assigned slots are still used. At a 70% load level, it takes longer to obtain a free assigned slot with both traffic types. This leads to longer waiting time at the node's queue, and the number of packets in the queue by the time a free assigned slot occurs will be larger. This will require nodes to make larger requests which subsequently blocks the return frame for longer periods of time, making free assigned slot arrivals even less regular and thereby increasing the delay.

5.5.2 CFDAMA with Round Robin Requests (CFDAMA-RR) strategy

CFDAMA with Round Robin requests (CFDAMA-RR) are originally introduced to get around the limitations of the Random Access, Packet Accompanied and Combined Request strategies, and to maintain unbiased access rights for all nodes. To maintain fairness between nodes in accessing the channel, the CFDAMA-RR scheme eliminates the possibility of losing the channel due to contention between nodes or channel domination by transmitting nodes. It uses the round robin technique to assign request slots to individual nodes. Therefore, nodes cannot be inhibited by other nodes from making requests, and the scheme is contention less. Owing to its simplicity and fairness, CFDAMA-RR is shown to be a good choice for a wider range of underwater scenarios. More importantly, it has the potential to be developed to a more underwater-specific CFDAMA variant that is introduced in chapter 6.

CFDAMA-RR devotes a region located at the start of the return frame to round robin request slots as shown in Figure 5.7. This particular format allows more equality in accessing request lots. Each sensor node will have to wait for its round-robin turn to make a request, if required, on a frame-by-frame basis. The number of slots to be requested is given by:

$$N_{rs} = N_{PQ} - N_{OR} \tag{5.4}$$

Where N_{rs} is the number slots requested, N_{PQ} is the number of packets queued and N_{OR} is the number of outstanding requests. Under certain conditions, CFDAMA-RR can be more suitable for particular UASN scenarios than others. The number of request slots must be carefully chosen for a given number of nodes. The scheme has three fundamental features:

- Its delay performance is heavily dependent on the number of nodes; gaining access to the channel becomes less regular as the number of nodes increases.

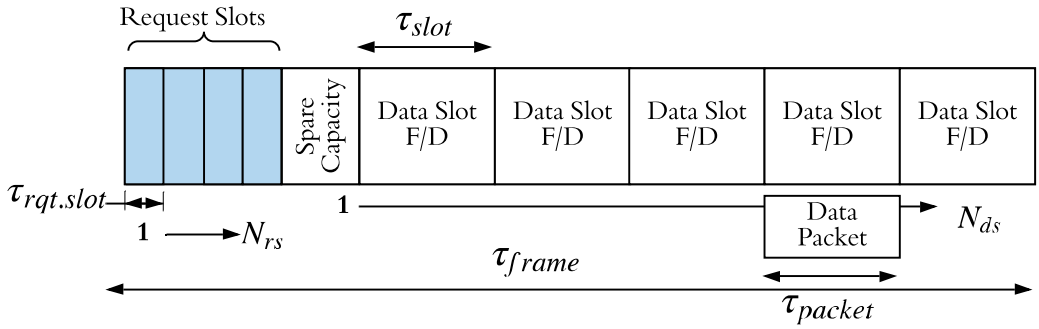

Fig. 5.7 CFDAMA-RR return frame

- The likelihood of wasting free assigned slots granted to nodes that have no data to send at the instance of a free slot arrival. This is not specific to CFDAMA-RR, but it is most likely to happen with it.
- Its delay performance also relies on the number of request slots per frame, but a large number of request slots can lead to unreasonably high overhead and low throughput performance.

Performance Investigation of CFDAMA-RR

With reference to Figure 5.7, the versatile simulated CFDAMA model outlined in the introduction of this chapter is adjusted to allow the implementation and investigation of the CFDAMA-RR scheme through the underwater scenario depicted in Figure 5.3. There, the sensor nodes are uniformly distributed, forming a ring topology. The delay-utilisation performance with both traffic models (Poisson and Pareto ON/OFF) has been studied. Table 4.3 lists the parameters of the simulated acoustic channel. Table 5.2 lists all the other parameters and required details.

In Figure 5.8, the mean end-to-end delays of the scheme with different numbers of nodes (20, 50 and 100) are shown against a full range of offered loads. Up to an offered load level of 50% of the channel capacity, the mean end-to-end delay has a flat pattern with both traffic types, owing to the fact that the average rate of packet arrivals is less than the rate at which slots occur. Under these circumstances, the mean end-to-end delay is close to its minimum and is greater with the Poisson than Pareto ON/OFF traffic models. This is attributable to the periodic ON/OFF nature of the traffic source and the length of arrival bursts which is in this case shorter than that with Poisson traffic in which a larger number of packets may arrive between successive free slot allocations in some cases.

Above this offered load level, demand assignment starts to contribute, causing the mean end-to-end delay to rise gradually. The end-to-end delay is much higher with Pareto ON-

Table 5.2 Simulation parameters for the CFDAMA-RR free assignment scheme

Attribute	**Value**
Transmission Range	$6 \times 6\ km$
Number of nodes	20, 50 or 100
Topology	see Figure 5.3
Number of data slots (N_{ds})	650
Number of request slots ($N_{req.slot}$) (N_{ds})	650
Request slot size	8 bit
Data slot size	64 bit
Packet size	64 bit
Pareto $\alpha_{on}\alpha_{off}$	1.2
Pareto k_{on}/k_{off}	1
Traffic load range	0.1 - 1 Erlangs

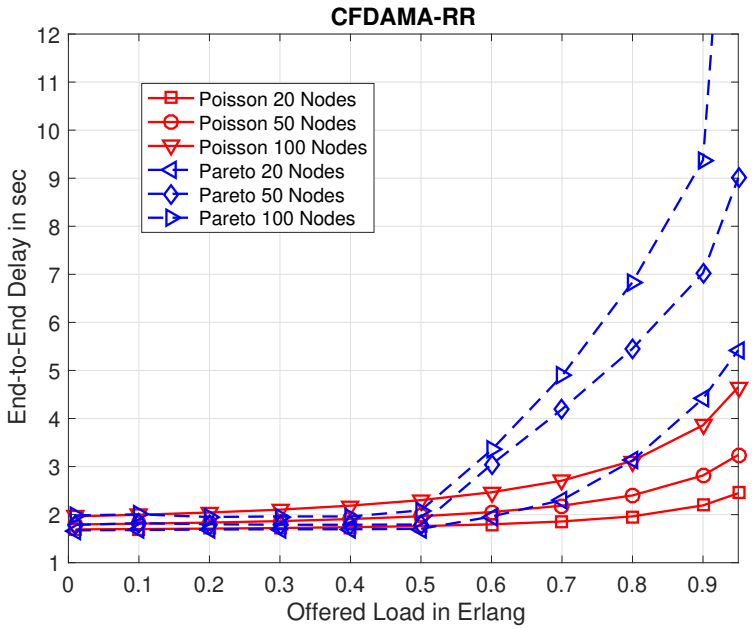

Fig. 5.8 Mean end-to-end delay as a function of channel load for CFDAMA-RR with Poisson and Pareto ON/OFF traffic sources, 64-bit packet size, and several numbers of nodes

OFF traffic because of the longer burstiness of the ON-OFF date traffic causing the mean delay to exceed the minimum DAMA delay boundary of 1.5 gateway hops at certain points, depending on the number of nodes. This is because of the statistics of Pareto ON/OFF data traffic which produce a longer period of time during which the number of nodes generating bursts exceeds a certain sustainable number. A key point to note from these results is that

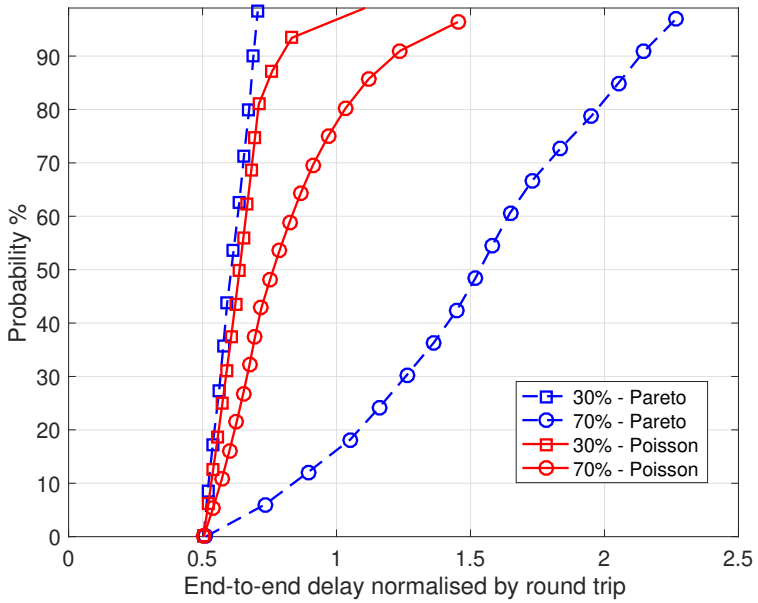

Fig. 5.9 Cumulative distribution function of end-to-end delay for CFDAMA-RR with Poisson and Pareto ON/OFF traffic sources, 64-bit packets, and 100 nodes at 30% and 70% channel loads

despite the significantly longer burstiness of the Pareto ON/OFF traffic compared with traditional Poisson, the CFDAMA-RR scheme is still capable of providing good end-to-end delay performance up to 95% of channel capacity with both traffic types. The performance, however, is heavily dependent on the number of nodes, especially with Pareto ON/OFF traffic. This is attributable to the nature of the round robin strategy on which the scheme relies. A large number of nodes can make the access to a request slot less regular for nodes. With 100 nodes, the mean delay exceeds 5 s at about 70% of the channel capacity, where it is just above 2 s with 20 nodes.

Figure 5.9 shows the CDF of the end-to-end delay of packet transmissions at two channel load levels (30% and 70%) offered by 100 nodes and with both traffic models (Poison and Pareto ON/OFF). At 30% channel load and with both traffic types, the end-to-end delay has uniformly distributed gradually increasing values. It can be seen that at this level of channel load, 100% of the packets experience end-to-end delays that are less than 1.5 gateway hops. This means each packet can skip using either its own free assigned slot (Scenario 1 in section 5.3) or an undue slot that is requested for a previous packet from the same node (Scenario 2 in section 5.3).

At 70% channel load, it can be seen that the slots of Scenario 1 and Scenario 2 are unable to accommodate the increasing number of Pareto packet arrivals causing the scheme

operation to be dominated by demand assignment (Scenario 3 in section 5.3). Therefore, around 50% of packet transmissions with Pareto ON/OFF traffic have an inevitable minimum end-to-end delay of 1.5 gateway hops due to the excessive use of demand slots. At this load level with Pareto ON/OFF traffic, the number of nodes generating bursts exceeds a certain sustainable number, forcing a substantial number of packets to start to build up in the node's queue. In spite of this level of loading, it can be seen that the free assigned slots and the undue demand slots are still used by up to 50% of the packets. However, it takes longer to obtain a free assigned slot with both traffic types, especially with Pareto ON/OFF. This leads to longer waiting time at a node's queue, and the number of packets in the queue by the time a free assigned slot occurs will be larger. This will require nodes to make larger requests which subsequently blocks the return frame for longer periods of time. Unlike with CFDAMA-RR, this is not an issue with CFDAMA-PAR, as all nodes will eventually have equitable access opportunities to the request slots owing to the underlying round robin strategy.

5.6 Comparative Performance of the CFDAMA Schemes Underwater

This section presents the comparative delay performance of both CFDAMA variants described in this chapter. It is worth reiterating the key features of the two schemes, prior to evaluation of the comparative performance. The primary benefit of both schemes is the contention-free nature in accessing the request slots, but CFDAMA-PAR is associated with the likelihood that some nodes will be prevented from making requests for substantial periods of time. CFDAMA-RR overcomes this disadvantage by sharing the available request slots equally among nodes using the round robin algorithm. In general, CFDAMA-RR outperforms CFDAMA-PAR in all scenarios, but not by a significant margin. The simulations of both schemes corresponding to the 100 node scenario with both Poisson and Pareto ON/OFF traffic types are used for the sake of this comparison. The related simulation parameters are given in Tables 5.1 and 5.2. The delay/utilisation performance for different packets sizes is shown in Figures 5.10, 5.11 and 5.12 against a full range of channel loads. The corresponding cumulative distribution function of end-to-end delay values is shown in Figure 5.13 at two channel load levels (70% and 90%) for Pareto ON/OFF traffic.

With moderate channel loads, all data slots in the CFDAMA return frame are freely assigned, and hence, the resulting delay/utilisation performance is independent of the request strategy. As the channel load is increased, the utilisation of demand assigned slots rises, resulting in an increased differentiation between the performance of the two CFDAMA

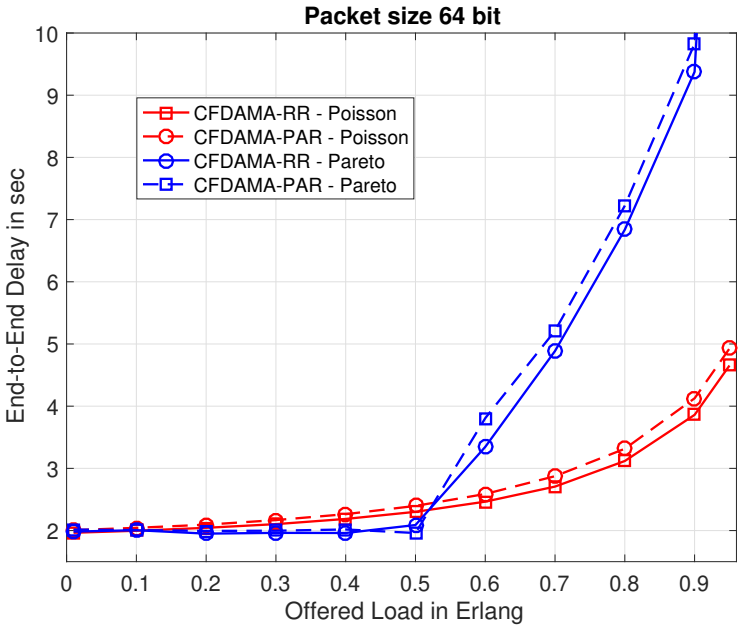

Fig. 5.10 Mean end-to-end delay as a function of channel load for both CFDAMA-RR and CFDAMA-PAR with Poisson and Pareto ON/OFF traffic sources, 64-bit packet size, and 100 nodes

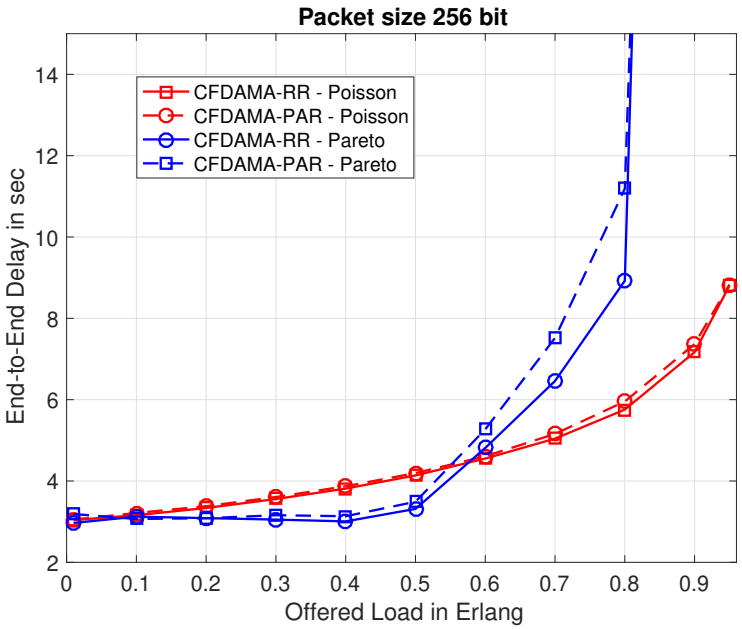

Fig. 5.11 Mean end-to-end delay as a function of channel load for both CFDAMA-RR and CFDAMA-PAR with Poisson and Pareto ON/OFF traffic sources, 256-bit packet size, and 100 nodes

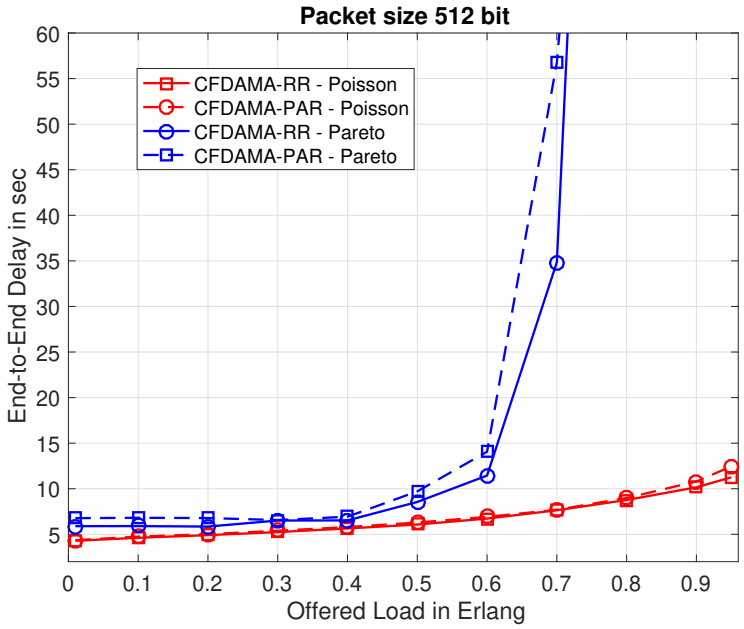

Fig. 5.12 Mean end-to-end delay as a function of channel load for both CFDAMA-RR and CFDAMA-PAR with Poisson and Pareto ON/OFF traffic sources, 512-bit packet size, and 100 nodes

variants. The contrast in performance is sharper with Pareto ON/OFF traffic at reasonably high channel load levels. In this instance, CFDAMA-RR offers superior performance, especially with small packet sizes. This is attributable to that nodes do not experience any significant backlogging. Despite the high traffic load, CFDAMA-RR still operates with a larger proportion of free assigned and undue demand assigned slots whilst ensuring that nodes are able to have access to the return channel through periodic round-robin request opportunities.

Comparing the performance of the two schemes at 70% channel load with a 64 bit packet size, as shown in Figure 5.10, it can be seen that CFDAMA-RR with Pareto ON/OFF traffic offers a mean end-to-end delay less than 4.9 s compared with 5.3 s for CFDAMA-PAR. With Poisson traffic, they maintain approximately the same delay difference at 2.7 s with CFDAMA-PAR and 2.4 s with CFDAMA-RR. With larger packet sizes, the achieved mean end to end delay is much less with CFDAMA-RR; at 65% channel load with 512 bit packet size as shown in Figure 5.12, it can be seen that with Pareto ON/OFF, CFDAMA-RR offers a mean end-to-end delay less than 20 s compared with above 25 s for CFDAMA-PAR. With Poisson, they maintain approximately the same delay difference that is experienced with 64 bit packet size.

The results in Figures 5.10, 5.11 and 5.12 also show that the delay/utilisation performance with Pareto ON/OFF traffic is significantly different to that obtained with Poisson traffic. A gradual increase in delay is observed with Poisson traffic as nodes become more active and the rate of independent packet generation becomes higher. Whereas, a two-phase rise in the delay is observed with Pareto ON/OFF starting with steady rise up to about half of channel capacity followed by a sharp rise afterwards. The reason behind this contrast in performance is the limited burstiness of the Poisson traffic that cannot offer substantial demands for an excessive period of time long enough to enable demand assigned slots to contribute effectively. In contrast, free assigned slots in this instance can contribute more effectively to support the transmission of independently generated packets. The overall delay distribution is much poorer with Pareto ON/OFF traffic, due to the much longer burstiness restricting a significant proportion of packet transmissions to the inherent DAMA delay bound. The delay distribution, in this case, is dominated by the number and size of node requests, determined by the duty cycle of the ON/OFF traffic generator.

The impact of different packet sizes on the delay performance of both schemes can also be seen in Figures 5.10, 5.11 and 5.12 with both data traffic types. The two schemes perform better with short packets. This is attributable to the low data rate used, which is the typical date rate of underwater modems. Long packets demand long slots in a CFDAMA frame, and long slots can make it less regular for slots to be freely assigned as the free slots are assigned using a round robin method in both schemes. This increases the average end-to-end delay for long packet transmissions. The resulting delay/utilisation characteristics with Pareto ON-OFF traffic are more sensitive to the packet size than those with the Poisson traffic model. These results put further emphasis on the notion that it is the periodic ON-OFF nature of the Pareto traffic that is behind most of the performance differential to Poisson traffic. For example, unlike with the Poisson traffic source, the CFDAMA delay performance with the Pareto ON-OFF traffic source and 512-bit packets experiences a degradation. This is due to the heavy tail of the Pareto distribution with a high probability of long ON and OFF periods causing longer queuing times.

Fig. 5.13 shows the CDF of end-to-end delays (normalised by the average length of round trips) of all packet transmissions for the two schemes with 100 nodes and with the two traffic models (Poisson and Pareto ON/OFF) at 70% and 90% load values. For the same reasons explained above, the superiority of RR is particularly manifested at high channel loads. However, at both 70% and 90% channel load levels, a considerable proportion of packet transmissions experience very similar end-to-end delay values regardless of the type of scheme. For example in the case of 70% channel load, with both schemes, about 20% of the packet transmissions experience delay values below a round trip time, and

another 20% experience delay values above 2 round trip times. The other 60% of the packet transmissions differ in their delay values based on the statistical behaviour of each scheme. This is attributable to the underlying variable rate demand assignment scheme and CFDAMA scheduling mechanism. Due to the high channel load, the demand assigned slots dominates CFDAMA operations. When a node happens to make a single request for more than one slot, which could happen with both schemes, a set of successive slots is then allocated in the frame allowing back to back packet transmissions. Subsequently, the end-to-end delay of back to back packet transmissions of both schemes becomes equal, determined by the inter-arrival time of packet generations with respect to the data slot duration. Any change in the packet inter-arrival time will have a direct consequent on the delay values as long as packet generations happen during the period of time between successive slot assignments. The difference between the two schemes in the end-to-end delay values becomes wider as a result to an increase in packet inter-arrival time allowing CFDAMA-RR to have smaller delay values owing to the more regular request opportunities compared with CFDAMA-PAR.

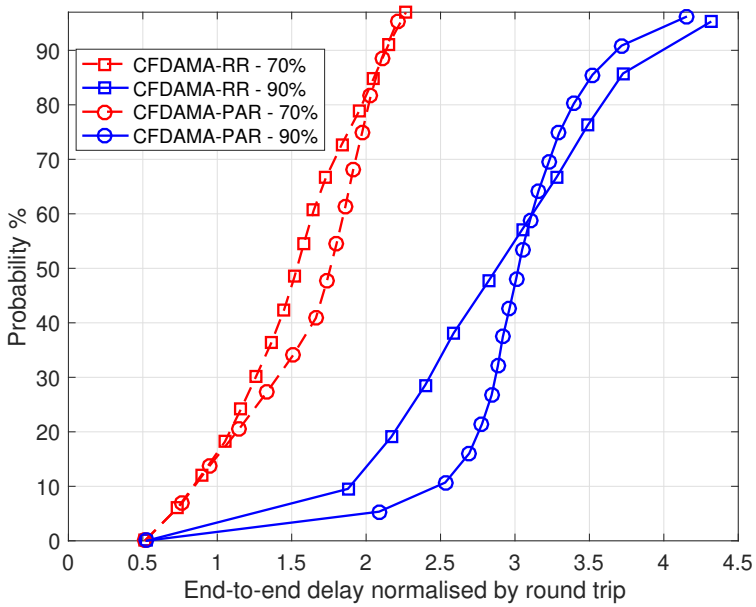

Fig. 5.13 Cumulative distribution function of end-to-end delay for both CFDAMA-RR and CFDAMA-PAR with Poisson and Pareto ON/OFF traffic sources, 64-bit packets, and 100 nodes at 70% and 90% channel loads

5.7 CFDAMA with Intermediate Scheduler (CFDAMA-IS)

The major advantage of the CFDAMA protocol is that it exploits the contention-less nature of the free assignment and the effectiveness of demand assignment in achieving high channel utilisation with a minimum end-to-end delay of only 1.5 gateway hops. This combination can optimise the balance between the end-to-end delay and channel utilisation. However, when implemented underwater, CFDAMA may have two drawbacks based on the depth of water. These two drawbacks can be summarised as follows:

- It will suffer from long round trip delays, proportional to the 1.5 gateway hops, between the sensor nodes and their transmission coordinator since the scheduler operates at the gateway. The gateway is typically located close to the surface of the intended water body to be facilitated with a high-speed terrestrial link. Hence, locating the scheduler approximately surface-to-bottom away from its sensor nodes can extensively reduce CFDAMA performance especially in deep water.
- Utilising the CFDAMA forward frame without any adaptation to the underwater scenario will cause a significant waste of capacity in the forward channel.

The CFDAMA-IS scheme works in a more efficient way by minimising the round trip delay. The centralised scheduler, required by CFDAMA, does not necessarily need to be near the surface to establish the communication links and coordinate transmissions of sensor nodes. In CFDAMA-IS, a node close to sensor nodes works as both a scheduler and a handover station to relay data packets to the gateway. CFDAMA-IS requires a change in the structure and use of the two CFDAMA frames to provide more efficient exploitation. During the forward frame, the intermediate scheduler essentially does two jobs: sending acknowledgements of allocated slots to sensor nodes and successively relaying data packets to the gateway. With respect to Figure 5.14 the time of a round trip is reduced significantly, and hence, the time needed to request capacity, receive its acknowledgement and transmit a packet is much less than one gateway hop and a half. Other than that, CFDAMA-IS is implemented in a similar way as CFDAMA as explained in section 5.3.

5.7.1 Fundamental CFDAMA-IS Characteristics

Similar to CFDAMA, each successfully received packet in CFDAMA-IS must have gone through one of the three possible scenarios described in section 5.4. With respect to the frame timing diagram depicted in Figure 5.14 and considering the behaviour in Scenarios 1

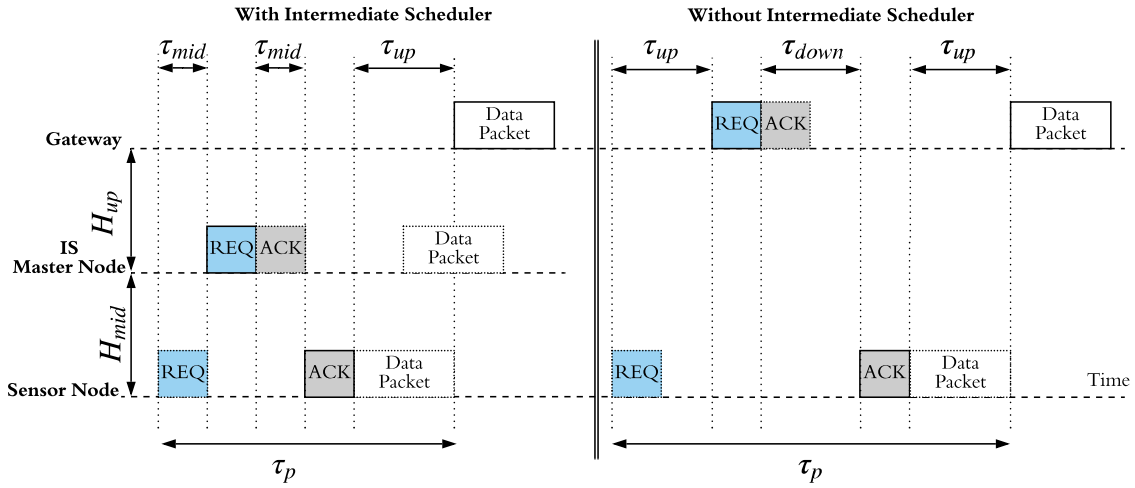

Fig. 5.14 CFDAMA propagation delay components with and without the intermediate scheduler

and 3, Equations 5.1 and 5.2 can be rearranged as follows:

$$E[D_{eted}] \approx \frac{N\tau_{slot}}{2} + 2\tau_{packet} + \tau_{up} \tag{5.5}$$

The third term accounts for the aggregate propagation delay required to travel to the gateway.

$$\begin{aligned} E[D_{eted}] &\approx \frac{\tau_{frame}}{2} + 3\tau_{packet} + \tau_p \\ \tau_{frame} &= N_{ds}\tau_{slot} + N_{rs}\tau_{rqt.slot} \end{aligned} \tag{5.6}$$

$$\tau_p = \begin{cases} 2\tau_{mid} + \tau_{up}, & \text{CFDAMA-IS} \\ 3\tau_{up}, & \text{CFDAMA} \end{cases}$$

It is clear from Equation 5.6 that the aggregate propagation delay τ_p that CFDAMA-IS allows is $2(\tau_{up} - \tau_{mid})$ less than that of CFDAMA. If the intermediate scheduler is located halfway between the gateway and sensor nodes, then $(\tau_{up} = 2\ \tau_{mid})$. This means that mean end-to end-delay of packets can be reduced by up to a gateway hop, enabling the demand assignment strategy in CFDAMA-IS to handle capacity requests faster than it does in CFDAMA.

5.7.2 Comparative performance of the CFDAMA-IS

This is a brief comparison prior to the next chapter which presents a more detailed CFDAMA performance evaluation with new request strategies. The RR request strategy is used with CFDAMA-IS to evaluate the impact of adding an intermediate master node to CFDAMA.

Table 5.3 Simulation parameters for the CFDAMA-IS scheme

Attribute	Value	Attribute	Value
H_{up} (see Fig. 5.14)	3.5 km and 400m	τ_{slot} (date slot duration)	6.6 ms (64 bit)
H_{mid} (see Fig. 5.14))	500m and 100m	τ_{rqslot} (req. slot duration)	0.83 ms (8 bit)
N (number of nodes)	300 and 20	N_{ds} (number of data slots)	32
Bandwidth	30 kHz	N_{rs} (number of req. slots)	32
Data Rate	9600bps	G in Erlangs	0.1 - 1

Figure 5.15 (a)(b)(c)(d) show the mean end-to-end delay against a variety of channel loads ranging from 0.1 to 1 Erlangs. The graphs are for the four capacity assignment strategies: free assignment, demand assignment, CFDAMA and CFDAMA-IS, with a Poisson traffic source and with a network of 20 and 300 nodes (sparse and dense networks). To reflect on two scenarios (deep and medium depths), Figure 5.15 (c)(d) show simulation results for the 4000m-depth scenario whereas Figure 5.15 (a)(b) show the 500m-depth scenario. With a large number of nodes, from Figure 5.15(a)(c), it can be seen that the mean end-to-end delay of the free assignment strategy grows significantly, for example, from 3.8 *s* at 1% channel load to 7.35 *s* at 95% channel load in the scenario with 4000m depth. The reason behind this is the long period between successive transmission slots allocated to each node due to the large number of nodes. On the other hand, at low channel loads, the results indicate that the free assignment strategy can provide small end-to-end delay values, approaching the minimum delay limit obtained from Equation 5.5.

The results in all the cases indicate that the delay performance of the demand assignment scheme is generally dominated by the fundamental lower bound of 1.5 gateway hops (7.860 s for 4000m depth and 0.93 s for 500m depth). The scheme shows a much slower increase in the mean end-to-end delay values over virtually the entire channel loads than the free assignment. This demonstrates the ability of the demand assignment scheme to support much higher channel load levels owing to the dynamic allocation of the available capacity based on instantaneous node requirements. The results, nevertheless, show a significant difference in the mean end-to-end delay compared to the free assignment strategy in all cases. In the 300-node scenario, for example in Figure 5.15 (c), the mean end-to-end delay of demand assignment ranges from 9.3 s at 1% channel load to 9.5 s at 95% channel load, which is on average greater than the mean end-to-end delay of the free assignment.

More importantly, the results show that the CFDAMA algorithm consistently outperforms its two constituent schemes in both mean end-to-end delay and channel utilisation. CFDAMA is inherently adaptive to the variation in channel conditions; it exploits the contention-less

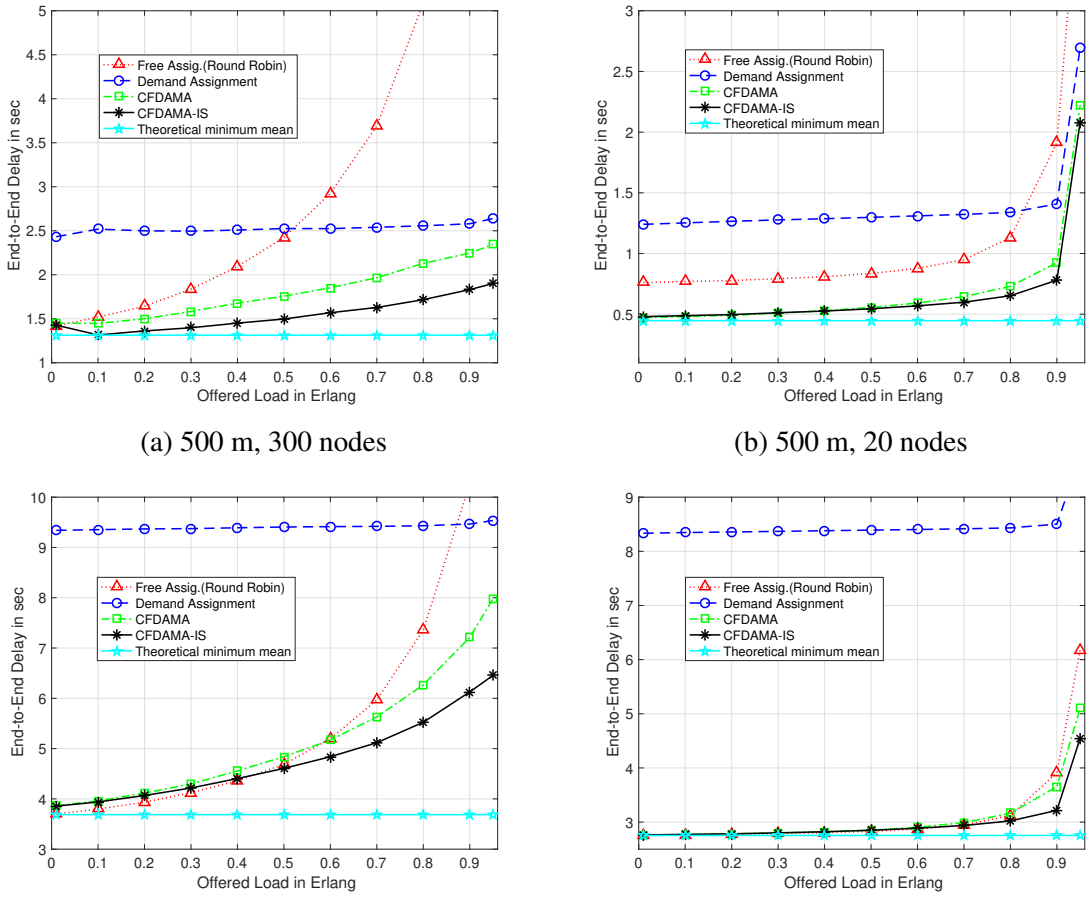

(a) 500 m, 300 nodes

(b) 500 m, 20 nodes

(c) 4 km, 300 nodes

(d) 4 km, 20 nodes

Fig. 5.15 Mean end-to-end delay against channel load, for CFDAMA-IS and its fundamental schemes with parameters shown in Table 5.3

nature of the free assignment and the effectiveness of demand assignment in achieving high channel utilisation efficiency. The results indicate that the CFDAMA-IS protocol has a significant advantage over the other three strategies in terms of both end-to-end delay and channel utilisation. Comparing with the other three schemes, CFDAMA-IS experiences the lowest mean end-to-end delay throughout almost all channel loads and number of nodes shown in the figures in all scenarios. The minimum end-to-end delay that CFDAMA-IS experiences in each scenario is at very low traffic loads when the majority of the slots are freely assigned. At high channel loads, the end-to-end delay increases steadily but is still less than the minimum delay limit of the CFDAMA scheme and its two constituent schemes. For example, as shown in Figure 5.15(c), at a channel utilisation of 1% of the channel capacity, the minimum end-to-end delay is only 3.8 s, which is less than the minimum delay of demand

assignment. At the highest channel load of 95%, the mean end-to-end delay is still the lowest at 6.4 s.

5.8 Summary and Conclusions

The chapter investigates the fundamental behaviour of two CFDAMA schemes in the context of UASNs. Through a versatile simulated CFDAMA model and representative underwater scenarios, the two CFDAMA variants, which differ in their provision of managing requests, are studied. Amongst many CFDAMA variants these two, which are CFDAMA-PAR and CFDAMA-RR, feature simplicity and maintain fairness. These two fundamental features put them at the top of the list of applicable CFDAMA variants suiting the underwater acoustic networks. When the selection of these two variants is made, a number of criteria are considered including:

- Simplicity.
- Fairness amongst nodes.
- Compatibility with existing underwater TDMA protocols and scheduling algorithms.
- Improvement of channel utilisation and end-to-end delays.
- Adaptability to the channel traffic conditions.

This selection does not necessarily mean the other CFDAMA variants unable to work with the underwater acoustic networks, but we argue that the peculiarity of the underwater environment and the nature of battery-powered sensor nodes communicating acoustically narrows down the list of economically applicable CFDAMA variants.

The performance of both schemes is evaluated with both Poisson and Pareto ON/OFF traffic sources. Simulation results indicate that Poisson modelled traffic is not intensive enough to place sufficient demands on the channel, leading to delay/utilisation performance independent of the request strategy. This limits the performance of both schemes to the DAMA delay boundary of 1.5 gateway hops except with free assigned slots intensively utilised for this type of traffic. With the ON/OFF traffic, the statistical behaviour of the traffic source predominates the delay performance of both schemes in all instances, especially at high channel loads. The primary limitation of the CFDAMA-PAR scheme is the possibility that a certain number of requesting nodes dominate the channel with heavy and regular demand, preventing other nodes from gaining access to the request slots. CFDAMA-RR uses the round-robin scheduling to share the request slots of every frame equally and regularly

between nodes causing the scheme to be subject to performance degradation with a higher number of active nodes. The larger the number of nodes there are, the less regular the round robin request slots are. However, it is shown that both schemes can provide good delay/utilisation performance under variant traffic loads and up to 100 nodes.

This chapter proposes a new form of the CFDAMA protocol underwater. Two changes are made to the traditional CFDAMA configuration as follows: Firstly, the CFDAMA scheduling node is repositioned from being in the gateway to be in or a master node located just above the sensor nodes. This leads to minimisation of round trip delays between sensor nodes and the scheduler. Secondly, the CFDAMA forward frame is exploited not only for transmitting acknowledgements from the master node to sensor nodes, but also for relaying data packets to the gateway. Simulation results have shown that the CFDAMA-IS protocol offers excellent performance in dealing with the trade-off between end-to-end delay and channel utilisation for Poisson data traffic through a simulated underwater scenario. The major advantage of the CFDAMA-IS protocol is the fact that it effectively combines the contention-less nature of the free assignment and the effectiveness of the demand assignment in achieving high channel utilisation. In CFDAMA-IS, the minimum demand assignment delay bound of 1.5 gateway hops is reduced, which results in a significant enhancement in the overall delay/utilisation performance. For a vertical channel with data rate of 9600 bit/s and up to a 4000 m depth/range with Poisson traffic offered by 20 and 300 nodes, CFDAMA-IS makes it possible to load the channel up to 95% of its capacity with a delay performance that is better than that of conventional CFDAMA and far superior to the demand assignment scheme, and more bounded than the free assignment scheme.

New insights into the implementation of CFDAMA are provided. Significant contributions and advances are made to the effectiveness of the scheme. However, the benefits of the scheme underwater are subject to the characteristics of underwater acoustic modems and the processing capability of sensor nodes. Compatibility of the scheme with the existing underwater TDMA protocols requires more investigation. A novel approach to CFDAMA-RR and CFDAMA-PAR have been invented to form the basis of some significant advances presented in chapter 6.

Chapter 6

Robust Capacity Assignment Schemes for UASNs

6.1 Introduction

Individually or combined, the free and demand assignment schemes are suitable MAC solutions for UASNs, provided that the built-in clocks are synchronised and all the design factors covered in chapters 4 and 5 are carefully considered for a given scenario (i.e. traffic type, packet duration, node population density and delay distribution, etc). However, in order to avoid any system failure or performance decline under extremely dynamic underwater conditions, these solutions must become more robust.

This chapter introduces two novel robust MAC protocols which have been exclusively designed for UASNs. The first scheme employs the round robin request strategy in a systematic manner (CFDAMA-SRR). Considering the spatial distribution of nodes, it has a bias against long-delay demand assigned slots and works in favour of exploiting a single request rather than multiple requests for the same demand, to enhance the delay/utilisation performance of CFDAMA-RR. The work associated with this scheme has led to a new publication [118]. The second scheme, namely CFDAMA-NoClock, is capable of providing adaptive TDMA to sensor nodes without the need for synchronisation between independent node clocks across a given UASNs. With a mechanism for regular calibration and compensation of propagation delay measurements, it enables relative timing amongst nodes and periodically informs them of the appropriate time for collision-free data transmissions. The work associated with this scheme is being documented for a new publication nearing submission.

The rest of the chapter is organised as follows: Section 6.2 introduces the CFDAMA-SRR scheme, section 6.3 evaluates the performance of CFDAMA-SRR, section 6.4 introduces the

CFDAMA-NoClock scheme, section 6.5 evaluates the performance of CFDAMA-NoClock, and finally, section 6.6 concludes the chapter.

6.2 CFDAMA-SRR: MAC Protocol for Underwater Acoustic Sensor Networks

6.2.1 Motivations

CFDAMA with Round Robin requests (CFDAMA-RR) is originally designed to overcome the limitations of its counterparts by maintaining unbiased access rights for all nodes. By using the round robin algorithm, the scheme ensures that nodes are not inhibited by other nodes from making requests. It eliminates the possibility of losing the channel due to either contention between nodes or channel domination by transmitting nodes. Under certain conditions, CFDAMA-RR may have the drawbacks that are described in section 4.5.2. Due to the long propagation delay underwater and the fact that sensor nodes in many applications are widely spread, implementing CFDAMA with the conventional CFDAMA-RR scheme and without considering the location of nodes results in poorer efficiency than the level of which the scheme is capable. We introduce in this section a new request strategy, CFDAMA with Systematic Round Robin requests (CFDAMA-SRR), to address this issue. The key contributions in this section include:

- Analysis of CFDAMA behaviour for representative underwater scenarios, through analytical and numerical simulations.
- Recommendations on the trade-off between CFDAMA parameters and strategies.
- A new request strategy, CFDAMA-SRR.
- Comprehensive simulation results based on a realistic underwater sensor deployment for seismic monitoring in oil reservoirs, with the use of the BELLHOP acoustic field computation program.
- Incorporation of well-known underwater propagation and ambient noise models.

6.2.2 The CFDAMA-SRR Scheme

In order to improve the performance of CFDAMA-RR, the correlation between the round trip delay τ_r and the type of granted transmission slot needs investigating. Every successfully received CFDAMA packet must have gone through one of three possible scenarios:

- Scenario 1: in which the packet gets through by the use of a free assigned slot.
- Scenario 2: in which the packet gets through by the use of an undue reserved slot, i.e. a slot requested for a preceding packet from the same node.
- Scenario 3: in which the packet gets through by the use of a due reserved slot, i.e. its own requested slot.

With reference to Figure 6.1, by considering an arbitrary n^{th} node and the case where there are N_{new} new packet arrivals in the current CFDAMA frame, we will find the expectation through which scenario the arbitrary k^{th} packet will be transmitted. For simplicity the data slot duration τ_{data} is used as a time unit in the following discussion. Each particular node can have one request slot per a CFDAMA frame. The duration of CFDAMA frame is denoted by T_{frame} and is given by:

$$T_{\text{frame}} = T_{\text{data}} + T_{\text{rqt}} \tag{6.1}$$

Where T_{rqt} is the total duration of request slots in the frame and T_{data} is the total duration of data slots in the frame. When $T_{\text{data}} \gg T_{\text{rqt}}$, which is usually the case for low frame overheads, then $T_{\text{frame}} \approx T_{\text{data}}$. In every CFDAMA frame, there will be two possibilities of the k^{th} packet arrival: arriving within the round trip delay denoted $\tau_{\text{r}}[n]$ time slots or arriving after it. We will assume that on average the N_{new} new packet arrivals happen uniformly within a CFDAMA frame, which contains T_{frame} time-slots, and thus, the expected number of new packets within $\tau_{\text{r}}[n]$ is given by:

$$x = \left\lceil \frac{N_{\text{new}} \tau_{\text{r}}[n]}{T_{\text{frame}}} \right\rceil \tag{6.2}$$

Therefore, if $1 < k < x$, called constraint C_1 in the following discussion, then the three packet transmission scenarios (defined above) could be possible. However, if $x < k < N_{\text{new}}$, called constraint C_2 in the following discussion, then Scenario 2 will be impossible as there will be no undue requested slots left. If C_2 is satisfied, the tagged packet arrives after $\tau_{\text{r}}[n]$ time-slots, and thus, will have to be granted either a free assigned slot (Scenario 1) which also must occur after $\tau_{\text{r}}[n]$ time-slots, or wait for its own requested slot (Scenario 3).

It is sensible to assume that the only way that the k^{th} packet escapes is via Scenario 3 when k exceeds a certain threshold. At high offered traffic levels, there must be a number of old packets N_{q} from previous CFDAMA frame(s) waiting in the node's queue ($N_{\text{q}} > 0$). Thus, the certain threshold is $(a+b)$, which is the maximum total number of free-assigned slots granted to the n^{th} node during the interval of $(\tau_{\text{r}}[n] + T_{\text{frame}} + \bar{S})$, where b represents the maximum number of free-assigned slots granted to a node during the interval of $\tau_{\text{r}}[n]$

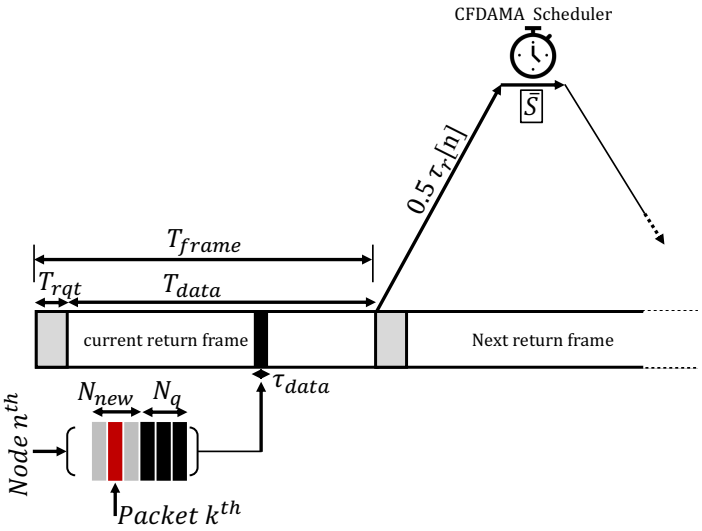

Fig. 6.1 Systematic round robin timing

time-slots, and for N (the number of nodes), it is given by:

$$b = \left\lceil \frac{\tau_r[n]}{N} \right\rceil \tag{6.3}$$

a represents the maximum number of free-assigned slots in a CFDAMA frame. In other words, the approximation can be made here is that if $N_q + k > a$, called constraint C_3 in the following discussion, the only way the k^{th} packet escapes is through its due demand requested slot (Scenario 3). Assuming $k\Delta$ is the expected instant of arrival of the k^{th} packet, the packet needs to wait for $(\tau_r[n] + T_{\text{frame}} + \bar{S} - k\Delta)$ slots in order to be granted its own demand-assignment slot. Since $\tau_r[n]$ is typically large underwater, $\bar{S}$ is insignificant compared to τ_r, on average the expected instant of the packet arrival $k\Delta$ can be close to $T_{\text{frame}}/2$, and T_{frame} is comparable to τ_r, this waiting interval can be approximated to $\gamma\tau_r[n]$. Where $\gamma \approx 1.5$ is a constant.

During the interval $\gamma\tau_r[n]$, there are: $\lceil \gamma\tau_r[n]/N(1-d) \rceil$ free-assigned slots available for the tagged n^{th} node, where $(1-d)$ is the fraction of free-assigned slots in a CFDAMA frame. This indicates that there will be a relatively large number of free-assignment slots available to use and the number increases with $\tau_r[n]$. The assumption ought to be made now is that if $[(N_q + k) < \lceil \gamma\tau_r[n]/N(1-d) \rceil]$, called constraint C_4 in the following discussion, then the k^{th} packet will certainly escape through a free-assigned slot (Scenario 1). This event occurs more frequently when $\tau_r[n]$ is large because the fraction of demand-assigned slots, d, in a CFDAMA frame is also reduced. Subsequently, the k^{th} packet will also have more chances to escape using an undue requested slot (Scenario 2).

Table 6.1 List of constraints

Denotation	**Constraint**	**Scenarios**
C_1	$1 < k < x$	Scenarios 1, 2, or 3
C_2	$x < k < N_{\text{new}}$	Scenarios 1 or 3
C_3	$N_{\text{q}} + k > a$	Scenario 3
C_4	$N_{\text{q}} + k < \lceil \gamma \tau_{\text{r}}[n]/N(1-d) \rceil$	Scenario 1

Considering Equations (6.2) and (6.3) and constraints (C_1, C_2, C_3 and C_4) summarised in Table 6.1, the round-trip delay $\tau_{\text{r}}[n]$ has a significant impact on determining the scenario through which a packet will be transmitted. More specificity, $\tau_{\text{r}}[n]$ will affect the transition from free assignment to demand assignment, and hence, the delay/utilisation performance. This transition will also depend on the position of the new packet in the node's queue with respect to the interval $\tau_{\text{r}}[n]$. Due to long propagation delays and sensor nodes that are typically located at different distances from the central gateway, implementing the CFDAMA-RR strategy without a form of location-based arrangement will cause the scheme to miss an opportunity of even better performance.

CFDAMA-SRR Solution Satisfying the constraint C_4 will depend not only on τ_{r} but also on the value of the offered traffic and the statistical behaviour of data traffic. They will be instantaneously determining the term $(k + N_{\text{q}})$ in the constraint C_4. Satisfying constraint C_4 means plenty of free assigned slots will be available. Nodes that are located farther away from the gateway will allow their new packets to have a higher chance to satisfy the constraint C_4 than the nodes that are located closer. The closer nodes will actually have a higher chance that their new arrived packets will satisfy the constraint C_3, and hence, have to wait for at least the period of τ_{r} to obtain a slot. If C_3 is satisfied and there are not enough request slots in the frame, newly arriving packets will have to wait for multiple frames before a capacity request can be made for them.

Given the above, this section introduces a new variant of CFDAMA-RR, namely CFDAMA-SRR. The new scheme works the same way as CFDAMA-RR does, described in section 5.5.2, except for the fact that the round robin algorithm works with respect to the location of sensor nodes. The nodes make their capacity requests not only in a round-robin fashion but also in a location-based manner with respect to the location of their centralised scheduling node. Opportunities to make a request are given successively to adjacent nodes one after another, starting from the centre to the edge of the network. CFDAMA-SRR can reduce the possibility that C_3 is satisfied and increase the possibility that C_4 is satisfied. At high channel loads,

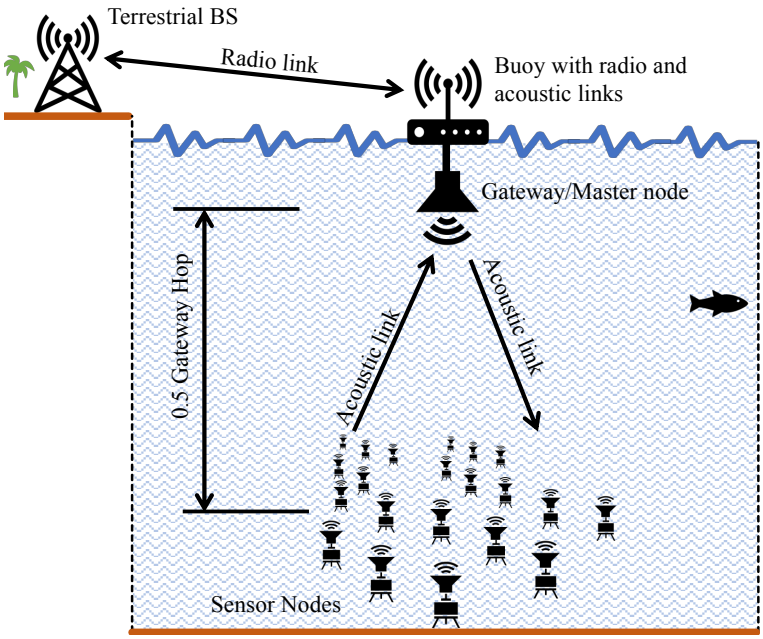

Fig. 6.2 A centralised UASN where the CFDAMA-SRR protocol is employed

this new scheme can maximise the use of each single request opportunity leading to an enhanced delay/utilisation performance. When a node makes a single request for more than one slot, a run of successive slots is then allocated allowing back to back packet transmissions. Subsequently, the end-to-end delay of back to back packet transmissions is determined by the inter-arrival time of packet generations with respect to the data slot duration. CFDAMA-SRR systematises the distribution of request opportunities which works in favour of the utilisation of a single request rather than multiple requests for the same demand. It also allows more time for those nodes located further away from the gateway to maximise the use of an increased number of free assigned slots owing to their longer round trips.

CFDAMA-SRR Scheduling Algorithm

With reference to the UASN deployment depicted in Figure 6.2, CFDAMA-SRR scheduling is performed using the two typical CFDAMA tables operating at the gateway, i.e. the free assignment table and the reservation request table. The cycle starts when a request is made. Allocation of both types of slots (free and demand) is done on a frame-by-frame basis. The global scheduler informs all sensor nodes of their allocations in a TDM fashion on the forward frame. Slots are initially assigned using the demand assigned mode, according to the entries in the reservation request table. Once all requests waiting in the queue have been dealt with, the scheduler then switches to free assignment mode and starts to freely assign slots to the remaining nodes in a round robin fashion. This is made by assigning

individual free assigned slots, one after another, to the nodes whose IDs are, at that moment, waiting at the top of the free assignment table. Following every slot allocation, each served node-ID is dropped to the bottom of the table. This approach maintains fairness between nodes. Likewise, each time a node is allocated a set of successive demand assigned slots based on the number requested, its ID is also moved to the tail of the free assignment table.

CFDAMA-SRR Frame Structures

To implement CFDAMA-SRR, the two typical CFDAMA frame structures are needed, i.e. forward frame and return frame. In the same way as CFDAMA-RR, the scheme devotes

Algorithm 1 CFDAMA algorithm implemented at the gateway, N_{RS}= Number of requested slots by a node, Tab_1=the free assignment table, Tab_2= the reservation request table, F= free slot, D= demand slot, j= pointer.

for every return frame **do**
  update Tab_2 based on new requests arrived during return frame(j)
  while available slots in forward frame (j) $\neq 0$ **do**
    if Tab_2 is not empty **then**
      in forward frame (j) assign N_{RS} D slots to 1^{st} node in Tab_2
      remove this entry id from Tab_2
      move this entry id to tail of Tab_1
    else
      assign 1 F slot to the node whose id is at the top of Tab_1
      move this entry to tail of Tab_1
    end if
  end while
end for

Algorithm 2 CFDAMA algorithm implemented at each sensor node, N_{PQ} = number of packets queued, N_{OR} = number of outstanding requests, N_{GS} = number of granted data slots

for every forward frame **do**
  if $(N_{\mathrm{GS}} \neq 0)$ in forward frame(j) **then**
    read due time of granted slots
    schedule N_{GS} transmissions as appropriate
  end if
  if a request slot is due in return frame (j+1) **then**
    count N_{PQ} and N_{OR}
    $N_{\mathrm{RS}} = N_{\mathrm{PQ}} - N_{\mathrm{OR}}$
    make a request of N_{RS} slots in return frame(j+1)
  end if
end for

a region located at the start of the return frame to round-robin request slots as shown in Figure 5.7. With complete fairness amongst sensor nodes, every node will have to wait for its round-robin turn to make a request, if required, on a frame-by-frame basis. Figure 6.3 illustrates an arbitrary transmission cycle in a randomly selected j^{th}return frame of CFDAMA-SRR. In this example, based on round-robin turns on a frame-by-frame basis, the turn at this instant is for the n^{th}, $(n+1)^{th}$ and $(n+2)^{th}$ nodes to make requests. In this instance, the sensor node can make a request, if required, and the number of slots to be requested by a node is given by:

$$N_{\mathrm{RS}} = N_{\mathrm{PQ}} - N_{\mathrm{OR}} \tag{6.4}$$

Where N_{RS} is the number of requested slots, N_{PQ} is the number of queued packets and N_{OR} is the number of outstanding requests. The illustrated example also shows that these nodes are transmitting data packets according to allocated D and F slots acknowledged in the $(j-1)^{th}$ forward frame. Algorithms 1 and 2 outline the implementation of this CFDAMA-SRR cycle. Furthermore, with reference to Fig 6.3, each node is responsible for aligning the arrival of its packet with the beginning of its allocated slot referenced at the gateway, by transmitting the packet $\tau_{\mathrm{p}}[n]$ seconds prior to the due time of the allocated slot. Where $\tau_{\mathrm{p}}[n]$ is the propagation delay between the n^{th} sensor node and the gateway. For practical synchronisation, guard intervals can also be added as appropriate in case of node clock/location drift. Nodes must synchronise their built-in clocks with the master node's clock. In practice, propagation delays need to be estimated in order to attain this synchronisation. Typically, this estimation of the long and time-variant propagation delay of acoustic waves is dealt with using a handshake technique as often as required [2]. Spare capacity can be inserted as required to make the frames equal in length for simplicity and an option to evaluate the performance under varying parameters, e.g. additional control overheads if required to reflect real implementations.

CFDAMA-SRR DELAY ANALYSIS

In order to gain useful insights, this section provides an analytical approach to evaluating the average end-to-end delay performance of CFDAMA-SRR. This approach follows similar steps to the derivation used in [116] to model the performance of a CFDAMA variant for satellite systems. However, the assumptions made for underwater scenarios are different. Packets make Bernoulli attempts continually until they get through either as Scenario 1, Scenario 2 or Scenario 3 described in Subsection (6.2.2). The average end-to-end delay of packets will depend on the scenario it goes through. The analytical approach here is to evaluate the average delay a tagged k^{th} packet would experience based on the probability of

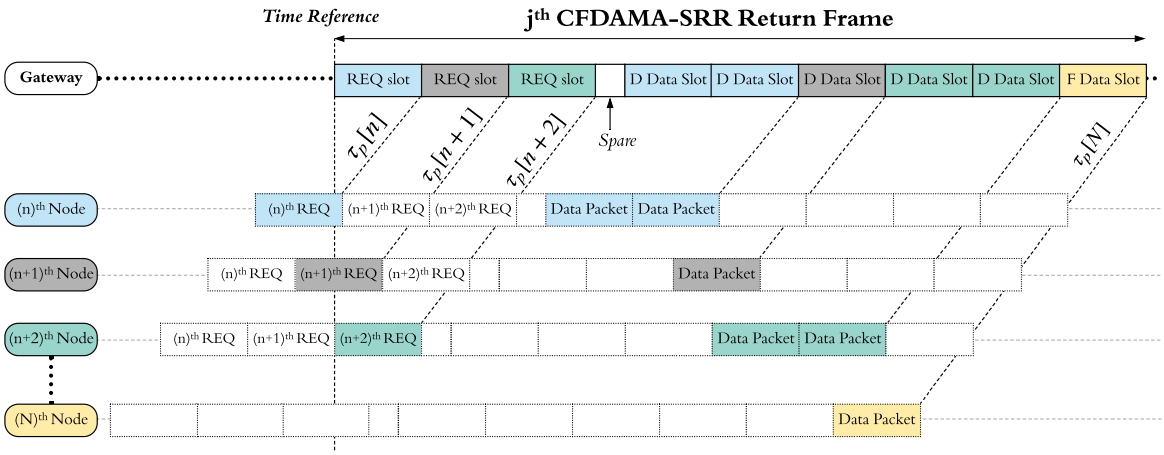

Fig. 6.3 An arbitrary CFDAMA-SRR return frame with some allocations

each of the three scenarios. For the reader's reference, Table 6.2 lists the mathematical terms used in this section.

In UASNs, the end-to-end delay of packets is heavily dominated by both the propagation delay and the number of sensor nodes in the network. The claim this section will fulfil is that the CFDAMA average waiting and service time can be modelled as a $M/G/1$ queue when the round-trip delays are long. Packet transmissions will be dominated by Scenario 1 and the round-robin free assignment scheme will be in operation most of the time when the round-trip delays are long. The following analysis steps will allow us to obtain the approximated mean and variance values of the waiting and service time. Plugging these values in the Pollaczek-Khinchin formula [119] of the $M/G/1$ queue will result in the total waiting and service time. Finally, the average end-to-end delay of packets can be calculated using this waiting and service time plus the average propagation delay. With respect to the CFDAMA-SRR frame illustrated in Figure 6.1, the frame has T_{frame} timeslots where T_{frame} is proportional to the total number of sensor nodes N. The frame size and data slot size can be chosen based on the desired throughput and transmission rate in a given underwater scenario. For convenience in the following discussion, the time-slot duration τ_{data} is used as the time unit. For example, the round-trip delay is denoted as τ_{r} time-slots. For a Poisson data traffic source, the probability that N_{new} new packets arrive in a CFDAMA frame is given by [116]:

$$P_{\text{r}}\{N_{\text{new}}\} = \frac{e^{-\lambda T_{\text{frame}}} \lambda^{N_{\text{new}}}}{N_{\text{new}}!} \tag{6.5}$$

where $\lambda = \Lambda/N$ is the arrival rate per time slot at each node. Λ is the network packet arrival rate per time slot. The beginning of the CFDAMA frame is defined to be the time origin. If a node's queue (at this instance) is not empty, it can send a request to the CFDAMA

Table 6.2 List of mathematical terms

Term	Description
N	Number of nodes
T_{frame}	CFDAMA frame duration
T_{data}	Total data slots duration in a frame
T_{rqt}	Total request slots duration in a frame
τ_{data}	Data slot duration
τ_{rqt}	Data slot duration
$\tau_{\text{r}}[n]$	Round-trip delay of n^{th} node
$\tau_{\text{p}}[n]$	Propagation delay between n^{th} node and gateway
N_{q}	Number of old packets
k	Packet's order in node's queue
n	Node's pointer
N_{new}	Number of newly arrived packets
x	Random variable = Number of new packets in τ_{r}
a	Number of free slots in CFDAMA frame
b	Number of free slots during τ_{r}
d	Fraction of demand assignment in CFDAMA frame
γ	Constant
λ	Packet arrival rate per nodes
Λ	System packet arrival rate
$E(Q)$	Expected queueing delay
η	A Ratio N/τ_{r}
$\bar{T}$	Waiting and service time
$\bar{T}_{\text{r}}$	Average propagation delay
$\bar{D}$	Overall CFDAMA mean delay

scheduler at the beginning of the next frame. The expected instant of arrival of the first due demand-assigned slot(s) is:

$$Y = \tau_{\text{r}}[n] + \bar{S} + T_{\text{frame}} \tag{6.6}$$

where $\bar{S}$ is queueing delay in the demand-assignment table of the scheduler, to be addressed later. The average period between two successive free assigned slots to a particular node is $N/(1-d)$, where $(1-d)$ is the fraction of free assigned slots in a CFDAMA frame. Provided that the free-assignment strategy is round-robin. Therefore, the probability that a packet at the front of the node's queue escapes by a free assigned slot (scenario 1) is:

$$p = \begin{cases} (1-d)/N & non-empty\ queue \\ 2(1-d)/N & empty\ queue \end{cases} \tag{6.7}$$

By considering an arbitrary k^{th} packet of the N_{new} new arriving packets at a tagged randomn^{th} node in the current CFDAMA frame, one of two potential cases the arriving packet will go through can be defined as follows:

- when the node queue is empty, i.e. $N_{\text{q}} = 0$
- when there are old packets queued up, i.e. $N_{\text{q}} > 0$

In the underwater scenarios some assumptions can be made, as shown later, which means that precise calculation of these probabilities is not required in this discussion. The scheduler queue delay $\bar{S}$ is generally negligible compared with the round-trip delay. Thus, the general unconditional mean queuing delay is:

$$E(D) = \sum_{N_{\text{q}}=0}^{T_{\text{frame}}} P_{N_{\text{q}}} E(D|N_{\text{q}}) \tag{6.8}$$

Computation of the k^{th} packet delay using Equation (6.8) becomes tedious as k increases. To reduce the computational complexity, some of the constraints from the discussion of section 6.2.2 can be used. If the constraint C_3 ($N_{\text{q}} + k > a$) is satisfied, then the only way the packet escapes is via its due demand assigned slot (Scenario 3). The expected end-to-end delay in this case will be equivalent to demand-assignment theoretical delay and given by the following:

$$E(D_{\text{k}}|N_{\text{new}}, N_{\text{q}}, N_{\text{q}} + k > a) = T_{\text{frame}} + \tau_{\text{r}}[n] + \bar{S} - k\Delta \tag{6.9}$$

As described in subsection 6.2.2, during this waiting interval there are $[\gamma\tau_{\text{r}}[n]/N(1-d)]$ free-assigned slots available for the tagged n^{th} node. This shows that the number of free-assigned slots will depend on τ_{r} and N. To reflect on the effect of both the long round-trip delays and number of UASNs nodes on the performance of CFDAMA-SRR underwater, a normalisation parameter is introduced to the analysis. It is denoted η and defined as the ratio between the two parameters $N\tau_{\text{slot}}/\tau_{\text{r}}$, i.e. $\eta = N\tau_{\text{slot}}/\tau_{\text{r}}$. By plugging η in the former expression ($[\gamma\tau_{\text{r}}/N(1-d)]$), the number of available free-assigned slots will be $[\gamma(1-d)/\eta]$. As η decreases, the benefits of free-assignment slots increase. With respect to the constraint C_2 and C_4 from the previous section, if $x < k < N_{\text{new}}$, then Scenario 2 will be impossible as the tagged packet cannot be transmitted via an undue requested slot, and if $[(N_{\text{q}} + k) < [\gamma(1-d)/\eta]]$ then the k^{th} packet will certainly escape through a free-assigned slot (Scenario 1). These two constraints will be satisfied more frequently when $\eta \ll 1$ ($i.e. \tau_{\text{r}} \gg N\tau_{\text{slot}}$).

Therefore, the average service time that the k^{th} packet will take when it reaches the head of the node's queue will rely mainly on Scenarios (1 and 3) and can be expressed as :

$$E(Q) \approx \sum_{i=1}^{\Omega} p(1-p)^{i-N_{\text{new}}} i + [1 - \sum_{i=1}^{\Omega} p(1-p)^{i-N_{\text{new}}}][\Omega] \tag{6.10}$$

The first term in (6.10) represents the delay of the k^{th} packet when transmitted as Scenario 1 and the second term gives the delay of the k^{th} packet when transmitted as Scenario 3, and p is given by expression (6.8). Equation (6.10) can be simplified to:

$$E(Q) = \frac{[1-(1-p)^{\Omega+1}]}{p} - (\Omega+1)(1-p)^{\Omega} + \Omega(1-p)^{\Omega} \tag{6.11}$$

where Ω is a constant given by:

$$\Omega = \lceil \gamma \tau_{\text{r}} \rceil, \text{ and } p = \frac{1-d}{N} = \frac{(1-d)\gamma}{\eta\Omega}$$

For ($\Omega \gg 1$), as it is typically the case with underwater scenarios due to the large τ_{r}, E(Q) can be simplified to:

$$E(Q) \approx \frac{(1-e^{-\nu})}{p} \tag{6.12}$$

Where $\nu = (1-d)\gamma/\eta$. This simplification is based on the relation $e^{-\nu} \approx (1-(\nu/\Omega))^{\Omega}$. For small values of η, d will be small and as a result the ν value will be relatively large. Thus, $e^{-\nu} \ll 1$. For example when η and $d < 0.1, e^{-\nu}$ will be less then $1.4x10^{-6}$ which is negligible. This suggests that for a small η, i.e. long round trip delays τ_{r}, the average service time of a packet at the head of the node's queue is approximated as:

$$E(Q) = \frac{1}{p} = \frac{N}{(1-d)} \approx N \; for \; d \ll 1 \tag{6.13}$$

Hence, the mean value and the variance of the service time are N and $N(N-1)$ respectively. Plugging in the mean and variance values in the Pollaczek-Khinchin formula will result in the total waiting and service time as follows:

$$\bar{T} = N + \frac{\lambda N(N-1)}{2(1-\lambda N)} \tag{6.14}$$

where λ is the arrival rate per node in packets/slot, i.e. equivalent to Erlangs. The average packet end-to-end delay is then given by:

$$\bar{D} = \bar{T} + \bar{T}_{\mathrm{r}} \tag{6.15}$$

where $\bar{T}_{\mathrm{r}}$ is the packets average propagation delay of N nodes and can be obtained from:

$$\bar{T}_{\mathrm{r}} = \sum_{n=1}^{N} \frac{\gamma \tau_{\mathrm{r}}[n]}{N} \tag{6.16}$$

Figure 6.6a, Figure 6.6b and Figure 6.6c illustrate a good agreement between the simulation and analytical results using Equation (6.15). The results are obtained for various underwater scenarios and CFDAMA parameters which are detailed in section 6.3.1.

6.3 Performance Evaluation of CFDAMA-SRR

To enable the full realisation of the effectiveness of CFDAMA-SRR, the scheme has been simulated and investigated in detail. Comparisons with CFDAMA-RR, Round-Robin Free assignment, demand assignment and with the analytical model given in Equation (6.15) are shown in this section. Comparison with the STUMP protocol is also provided. In all the results presented, channel load is measured in Erlangs and represented as a fraction of the transmitted data. The channel is loaded up to its maximum useful data carrying capacity.

6.3.1 Simulation Setup

Our versatile simulation model built in Riverbed modeller (See section 5.1) is used to evaluate the performance of CFDAMA-SRR. To reflect on more realistic propagation of acoustic waves underwater, the BELLHOP program is employed to provide our Riverbed-based acoustic link with the actual acoustic propagation speed based on a realistic Sound Speed Profile (SSP). This section provides the simulation Setup details.

Speed of sound underwater

Figure 6.4 depicts a realistic SSP of a case derived by Dushaw [120] from the 2009 World Ocean Atlas temperature, pressure and salinity data at $(56.5^{o}N, 11.5^{o}W)$ in April, i.e. around the North Atlantic Ocean off the coast of the UK and Ireland. The SSP causes refraction of the propagated acoustic rays, which in turn results in curved trajectories. These trajectory

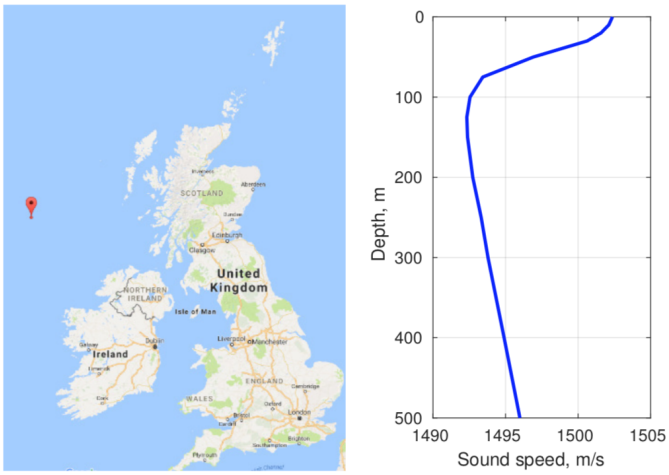

(a) Google Maps location (b) Sound speed profile

Fig. 6.4 Example of a SSP in the North Atlantic Ocean [2]

traces have been extracted using the BELLHOP ray tracing program and accurate propagation delays have been obtained.

Underwater acoustic channel model

With respect to the channel parameters utilised in section 4.3, a RM-based acoustic channel has been simulated. A vector containing the actual values of node-to-node propagation delays based on the SSP depicted in Figure 6.4 have been extracted from BELLHOP and imported into RM. An empirical model [1] is used to predict the underwater ambient noise based on the channel bandwidth given in table 6.3. The Thorp model is used to calculate the absorption coefficient in order to be used to estimate received power. Based on these parameters, the signal to noise ratio (SNR) experienced by each transmitted packet is evaluated, and subsequently, the Bit Error Rate (BER) is estimated to determine the packet's eligibility for a successful reception at its receiver. This BER is not the empirical rate of bit errors, but rather the expected rate based on a look-up table and the corresponding SNR value. The RM counts the number of bit errors in each packet and maintains a bit-error accumulator. The acceptability test of a packet at the receiver is based on both the interference between packets as well as the proportion of bit errors due to noise. If a non-zero-length packet overlap between successive packet arrivals is detected, the receiver rejects all packets involved in the overlap. If the number of bit errors in a packet exceeds a certain threshold, the receiver rejects the packet.

Table 6.3 Simulation parameters

Attribute	**Value**
Transmission Range	6×6 *km*
Number of Nodes	20, 50 or 100
Bandwidth	30 kHz
Data Rate	9600bps
Packet Size = Data Slot Size	64, 256, 512 bits
Data Slot Duration (τ_{data})	6.66, 26.66, 53.33 ms
Request Slot Size	8 bit
Request Slot Duration (τ_{rqt})	0.833 ms
Number of Data Slots in Frame (N_{ds})	650, 256 and 128
Number of Request Slots in Frame (N_{rs})	30, 40 and 50
Traffic Load Range	0.1 - 1 Erlangs

Network Topology and Simulation Parameters

With reference to Figure 6.2, different scenarios of three different network sizes (20, 50 and 100 nodes) and several packet durations are studied. Sensor nodes are distributed randomly across a coverage area of 6×6 *km*, using the RM simulator with a centralised gateway at a 20m depth just above the central point of the coverage area. The depths of sensor nodes obey a uniform random distribution and are located between 470 and 490 m. The selection of these parameters corresponds to a typical oil reservoir seismic monitoring scenario, e.g. [110]. They are chosen to be within the range of operating parameters of current commercial modems. For example, but not limited to, the EvoLogics S2CR 15/27 modem [111]. The trade-off between CFDAMA parameters is assessed. These scenarios can provide a range of different test options for performance evaluation of the CFDAMA schemes or comparison with other approaches in the literature. The simulation parameters are listed in Table 6.3. Using the given data slot duration (τ_{data}), request slot duration (τ_{rqt}), number of data slots (N_{ds}) and number of request slots (N_{rs}), one can obtain T_{frame} from Equation (6.1), which can be rewritten with respect to the aforementioned parameters as follows:

$$\begin{aligned} T_{\text{frame}} &= T_{\text{data}} + T_{\text{rqt}} \\ &= N_{\text{ds}}\tau_{\text{data}} + N_{\text{rs}}\tau_{\text{rqt}} \end{aligned} \tag{6.17}$$

6.3.2 Comparative Performance of CFDAMA-SRR

Figure 6.5 shows the mean end-to-end delay performance against a variety of channel loads ranging from 0.1 to 1 Erlang and based on both Poisson and Pareto ON/OFF traffic models. The graphs shown in the figure are for CFDAMA-SRR while the other variants of CFDAMA with different request strategies are shown later. The results show that like other CFDAMA variants, the CFDAMA-SRR scheme consistently outperforms its two constituent schemes (free and demand assignment) in both mean end-to-end delay and channel utilisation. The reason behind this is the nature of the CFDAMA mechanism in general which is more adaptive to variation in channel conditions; it exploits the advantages of its two underlying schemes based on the instantaneous channel load.

At low to medium channel loads, the delay performance with both traffic models is similar to the delay performance of the free assignment scheme, indicating that the DAMA scheme under these conditions is not invoked yet. This is attributable to the fact that the average packet arrival rate is slower than the rate of assigning free slots in a round-robin fashion due to the low level of burstiness. Up to approximately 50% of the channel capacity, the mean end-to-end delay is close to its minimum and is greater with Poisson than Pareto ON/OFF traffic types. This behaviour is attributable to the periodic ON/OFF nature of the traffic source and how often the packet arrivals within bursts are. In this instance, the uniform regularity of low traffic ON/OFF source leads to that every packet could potentially be transmitted in the first free allocated slot just after its arrival. Whereas, with Poisson traffic, the scenario is different in that several packets could arrive between successive free slot allocations in some cases.

Above 50% of channel capacity, the end-to-end delay is much higher with the Pareto ON-OFF traffic because of the greater burstiness of the ON-OFF data traffic. This is because of the statistics of Pareto ON/OFF data traffic which produce a longer period of time during which the number of nodes generating bursts exceeds a certain sustainable number. If a long burst of packets is generated from a Pareto ON/OFF source, a substantial number of packets will start to build up in the node's queue. This will then result in significant demand by this node and subsequent slot allocation. It means the node will dominate the return frame for a significant period of time. All this will eventually cause a dramatic increase in the mean end-to-end delay at very high channel loads. A key point to note from these results is that despite the significantly longer burstiness of the Pareto ON/OFF traffic compared with traditional Poisson, the CFDAMA-SRR scheme is still capable of providing good end-to-end delay performance up to 90% of channel capacity.

It is worth mentioning that the free and demand assignment schemes begin to suffer from instability after the channel load exceeds 85%, especially with the Pareto ON/OFF traffic

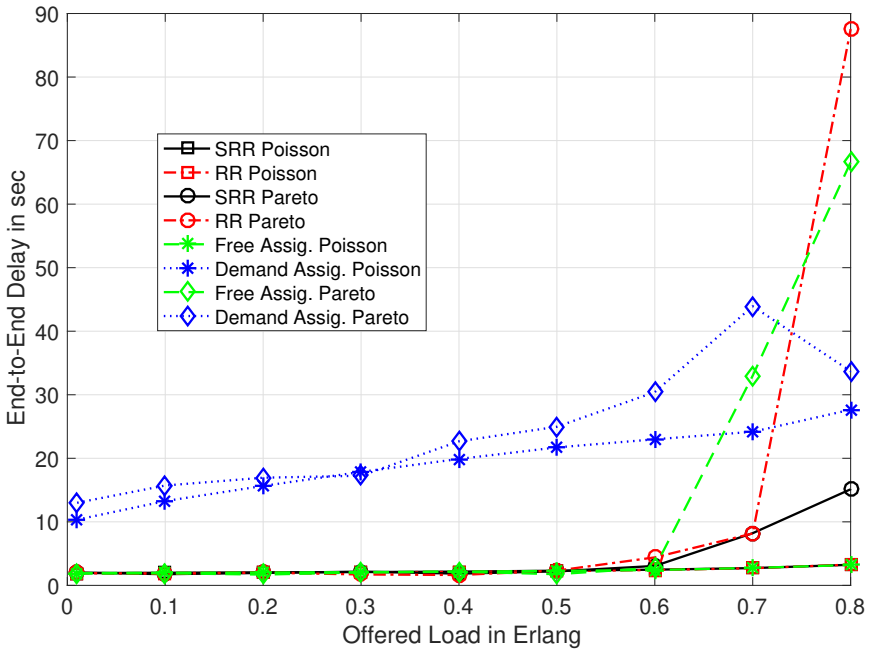

Fig. 6.5 Comparative delay/utilisation performance - 100 Nodes

source. This causes a significant increase in the spread of end-to-end delay values with a considerable increase in the proportion of packets experiencing very long end-to-end delay. At such very high channel load, the traffic source becomes able to offer instantaneous load levels exceeding the channel capacity over a significant periods of time. During these periods, packets continue to build up in the sensor node queues until the load level drops below the channel capacity. The CFDAMA-SRR scheme can cope with such statistical variations in the traffic source level up to higher channel load levels as the following section describes.

SRR vs. RR The results in Figure 6.6a, Figure 6.6b and Figure 6.6c clearly indicate that the CFDAMA-SRR scheme outperforms its underlying scheme CFDAMA-RR in terms of end-to-end delay and channel utilisation with the Poisson traffic model and different numbers of nodes (20, 50 and 100 nodes respectively). CFDAMA-SSR experiences the lowest end-to-end delay throughout almost all channel loads shown in the figures with all simulated network sizes. The minimum end-to-end delay that CFDAMA experiences is at very low traffic load; when the majority of the slots are freely assigned. At high channel loads, the end-to-end delay steadily increases, but the experienced delay rises more slowly with CFDAMA-SRR compared with CFDAMA-RR. As shown in Figure 6.6c, at a channel utilisation of 1% of the channel capacity and 100 nodes, the minimum end-to-end delay is only 2 s with both traffic models. At a high channel load of 80%, the mean end-to-end

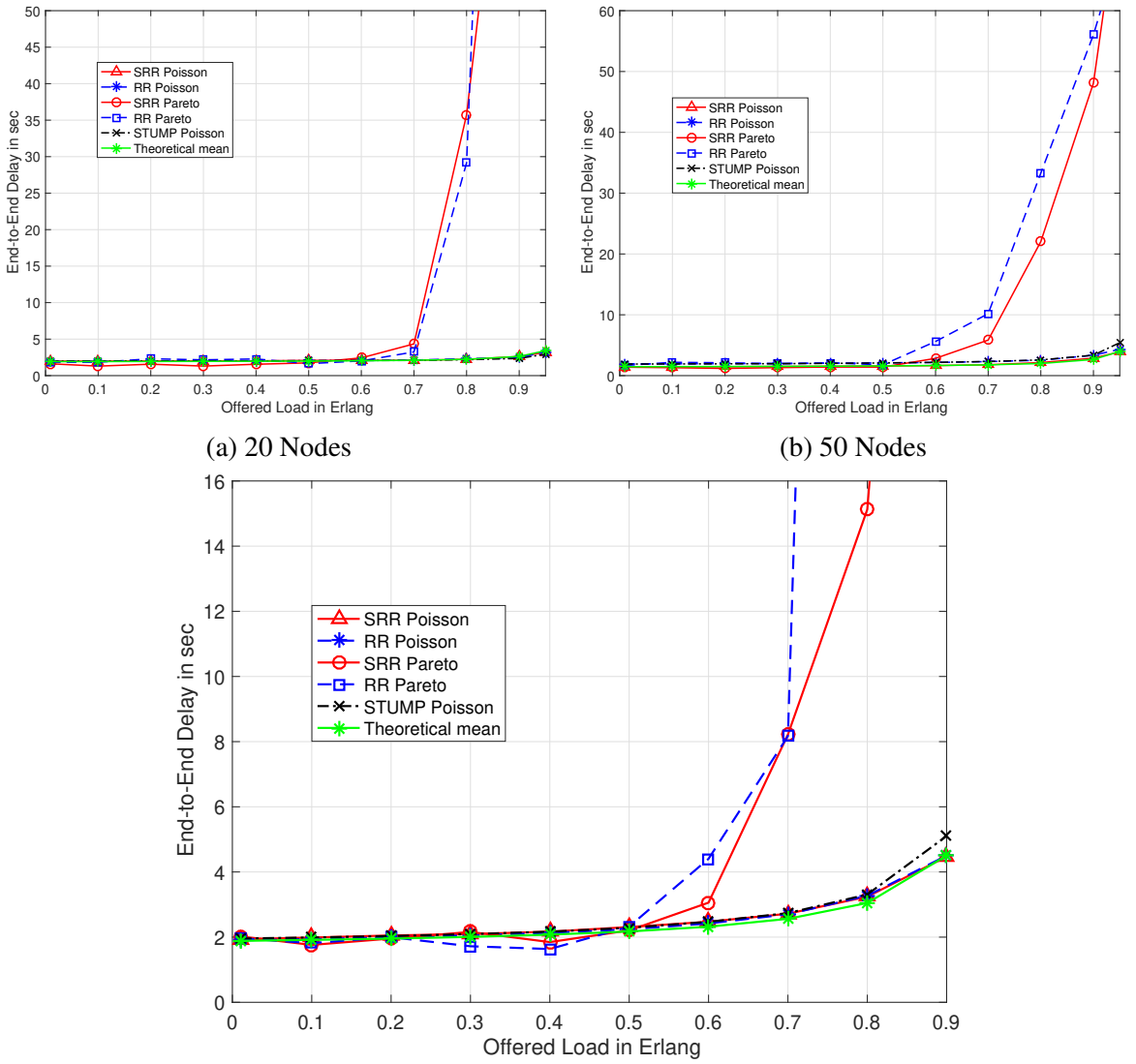

(a) 20 Nodes

(b) 50 Nodes

(c) 100 Nodes

Fig. 6.6 The delay/utilisation performance of CFDAMA-SRR vs Round Robin Free assignment vs STUMP with different number of nodes. 64-bit packets and 9.2 bit/s

delay is still the lowest at 3 s with Poisson and 15 s with Pareto ON/OFF. This enhanced performance of CFDAMA-SRR can be attributed to a number of reasons:

- The scheme has a bias against transmissions associated with long round-trip demand assigned slots. The queuing time is correlated to the location of the node. Nodes that are located further from the gateway will have more availability of queued packets. Far nodes will also be able to efficiently exploit their request opportunities, and hence, the farther away the node is, the larger number of packets will be served in a request opportunity.

- It allows those nodes which are located closer to the gateway to make their requests first rather than potentially waiting for multiple CFDAMA frames. In the meantime, it allows more time for those nodes which are located further away from the gateway to maximise the use of the available free assigned slots rather than wasting them.
- For the same two reasons above, the likelihood of wasting free assigned slots in some cases due to the potential absence of queued packets at sensor nodes is very low.

Not only is the validity of these reasons supported by the delay analysis done in section 6.2.2, which proves the direct relationship between the round trip delay and free request slots availability, but it is also supported by the CDF results described in section 6.3.4.

SRR vs. STUMP STUMP represents an excellent TDMA-based solution in terms of throughput, by transmitting data packets without MAC overhead. It achieves high utilisation by exploiting node location diversity to overlap node transmissions and enable ordered packet arrivals. However, its delay/utilisation performance dependent on the accuracy of its ordering algorithm. Also, it does not have a mechanism to respond to individual node requirements. Its waiting and service time increases as the value of channel load increases.

Figure 6.6a, Figure 6.6b and Figure 6.6c indicate that in virtually all cases both schemes perform similarly. The reason behind this similarity in performance is the limited burstiness of the Poisson traffic that cannot offer substantial demands for excessive periods of time long enough to enable demand assigned slots to contribute effectively. In contrast, free assigned slots in this instance can contribute more effectively to support the transmission of independently generated packets. The overhead of CFDAMA-SRR is negligible in these scenarios owing to long CFDAMA frames. With low channel loads, most of the data slots in the CFDAMA return frame are freely assigned, and hence, the resulting delay/utilisation performance is independent of the request strategy. At high offered load values and 100 nodes, CFDAMA-SRR has a small advantage over STUMP in terms of end-to-end delay. This is attributable to the increased demand made for packets having exponential inter-arrival time, and the fact that the TDMA slots assigned periodically by STUMP cannot be as effective as the on-demand slots assigned by CFDAMA-SRR at such high load levels. At a high channel load of 90%, the mean end-to-end delays are around 4.5 s with CFDAMA-SRR and 5.1 s with STUMP.

6.3.3 Performance of CFDAMA-SRR with Different Parameters

Request Strategy Figure 6.7a illustrates the delay/utilisation performance of CFDAMA with Poisson modelled traffic and different request strategies. It can be seen that the choice

of request strategy has a small effect on the performance over some parts of the offered load range, becoming clearer at high channel loads with the Pareto ON/OFF traffic whose results are shown in the opposite figure - Figure 6.7b. Considering the results in Figure 6.7b obtained with Pareto ON-OFF traffic source, it can be seen that the SRR strategy exhibits superior delay/utilisation performance at high channel loads due to its substructure - the RR strategy. This is primarily attributable to the fact that CFDAMA-SRR limits the chances of wasting free assigned slots and also biases against demand assigned slots associated with long round trip delays.

Moreover in Figure 6.7b, at high channel loads, the end-to-end delay rises rapidly and CFDAMA with both request strategies becomes less effective under Pareto ON/OFF traffic when the channel is loaded beyond 80% of its capacity. Despite the long burstiness and high channel load, the CFDAMA-SRR scheme is still able to provide acceptable utilisation performance up to 85% of channel capacity. Results in both figures (Figure 6.7a and Figure 6.7b) also show that the other request strategies (PA and CR) are also outperformed by SRR with Pareto ON/OFF traffic. In the PA strategy, a small number of nodes hog the channel, which inhibits other nodes from making strongly needed requests. The CR strategy overcomes this issue by combining the PA strategy with the RA strategy, but it still cannot outperform SRR. The CFDAMA-SRR scheme with Pareto ON/OFF traffic has a mean end-to-end delay of around 14 s at channel load of 80% whereas it is above 40 s with the RR scheme.

Considering different numbers of request slots for the CFDAMA-SRR schemes, Figure 6.8a and Figure 6.8b show the delay/utilisation performance with both Poisson and Pareto ON/OFF traffic respectively. It can be seen that changing the number of request slots has almost no noticeable impact on the delay performance at low and medium channel loads with either traffic model.

Number of Request Slots Over the first half of the load range, CFDAMA-SRR relies mainly on the free assignment strategy where request slots are not necessarily required. At high channel loads of Pareto ON/OFF traffic up to 80% of channel capacity, the performance shows a much more sensitive response to the changes in the number of request slots. This is because the increasing number of request slots results in a rise in the frame overhead and a growth in wasted capacity due to unused request slots. However, a small number of request slots cannot cope with the increasing channel demand, causing an increase in the delay to make requests and obtain assigned slots. With 50 request slots, the mean end-to-end delay is around 8 s at a load of 70% of channel capacity. At high channel loads, decreasing the

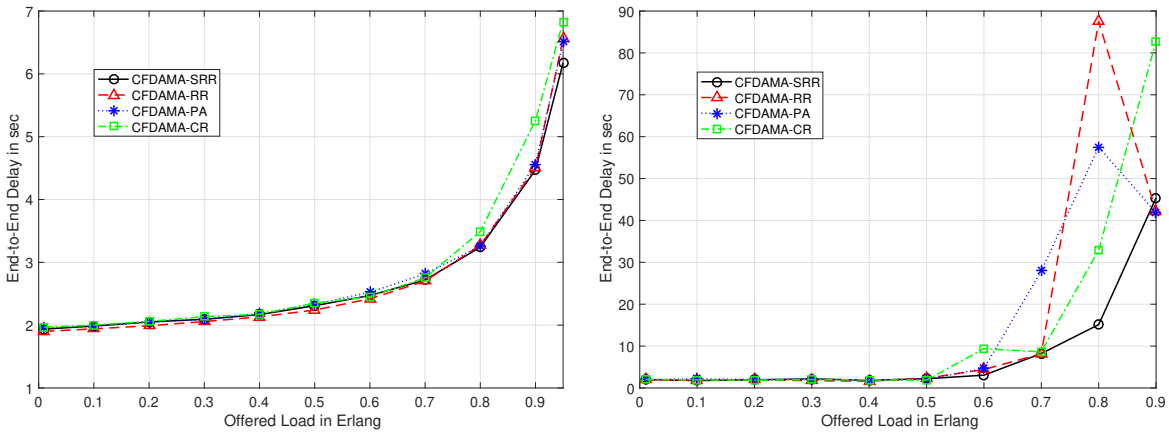

(a) With Poisson traffic (b) With Pareto ON/OFF traffic

Fig. 6.7 The delay/utilisation performance of CFDAMA with different request strategies and two distinct traffic types; 64-bit packets; 9.6 kbit/s

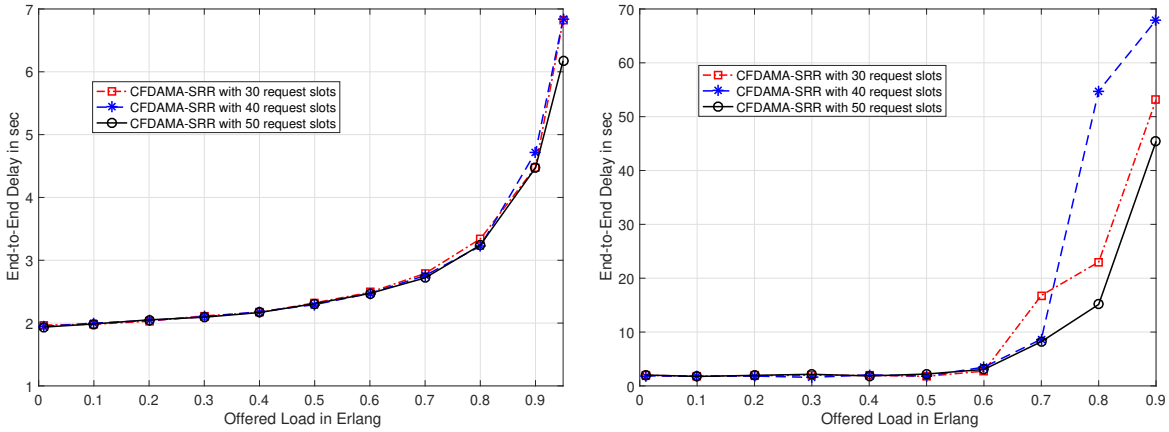

(a) With Poisson traffic (b) With Pareto ON/OFF traffic

Fig. 6.8 The delay/utilisation performance of CFDAMA with different number of request slots and two distinct traffic types; 64-bit packets; 9.6 kbit/s

number of request slots to 40 slots and then 30 slots resulted in longer delays and inferior channel utilisation at high channel loads with Pareto ON/OFF traffic.

Data Packet Size The impact of different packet sizes on the CFDAMA-SRR performance is shown in Figure 6.9a and Figure 6.9b with Poisson and Pareto ON/OFF traffic types respectively. The scheme performs better with short packets. This is attributable to the low data rate used, which is the typical data rate of underwater modems. Long packet demand long slots in a CFDAMA frame and long slots can make it less regular for slots to be freely assigned as the free slots are assigned using a round robin method. This increases the average

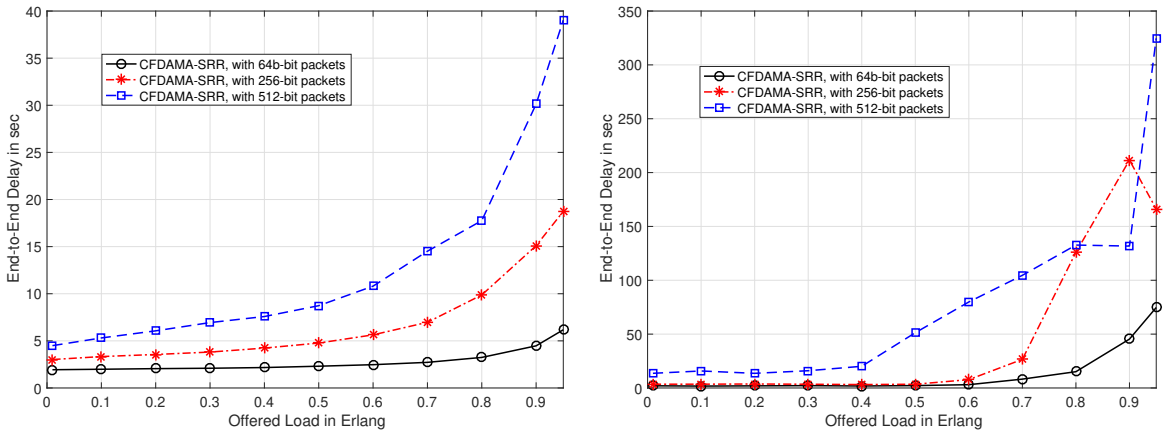

(a) With Poisson traffic (b) With Pareto ON/OFF traffic

Fig. 6.9 The delay/utilisation performance of CFDAMA-SRR with different packet lengths and two distinct traffic types; 9.6 kbit/s

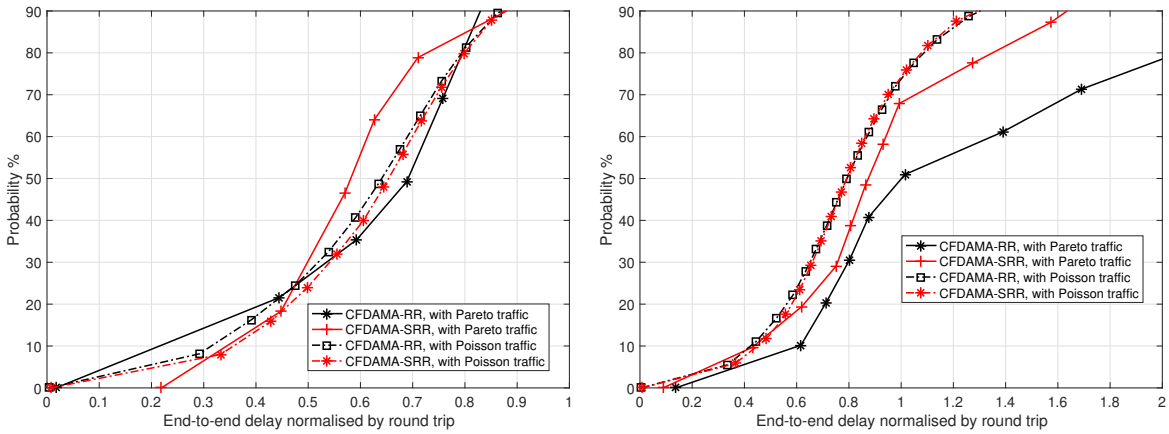

(a) 30% offered load (b) 60% offered load

Fig. 6.10 End-to-end delay distribution with two distinct traffic types; 650 of 64-bit data slots and 50 of 8-bit request slots per frame

end-to-end delay for long packets transmission. The resulting delay/utilisation characteristics with Pareto ON-OFF traffic are more sensitive to the packet size than the characteristics resulting from Poisson traffic. These results put further emphasis on the notion that it is the periodic ON-OFF nature of the self-similar traffic type that is behind most of the performance differences with the Poisson traffic type. Unlike with Poisson traffic source, the CFDAMA delay performance with Pareto ON-OFF traffic source and 1024-bit packets experienced a degradation. This is due to the heavy tail of the Pareto distribution with a high probability of long ON or OFF periods when such long packets are used.

6.3.4 End-to-End Delay Distribution

Figure 6.10a and Figure 6.10b shows the CDF of the end-to-end delay (normalised by the average length of a round trip) of all packet transmissions for the two strategies (SRR and RR) with 100 nodes and with the two traffic models (Poisson and Pareto ON/OFF) at both 30% and 60% load values. For the same reasons explained above, the superiority of SRR is particularly manifested at high channel loads with Pareto ON-OFF traffic. At the 30% offered load value, 90% of packets with both traffic models do not exceed the delay boundary of a round trip. This indicates all these packets are transmitted through free assigned slots. At the 60% offered load value, 35% of RR packets with Pareto ON/OFF experienced longer delays than a round trip delay, whereas 85% of SRR packets do not exceed the boundary of a round trip time. This supports the theory of how the SRR packet transmissions benefit from systematising the distribution of request opportunities based on node locations. Because 85% of SRR packets did not exceed the delay limit of an average round trip, they must have been transmitted either through free or undue transmission slot (Scenario 1 and 2 described in section 6.2.2). This meets the expectation that SRR increases the probability that a single request is utilised rather than multiple requests for the same demand. With Poisson traffic, both strategies perform similarly and allow 90% of packets to arrive at the destination node within a round trip time.

6.4 CFDAMA-NoClock: MAC Protocol for Underwater Acoustic Sensor Networks

The primary notion behind the CFDAMA without clock synchronisation (CFDAMA-NoClock) scheme proposed in this section is to achieve an adaptive TDMA protocol enabling back-to-back packet reception at the gateway node without the need of global timing (i.e. a synchronised clock at every node). This is attained using a method of relative timing in which the clock of each individual node is independent of other nodes and each node is regularly given the necessary instructions in order to track timing drift and data transmission offset. With respect to Figure 5.3, the gateway node, acting as a usual CFDAMA coordinator, needs to be able to estimate the propagation delay to every sensor node and piggyback timing instructions in the acknowledgement packet transmitted during the CFDAMA forward frame. The following subsections describe the principle of the CFDAMA-NoClock scheme.

6.4.1 Motivations and Related Work

Morozs et al. [2] introduced an underwater MAC protocol, called Transmit Delay Allocation MAC (TDA-MAC), incorporating a scheduling algorithm that allows a TDMA-like slotted packet reception at the gateway without the need for local synchronisation with a global clock. There, for each data transmission cycle (i.e. TDMA frame), the gateway broadcasts a single packet (REQ in Figure 6.11) to trigger the transmission of one data packet, if any, per sensor node, in a timely manner. In every sensor node, the transmission of a data packet is timed to happen in a certain instructed period of time referenced to the reception of the REQ packet. To this end, the protocol requires a set-up stage in which propagation delays between ever sensor node and the gateway are estimated and a transmit delay instruction (TDI) packet is sent to every sensor node ($\tau_{\mathrm{p}}[n]$ in Figure 6.11). The gateway is able to periodically assess the accuracy of the measured propagation delays by comparing the expected and the actual time of arrival of data packets. If error values exceed a certain sustainable limit, the gateway node can then update the TDI packets accordingly. The advantages of TDA-MAC over previous schedule-based protocols is the practicality and simplicity of its synchronisation algorithm, making it suitable for large-scale UASNs. The developers of TDA-MAC highlight some limitations which are overcome via an enhanced variant called Accelerated TDA-MAC (ATDA-MAC), also proposed in [2]. These limitations are primarily related to the achievable channel utilisation and can be outlined as follows:

- The waiting time between triggering the transmission from sensor nodes and receiving the first subsequent data packet brings about an equivalent channel utilisation gap proportional to the shortest round trip propagation time from the gateway to sensor nodes.
- The protocol is sensitive to the duration of data packets, the population density and the spatial distribution of nodes. The achievable channel utilisation is inversely proportional to the duration of data packets with respect to the average round trip propagation time from the gateway to the sensor nodes.
- In certain cases depending on the statistical behaviour of the data traffic source (i.e. packet inter-arrival time), in-between gaps may occur amongst the successive data packets received at the gateway, gaps that cannot be utilised for useful data transmissions no matter how short the allocated transmit delay is.

In order to overcome the aforementioned limitations, [2] suggests the possibility of using two channels one of which is dedicated to data packets only, while the other is dedicated for REQ packets. Unlike in TDA-MAC, the two-channel protocol can allow the broadcast

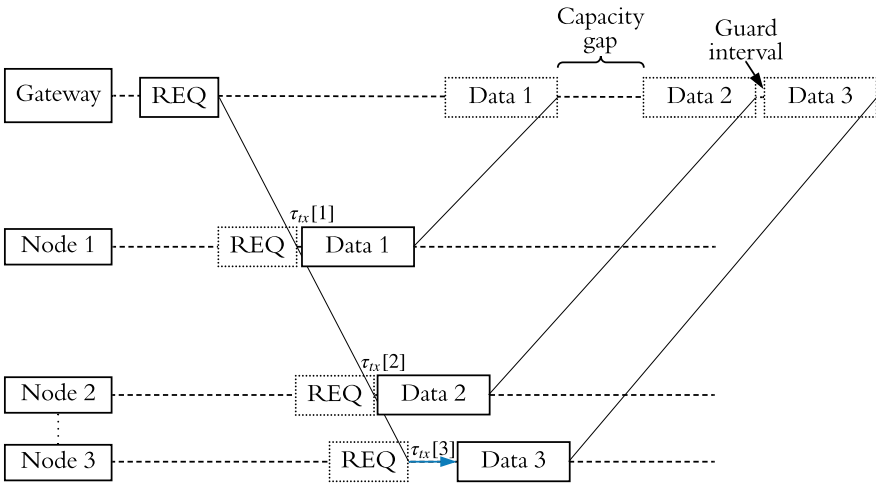

Fig. 6.11 Packet flow in TDA-MAC; REQ - data request packet, gaps in channel utilisation using TDA-MAC due to nodes' spatial distribution and short packet

of the next REQ packet before the end of the current TDMA frame rather than waiting until receiving the data packets from all sensor nodes. With ATDA-MAC, only the guard intervals, if any, will hold the protocol from achieving 100 % throughput, provided the use of appropriate packet and frame lengths with optimal REQ packet scheduling. However, like with any other fixed TDMA protocols, achieving high channel utilisation is subject to the presence of full buffer traffic source. ATDA-MAC does not incorporate a mechanism allowing adaptation to the changes in the statistical behaviour of the data traffic source and the instantaneous demand of individual sensor nodes. If every node is enabled to transmit a run of successive packets as demanded after receiving the REQ packet, then the protocol will act as an adaptive TDMA. In the next subsection, we introduce a new CFDAMA variant inspired by the notion of no clock synchronisation. The primary motivations for this new scheme can be summarised as follows:

- It boosts the practicality of CFDAMA underwater as it allows its scheduling algorithm to operate with no clock synchronisation amongst the network nodes.
- It can provide high channel utilisation and allows it to approach the theoretical maximum with controlled end-to-end delay performance.
- It enables instantaneous adaptation to the variation in data traffic conditions in terms of the duration of a specific burst, inter-burst gaps, the duty cycle of bursts and the channel load level.

6.4.2 The CFDAMA-NoClock Scheme

The original CFDAMA variant suiting the new scheme is CFDAMA-PB, which piggybacks capacity requests onto data packets. Being a TDMA-like protocol increases its compatibility with our NoClock scheduling algorithm. The implementation of CFDAMA-PB in the context of ATDA-MAC requires an initial set-up stage prior to the actual data transmissions. In this initial stage, the propagation delays between the gateway and sensor are accurately measured via a handshaking technique, described in detail in section (3.1). This process lasts for a short period of time typically of the order of several minutes depending on the density of nodes and their spatial distribution.

Once it works out all the propagation delays, the scheme can begin the data packet transmission stage. To enable CFDAMA-PB to operate without a synchronised clock, a number of adjustments are required. The acknowledgement packets sent during the CFDAMA forward frame will be replaced by a packet acting similarly to the REQ packet of TDA-MAC, but with an extra payload. Instead of sending an exclusive packet to every sensor node to inform them with their allocated free or demand slots, a single packet denoted by ACK-REQ is broadcast to inform every node the number of successive slots allocated (N_{rs}) to it and the amount of time, delay-to-slot (DTS), the node has to wait before it can start a run of successive packet transmissions as allocated. DTS acts similarly to the TDI packet of TDA-MAC, but the Tx delays are calculated significantly differently. The CFDAMA return frame will remain operating as usual, as described in section (CFDAMA-PAR), except for the fact that at every snore node, the transmission of N_{rs} data packet(s) cannot begin until it receives the ACK-REQ and waits the amount of time that is stated in the DTS segment of the ACK-REQ packet. This process is depicted in Figure 6.12. There, the gateway broadcasts an ACK-REQ packet on the forward channel to be received by every node at different arrival times due to them being located at different locations. Upon the arrival of the ACK-REQ packet, the concerned node waits the appropriate amount of time, and then, transmits a run of N_{rs} data packets. On condition that the appropriate CFDAMA frame length and forward frame delay are used, this process leads to CFDAMA-like packet arrival at the gateway without the need for clock synchronisation amongst sensor nodes. This packet reception is illustrated in Figure 6.12.

6.4.3 CFDAMA-NoClock: Calculating Delay-to-Slots

The gateway node constructs the DTS segment of the ACK-REQ packet that needs to be transmitted to every sensor node on a frame-by-frame basis in order to assign the Tx delays. The Tx delay for the n^{th} node, where $n = 2,3,...,N$ is given by:

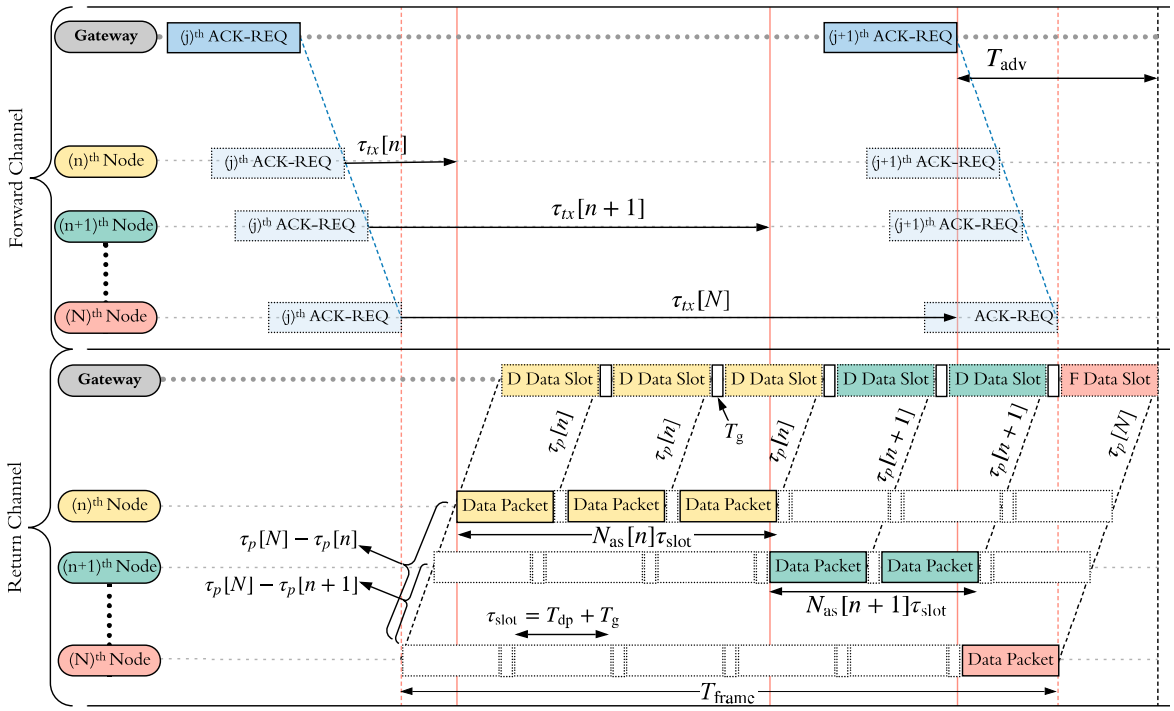

Fig. 6.12 An arbitrary CFDAMA-NoClock transmission cycle with its two channels working concurrently; ACK-REQ - acknowledgement and data request packet

$$\tau_{\mathrm{tx}}[n] = 2(\tau_{\mathrm{p}}[N] - \tau_{\mathrm{p}}[n]) + \sum_{i=1}^{n-1} (N_{\mathrm{as}}[i]\tau_{\mathrm{slot}}) \tag{6.18}$$

where $\tau_{\mathrm{p}}[n]$ is the propagation delay from the gateway to the n^{th} sensor node, N^{th} sensor node is the farthest node from the gateway, $\tau_{\mathrm{tx}}[n]$ is the delay-to-slot assigned to the n^{th} sensor node, N_{as} is the number of data slots assigned to the n^{th} node in the current frame and τ_{slot} the duration of data slot which must satisfy the following constraint:

$$\tau_{\mathrm{slot}} \geqslant T_{\mathrm{dp}}[n] + T_{\mathrm{g}}[n] \tag{6.19}$$

Where $T_{\mathrm{dp}}[n]$ is the duration of the n^{th} node's data packet including the segment of its capacity requests and $T_{\mathrm{g}}[n]$ is the guard interval after the n^{th} node's data packet reception at the gateway. If the CFDAMA-PAR variant is used rather than CFDAMA-PB, an additional term must be added to 6.19 to take into account the duration of interleaved capacity request slots. In every round of transmitting an ACK-REQ packet, two vectors: $\tau_{\mathrm{tx}} = (\tau_{\mathrm{tx}}[1], \tau_{\mathrm{tx}}[2], ..., \tau_{\mathrm{tx}}[N])$ and $N_{\mathrm{as}} = (N_{\mathrm{as}}[1], N_{\mathrm{as}}[2], ..., N_{\mathrm{as}}[N])$ are constructed at the gateway node, sorted based on the n^{th} node's location from nearest to farthest from the gateway and loaded onto the ACK-REQ packet. There is an exception for the first round, in which the gateway assigns a free slot to

Algorithm 3 CFDAMA-NoClock algorithm implementation on the gateway node; ACK-REQ - CFDAMA acknowledgement and data request packet

for every sensor node ($n = 1, 2, 3, \ldots N$) **do**
  Transmit PING packet to n^{th} sensor node
  Wait for PING packet back from n^{th} sensor node
  Calculate propagation delay $\tau_{\mathrm{p}}[n]$ to n^{th} sensor node
end for
Calculate Tx delay $\tau_{\mathrm{tx}}[n]$ for every n using (6.18)
Determine the D/F slot allocation according to CFDAMA-PB rules
Construct τ_{tx} and N_{as} vectors and Load them onto ACK-REQ packet
Broadcast the ACK-REQ packet
while CFDAMA slot jitter is below threshold (no collisions) **do**
  Measure the errors between expected and actual data packet arrivals
  if CFDAMA slot jitter is above a threshold **then**
    Compensate for propagation delay estimation errors using the actual value
    Go to Step 6
  end if
end while

Algorithm 4 CFDAMA-NoClock algorithm implementation on a sensor node; TDI - ACK-REQ - CFDAMA acknowledgement and data request packet

if PING packet received from gateway node **then**
  Transmit PING packet back to gateway node
end if
if ACK-REQ packet received from gateway node **then**
  Schedule packet transmission with allocated delay and for N_{as} successive data packets
end if

every sensor node ($N_{\mathrm{as}}[n] - 1$) because capacity requests have not been made at this point in time.

Algorithm 3 shows the implementation steps taken at the gateway node to run the CFDAMA-NoClock protocol. Algorithm 4 shows the implementation steps taken at every sensor node to operate in accordance with the proposed protocol. The complexity and computing requirements are low at the sensor nodes; The algorithm demonstrates these vital features with only two basic reactive operations. Most of the processing requirements of the scheme are at the gateway node.

6.4.4 CFDAMA-NoClock: Scheduling the CFDAMA Forward Frame

Following the process of measuring all propagation delays to the sensor nodes, the gateway has to establish the offset time between the CFDAMA forward and return frames (known as

forward frame delay, see Figure 6.3). In other words, it has to determine during the current return frame the proportion of slots over which the transmission of the next ACK-REQ packet takes precedence. For instance, the illustrative chronology in Figure. 6.12 shows that the gateway brings forward its ACK-REQ packet transmission by more than 1.5 data slots. This proportion is denoted by T_{adv} in the following description. Theoretically, the larger the T_{adv} is, the less the gap between successive CFDAMA return frames will be, which results in better channel throughput. However, a constraint has to be satisfied in order not to over accelerate the next return frame and cause frame overlap with the current return frame at the gateway:

$$T_{\text{adv}} = \max_{n=1\ldots N} \left\{ n \mid n\tau_{\text{slot}} \leqslant 0.5\tau_{\text{p}}[N] \right\} \tag{6.20}$$

where $T_{\text{g,rp}}$ is the guard interval between the transmission of an ACK-REQ packet and the adjacent data packet reception. This constraint ensures that, for every slot over which the transmission of ACK-REQ takes precedence, the new ACK-REQ packet does not arrive at the concerned node, which will utilise this slot, before it completes the transmission of the previous data packet.

6.4.5 CFDAMA-NoClock: Optimal CFDAMA Frame Length

Whilst the maximum limit of the CFDAMA return frame interval is extendible based on the desired delay/utilisation performance, its shortest interval has a certain limit given the no-synchronised-clock circumstances. Ideally, the gateway node is required to transmit at least one broadcast ACK-REQ packet during the interval over which the data packets from all sensor nodes assigned capacity are received. This interval will then be the minimum duration of the CFDAMA return frame T_{frame}. Therefore, this T_{frame} has to satisfy the two constraints:

$$\begin{aligned} T_{\text{frame}} &\geq T_{\text{min,delay}} \\ T_{\text{frame}} &\geq T_{\text{min,demand}} \end{aligned} \tag{6.21}$$

where $T_{\text{min,delay}}$ is the constraint placed by the longest round-trip propagation delay, $\tau_{\text{p}}[N]$, between the gateway and the sensor nodes, and $T_{\text{min,demand}}$ is another important constraint placed by the channel full capacity in terms of data carrying capacity, i.e. if the former constraint is not the limiting factor, the latter is, in which case the performance is limited by the packet duration, capacity demand and statistical behaviour of the data traffic source.

The first constraint $T_{\text{min,delay}}$ is calculated using the following expression:

$$T_{\text{frame}} \geq \max_{n} \tau_{\text{p}}[n] - \min_{n} \tau_{\text{p}}[n] \tag{6.22}$$

where T_{frame} is the frame interval. This expression states that the frame length cannot be shorter than the difference between the longest and the shortest round-trip delays to ensure receiving at least one data packet, if any, from the farthest sensor node.

In the second case, he data carrying capacity constraint on T_{frame} is given by the following expression:

$$T_{\text{min,demand}} = \sum_{n=1}^{N} N_{\text{as}}[n] \left(T_{\text{dp}}[n] + T_{\text{g}}[n] \right) \tag{6.23}$$

The expression ensures that the minimum T_{frame} should not be smaller than the duration of all data packets of the current cycle plus the guard intervals amongst them. Taking both constraints into account, the minimum possible interval between two consecutive ACK-REQ packet transmissions can then be expressed as:

$$T_{\text{frame,min}} = \max \left(T_{\text{min,delay}}, T_{\text{min,demand}} \right) \tag{6.24}$$

In practice, this frame interval is typically specified to a given application based on how frequently the sensor readings require gathering. The CFDAMA-PB scheme can give its best delay/utilisation performance when $N\tau_{\text{slot}}$ is set to be close to the $2\max_n \tau_{\text{p}}[n]$, composed of N_{slots} data slots where $N_{slots} \geqslant N$. This ensures that a larger number of nodes, if not all nodes, can make a capacity request in every return frame. The suitable frame and data-slot durations are chosen on the basis of the desired channel capacity and transmission rate of a given application taking into consideration constraint 6.24.

6.4.6 CFDAMA-NoClock: Achievable Channel Utilisation

The maximum achievable channel utilisation of CFDAMA-NoClock is limited to the maximum channel utilisation of the no-synchronised-clock algorithm and CFDAMA-PB capacity overhead, which can be approximated as follows:

$$\gamma_{max} = \frac{(1-\vartheta) \sum_{n=1}^{N_{\text{slots}}} T_{\text{dp}}[n]}{\sum_{n=1}^{N_{\text{slots}}} \left(T_{\text{dp}}[n] + T_{\text{g}}[n] \right) + T_{\text{rs}}[n]} \tag{6.25}$$

Where ϑ is the fraction of packet overhead due to the embedded capacity requests. This expression states that the guard intervals and packet overheads are the primary cause of throughput loss. Achieving this throughput is conditional on the elimination of any potential gaps interleaving adjacent CFDAMA-PB frames (i.e. gaps separating every set of packet reception). To achieve this optimal throughput performance, the interval of the frame should

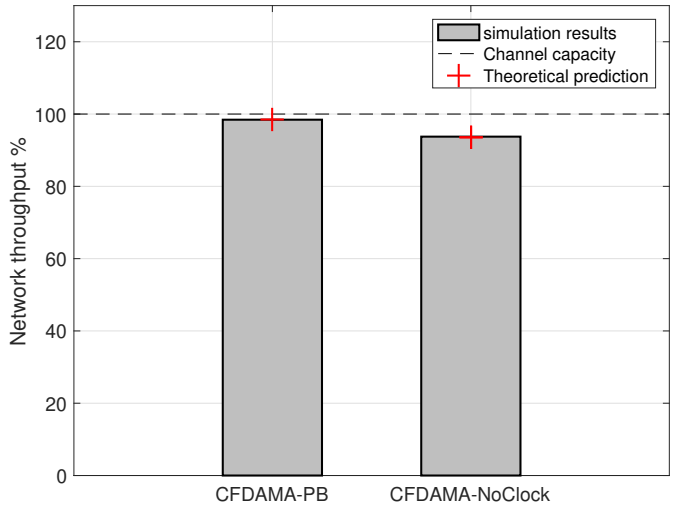

Fig. 6.13 Network throughput achieved by CFDAMA-NoClock and CFDAMA-PB under Poisson data traffic. The simulation results are compared with the analytical prediction given by Equation (6.25); packet size 512 bit and data rate 9.2 kbit/s

be at least $2\tau_p[N]$, and the proportion of data slots over which the transmission of the next ACK-REQ packet takes precedence should be: $T_{adv} = 0.5\tau_p[N]$.

6.5 Performance Evaluation of CFDAMA-NoClock

In this section, the performance of CFDAMA-NoClock is evaluated using our versatile CFDAMA simulation model built in Riverbed Modeller for the UASN model depicted in Figure 6.2. We compare the performance of the proposed scheme with that of an optimal CFDAMA-PB scheme, under both periodic data gathering obeying Pareto ON/OFF traffic and random Poisson traffic conditions. The simulation setup described in section 6.3.1 is used for this performance evaluation. With reference to Figure 6.2 and Table 6.3, the network topology and simulation parameters described in section 6.3.1 are used respectively. Figure 6.13 is a bar chart representing the network throughput achieved at the gateway working as a sink receiving collected data from all sensor nodes. Here, throughput is defined as the proportion of the successful data transmission that is effectively used to transfer new information after an amount of traffic is placed on the channel, expressed in Erlangs or as a percentage of the channel capacity, i.e the overall data carrying capacity. Achieving 100% channel utilisation is attained by a corresponding channel load of 100%, or 1 Erlang to achieve a certain level of throughout determined by the MAC scheme. The chart shows

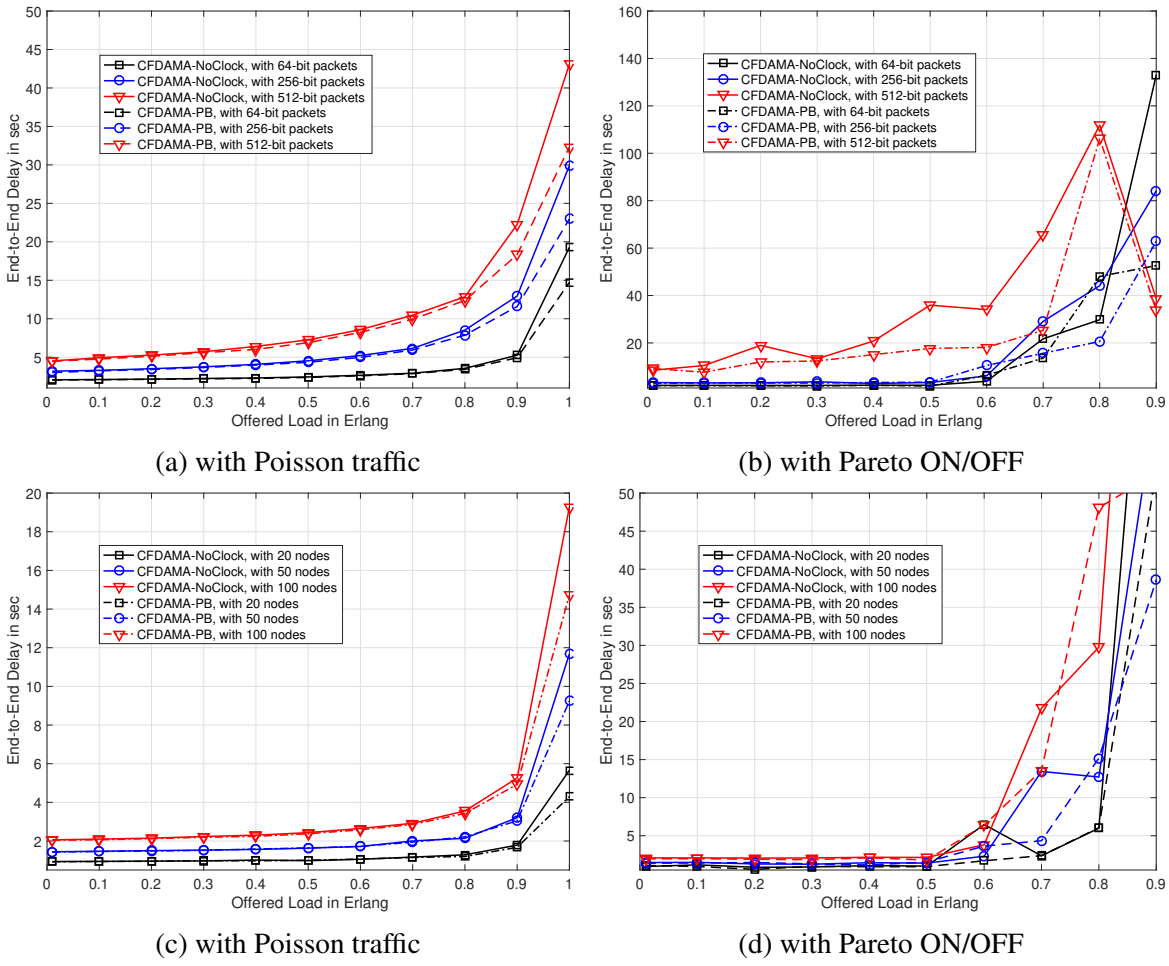

(a) with Poisson traffic

(b) with Pareto ON/OFF

(c) with Poisson traffic

(d) with Pareto ON/OFF

Fig. 6.14 The delay/utilisation performance of CFDAMA-NoClock vs CFDAMA-PB with different 20, 50 and 100 nodes; 64, 256 and 512 bit packets and 9.2 bit/s; and two distinct traffic conditions

the throughput performance of CFDAMA-NoClock and the synchronised CFDAMA-PB for a baseline comparison. It also compares with the analytical predictions of the optimal CFDAMA-NoClock throughput given by Equation (6.25).

The results in Figure 6.13 indicate that there is a negligible difference in throughput performance between CFDAMA-NoClock and synchronised CFDAMA-PB in all three simulated scenarios. This demonstrates that CFDAMA-NoClock can achieve the performance of ideal CFDAMA-PB without the need for a synchronised clock in every sensor node. The primary source of capacity waste in the case of CFDAMA-NoClock is the guard intervals amongst data packets, suggested being 5% of the data packet length. In practice, the length of the guard interval can be set to be a more realistic value suiting a given network deployment experiencing certain multipath spread, motion of nodes, and/or propagation delay jitter. Fur-

thermore in Figure 6.13, the comparison with the analytically predicted values of the network throughput indicates that Equations (6.25) provides a good performance estimate based on the system parameters, e.g. packet duration, guard intervals and packet overhead. The very slight disagreement between the analytically predicted optimal throughput performance of CFDAMA-NoClock and the simulation outcome is attributable to the collection time, i.e. the time between the very first ACK-REQ packet and the subsequent set of data collection (i.e. first CFDAMA return frame). This inevitable gap in channel utilisation cannot be filled due to not being preceded by any data packets and followed by the first set of data packet reception. This gap is proportional to the longest round-trip propagation delay.

Another important performance metric is the end-to-end delay achieved by our NoClock scheme under the two distinct traffic conditions, i.e. Poisson and Pareto ON/OFF. CFDAMA-NoClock should not experience very different delay/utilisation performance from the typical CFDAMA-PB delay performance. Figure 6.14 shows the delay/utilisation performance of CFDAMA-NoClock with the two traffic types (Poisson and Pareto ON/OFF), different numbers of nodes (20, 50 and 100) and different data packet sizes (64, 256 and 512 bits) at a data rate 9.6 kbit/s. In general, the mean end-to-end delay starts to increase exponentially as the offered load value approaches the maximum network throughput of a given scenario. Like CFDAMA-PB, the CFDAMA-NoClock scheme is still capable of providing the expected end-to-end delay performance with both traffic types. At low to medium channel loads, the mean end-to-end delay with both traffic models is similar. Above 50% of the channel capacity, the end-to-end delay is much higher with the Pareto ON-OFF traffic. With full channel load, 100 nodes and several packet durations, the shortest mean end-to-end delay achieved with the shortest packet duration of 6.66 ms. There, as Figure 6.14a-6.14b shows a data packet can be collected approximately every 19 s with Poisson traffic and 135 s with Pareto ON/OFF. With full channel load and different numbers of nodes, the shortest mean end-to-end delay is achieved with the smallest network size of 20 nodes. There, as Figure 6.14c-6.14d shows a data packet can be collected approximately every 5.8 s on average with Poisson traffic and 96 s with Pareto ON/OFF. For full details about the reasons behind this particular delay/utilisation performance refer to section 5.5.1 discussing the performance of CFDAMA-PAR.

6.6 Summary and Conclusions

This chapter proposes and examines two new robust MAC solutions for UASNs. We refer to them as CFDAMA-SRR (CFDAMA with Systematic Round Robin) and CFDAMA-NoClock (CFDAMA without clock synchronisation). The former scheme is more suitable for large-

scale and widely-spread UASNs, whereas the latter is a more feasible MAC solution when synchronisation amongst node clocks cannot be attained. The major challenge for coordinating access of nodes communicating acoustically underwater, subsea in particular, is the propagation delay distribution determined by the population density and spatial distribution of nodes. Another major challenge is the existence of disturbances caused by waves, sea currents and wind loading while deploying the nodes onto structures that may be in unpredictable motion. Moreover, the sound speed profile indicates that acoustic waves do not propagate in straight lines underwater. All these factors may bring about particularly challenging temporal-spatial uncertainty while a given UASN is deployed in a subsea location.

The CFDAMA-SRR scheme exhibits excellent performance in dealing with the trade-off between end-to-end packet delays and channel utilisation with both Poisson and Pareto ON/OFF data traffic conditions. Comprehensive event-driven Riverbed simulations of a network deployed on the sea bed show that CFDAMA-SRR outperforms its underlying scheme, CFDAMA-RR, especially when sensor nodes are widely spread. Considering node locations, the novel scheme has a bias against long delay demand assigned slots to enhance the performance of CFDAMA-RR. Illustrative examples show good agreement between analytical and simulation results. The Simulation results show that CFDAMA-SRR is able to provide a superior delay/utilisation performance to other request strategy, with consistent throughput and stable end-to-end delay performance for a wide range of scenarios. For a vertical channel with data rates up to 10 kbit/s and with 20, 50 and 100 nodes over a large coverage area, CFDAMA-SRR makes it possible to load the channel up to higher levels of its capacity with a delay performance superior to that achievable with CFDAMA-RR. It systematically organises the distribution of request opportunities which works in favour of the utilisation of a single request rather than multiple requests for the same demand. At a high channel, for instance, the load of 80%, the mean end-to-end delay is lower with CFDAMA-SRR than with CFDAMA-RR at 3 s with Poisson and 15 s with Pareto ON/OFF.

The CFDAMA-NoClock scheme exhibits excellent delay/utilisation performance. Comprehensive event-driven Riverbed simulations of a network deployed on the sea bed show that the proposed protocol is able to closely match its underlying scheme CFDAMA-PB with the advantage of independent unsynchronised node clocks. In all simulated scenarios, ranging from a network of 20, 50 to 100 nodes and packet sizes from 64, 256 to 512 bits, with a data rate of 9.2 kbit/s and two data traffic types (Poisson and Pareto ON/OFF), the proposed protocol achieves the expected very close delay/utilisation performance to that can be achieved with CFDAMA-PAR addressed in the previous chapter. The elimination of synchronised clocks increases the practicality of this CFDAMA variant. The MAC operations required to be processed on the sensor nodes are minimal; they wait for a particular type of

acknowledgement/control packet after which they, in the informed time, transmit as many packets as informed. All the complexity associated with the functionality of the scheme is at the gateway node. These features make the proposed scheme a feasible networking solution for robust and efficient deployments in the real world.

Chapter 7

Conclusions and Further Work

7.1 Summary and Conclusions

UASNs feature time-variant channel and traffic characteristics which place constraints and limitations on the functionality of MAC protocols as well as challenges to designing them. This thesis has discussed these time-variant characteristics and the resulting constraints, limitations and challenges and argued that MAC protocols incorporating combined capacity assignment strategies can provide UASNs with the necessary adaptability to achieve excellent delay/utilisation performance and fairness among nodes.

As described in more detail in chapter 3, the primary environmental constraints and consequent limitations are: 1) The variable propagation speed of acoustic waves, following curved paths based on several environmental parameters, and the unpredictable node motions underwater place the limitation of spatial and temporal uncertainty and cause the phenomena of space unfairness. 2) The relationship between the frequency of acoustic waves and the underwater acoustic background noise is non-linear causing the noise to affect the low-frequency components in particular. This places a certain lower limit to the channel bandwidth. A limit at which the background noise is tolerable and the desired SNR is attainable without the need for excessive transmission power that may harm the life of marine animals and their communications. Whereas, the upper limit is determined by the reverse relationship between the frequency and the acoustic signal attenuation for a given transmission range. This means that the underwater acoustic channel is characterised with a limited operating frequency band that is both noise-dependent and distant-dependent. The current underwater acoustic modems and the current modulation techniques are still unable to achieve high data rates with such limited bandwidth. This is a major limitation if a MAC protocol involves substantial packet overheads or relies on FDMA. 3) Sensor nodes are typically battery-powered, and their energy is limited. The limited battery life of the

sensor nodes necessitates the need for MAC protocols that can enable nodes to survive in the underwater long-term operations without a regular need of recharging or replacing their batteries.

It has also been found that, in addition to the previous environmental factors, there are non-environmental factors influencing the functionality of MAC protocols and considered as key design factors. They include the network topology, hop length, network size, packet duration, data rate, data traffic conditions. The latter is an issue of particular interest; the variation in traffic characteristics of the wide-ranging applications of UASNs poses a challenge to any attempt to design a single MAC protocol that can demonstrate resilience to the random statistical behaviour of traffic sources. Many underwater wireless sensor applications are characterised by periodic data traffic models rather than random bursty traffic; applications such as environmental monitoring tasks. To this type of traffic, collision-free scheduling-based MAC protocols, e.g. TDMA, are infinitely preferable owing to their customised frames enabling well-structured packet reception patterns. Other applications are characterised by independent events occurring naturally with no correlation amongst different sensor nodes. To this type of traffic, opportunistic and contention-based MAC protocols are preferable. Designing a single MAC protocol that is able to meet the requirements of these two distinct traffic types is particularly challenging.

The functionality of MAC protocols should be stable despite the presence of the aforementioned constraints and limitations. The performance of a MAC protocol is determined by the ability to adapt to different underwater scenarios. Underwater scenario means not only the surrounding environmental factors but also the non-environmental factors. All things considered, the above constraints and limitations pose challenges to the design of MAC protocols for UASNs including attempts to achieve low end-to-end delay, high channel utilisation, fairness and low complexity. It is clear from the literature review in chapter 3 that contention-based MAC protocols are less efficient for centralised topologies due to the potentially high level of contention in winning the channel. Under the scenario of bursty short-packet traffic, contention increases data packet loss rate and decreases throughput. They are more practical for small distributed networks. Scheduling-based schemes can enable the allocation of variable data rates by just changing the number of time slots allocated to each node. They can also be combined with contention-based schemes. This combination is classified as Adaptive TDMA, where capacity is usually assigned on demand. Scheduling-based schemes are shown as the most common MAC solutions for UASNs. Scheduling is found to be the main concern in such a dynamic environment. The most common synchronisation technique underwater is the use of a global scheduler, exchange of timing signals via a handshaking technique as well as the use of guard intervals to eliminate potential packet

overlaps. To this end, single-hop topologies lend certain compatibility to underwater sensing applications. What emphasises the compatibility of single-hop is simplicity alleviating the impact of the typical dilemma of energy facing battery-powered sensor nodes.

In chapter 4, random access demonstrated in the form of slotted ALOHA is shown to enable virtually instantaneous channel access but with very poor channel utilisation performance due to the channel access contention. Free assignment exhibits simplicity of implementation and is shown to offer close to the theoretical minimum end-to-end delay, but only at low channel loads, with modest node numbers and relatively short packet durations. With both Poisson and Pareto ON/OFF traffic types, the scheme outperforms the demand assignment scheme in terms of packet end-to-end delays over the entire range of channel loads for a typical UASN scenario. Demand assignment is shown to offer higher channel utilisation levels owing to the responsive allocation of capacity based on individual node requirements; however, it is limited to a minimum end-to-end delay bound of 1.5 gateway hops. This justifies the purpose of the following chapter investigating the combined capacity assignment schemes to provide both high channel utilisation and controlled delay performance.

In Chapter 5, the MAC schemes that combine free assignment with demand assignment are developed and examined in the context of UASNs. A detailed description of the CFDAMA scheme is presented including its scheduling algorithm, frame structures and underlying request strategies. CFDAMA is found to be capable of minimising the end-to-end delay and maximising the channel utilisation of UASNs. The presence of the free assignment strategy in CFDAMA works as a backup slot provider. It means that CFDAMA can adapt to the severe underwater conditions that may bring about instantaneous connection loss, preventing sensor nodes from sending requests. Combining two different MAC schemes with the possibility of using several request strategies gives CFDAMA the flexibility to meet different network requirements and applications. Simplicity is a fundamental feature of CFDAMA as most of the processing is done at a master node, typically equipped with a high-speed terrestrial link and a more sustainable power source. Amongst many CFDAMA variants, two schemes are of particular interest in chapter 5, i.e CFDAMA-PAR and CFDAMA-RR. Due to the nature of the underwater environment as well as the battery-powered sensor nodes communicating acoustically, these two CFDAMA variants which differ in their provision have been selected for UASNs. A number of criteria are considered for this selection including simplicity, fairness amongst nodes, compatibility with existing underwater TDMA protocols and scheduling algorithms. The two schemes are simple, attain fairness by employing the round robin algorithm and are able to work with the existing underwater TDMA protocols. They are investigated in the context of UASNs with both Poisson and Pareto ON/OFF traffic sources. Virtually in all scenarios, Poisson traffic with exponentially packet inter-arrival times

is shown to be unable to place sufficient demands on the channel to show a difference between the two request strategies in their delay/utilisation performance. The delay performance of both schemes is shown to be within the DAMA limit of 1.5 gateway hops. With the ON/OFF traffic type, the statistical behaviour of the traffic source governs the delay performance of both schemes in all instances, especially at high channel loads. Generally, both schemes are shown to be able to provide good delay/utilisation performance under reasonable traffic loads and up to 100 nodes. The potential drawback associated with the CFDAMA-PAR scheme is exhibited in the high likelihood of channel overuse by a certain number of nodes with heavy demand preventing other nodes from gaining access to the request slots. CFDAMA-RR is shown to uphold more fair access rights to all nodes, but its performance is subject to degradation when a large number of nodes is used. The larger the number of the node, the less regular the round robin request slots.

Chapter 5 proposes a new setup for the CFDAMA protocol suiting underwater scenarios. Two changes have been made to the traditional CFDAMA setup: 1) The CFDAMA scheduling node is no longer implemented in the gateway; it is rather implemented in an additional master node located just above the sensor nodes part way through to the gateway node. This allows shorter round trip delays between sensor nodes and the scheduler. 2) The CFDAMA forward frame is exploited not only for transmitting acknowledgements from the master node to sensor nodes, but also for relaying data packets to the gateway. Simulation results show that the CFDAMA-IS protocol can boost the effectiveness of CFDAMA in terms of delay/utilisation performance with both request strategies.

Chapter 6 introduces our two novel robust MAC solutions for UASNs, called CFDAMA-SRR (CFDAMA with Systematic Round Robin) and CFDAMA-NoClock (CFDAMA without clock synchronisation). CFDAMA-SRR is suggested for large-scale and widely-spread UASNs, whereas CFDAMA-NoClock is suggested for application of particular synchronising difficulties. Both analytical and comprehensive event-driven Riverbed simulations of a network deployed on the seabed show that the proposed schemes can adapt to the time-variant channel conditions and offer enhanced delay/utilisation performance with various scheme parameters and network sizes selected based on a realistic deployment of UASNs. The CFDAMA-SRR scheme is shown analytically and empirically to be able to outperform its underlying scheme CFDAMA-RR in both end-to-end delay and channel utilisation, with the two distinct traffic models - Poisson and Pareto ON/OFF - and a different number of nodes 20, 50 and 100 nodes. This enhanced performance of CFDAMA-SRR is attributable to the systematic way of implementing the round robin algorithm in assigning free slots to sensor nodes. This allows the scheme to have a bias against transmissions associated with long round-trip demand assigned slots. At high channel loads, the scheme enables sensor nodes to

maximise the use of every single request opportunity leading to an enhanced delay/utilisation performance. It also allows more time for far nodes to maximise the use of an increased number of free assigned slots owing to their longer round trip times. The CFDAMA-NoClock scheme is shown analytically and empirically to be able to achieve throughput performance very close to the throughput the performance of ideal CFDAMA-PB, and without the need for a synchronised clock in every sensor node. The end-to-end delay NoClock scheme is also evaluated under the two distinct traffic conditions - Poisson and Pareto ON/OFF - with different number of nodes (20, 50 and 100) and different data packet sizes (64, 256 and 512 bits) at a data rate 9.6 kb/s. Like CFDAMA-PB, the CFDAMA-NoClock scheme is shown to be able to provide excellent end-to-end delay performance. At low to medium channel loads, the mean end-to-end delay with both traffic types is similar. Above 50% of channel capacity, the end-to-end delay is much higher with the Pareto ON-OFF traffic. With full channel load and 100 nodes, for example, on average a data packet is collected by the gateway from a sensor node approximately every 19 s with Poisson traffic and 135 s with Pareto ON/OFF. Eliminating the node synchronised clocks typically required by CFDAMA encourages us to have a marked preference for it when implementing CFDAMA in a UASN deployed in particularly dynamic underwater conditions.

7.1.1 Original Contributions

Underwater acoustic networking is an immature area of knowledge. To the best of the author's knowledge, every main chapter of this thesis contributes to the body of knowledge. Some contributions are based on the author's thorough and critical review of the literature (chapter 2 and chapter 3), whereas others are based on extensive research of the subject matter using both analytical and empirical approaches (chapter 4, chapter 5 and chapter 6). Original MAC solutions are presented in the later chapters to contribute to the efforts put into making underwater acoustic networking possible. A chapter-by-chapter description of the original contributions of the thesis can be summarised as follows:

- The novel contributions of chapter 2 and chapter 3 are limited to proposing a classification perspective and putting together a summary of the background and the related work of UASNs. Chapter 2 proposes a new taxonomy of underwater networks, which is useful in giving the reader an idea about the position of this research with respect to the different classifications of underwater networks. It can be developed further to contribute towards the efforts put into standardising the framework of underwater networks. This chapter also sheds some light on the traffic requirements of UASNs, which is an unexplored area of research. By exploiting the wealth of knowledge of

terrestrial sensor networks, it is argued that at least two distinct data traffic types are required for the evaluation of MAC protocol performance to represent a wide range of applications. Using the Poisson traffic type for this performance evaluation is very common, but we are not aware of other studies involving a significantly burstier traffic model such as Pareto ON/OFF in the context of UASNs. The contributions of chapter 3 are the presence of a comprehensive background and thorough related work survey, which is represented graphically and tabularly in addition to the detailed text.

- A novel adaptation of the event-driven Riverbed modeller and combination with the BELLHOP acoustic field computation program in order to provide an underwater acoustic channel simulated based on well-known underwater propagation and ambient noise models. A number of the Riverbed Modeller pipeline stages have been modified to reflect several underwater propagation mechanisms, based on a realistic underwater sensor deployment for seismic monitoring in oil reservoirs. A vector containing the actual values of node-to-node propagation delays based on a realistic SSP derived from the World Ocean Atlas temperature, pressure and salinity, are extracted from BELLHOP and imported into the modeller. The simulated channel is described in chapter 2 and developed in chapter 4 and made more advanced in chapter 6 to be used for most of the simulated underwater scenarios throughout the thesis.

- It is the first study to consider capacity assignment schemes, i.e. free assignment, demand assignment and CFDAMA, in the literature of underwater acoustic networks. The three capacity assignment schemes are investigated in the context of UASNs in chapters 4 and 5. Comprehensive event-driven Riverbed simulations have been developed to evaluate the performance of the three schemes via the simulated acoustic channel. CFDAMA is found capable of minimising the end-to-end delay and maximising the channel utilisation and outperforms its two underlying schemes, i.e. free assignment and demand assignment. CFDAMA demonstrates simplicity and adaptability to the time-variant traffic and channel conditions underwater.

- A novel approach to implementing CFDAMA in the context of UASNs is proposed in chapter 5. Two major changes have been made to the traditional implementation of CFDAMA. Scheduling is implemented in a subordinate master node rather than the gateway node to significantly reduce the propagation delay across the acoustic link between the sensor node and the scheduler to eliminate the 1.5 gateway hop minimum end-to-end delay boundary. The acknowledgement packets are exploited to relay data packets to the gateway from the master node. These adjustments have enhanced

the overall delay/utilisation performance of CFDAMA underwater and boosted its effectiveness.

- In the preceding chapters, the analysis of delay performance focused on the dominant factors determining the average end-to-end delay of packets. Queueing time at sensor nodes is not covered. The spatial distribution of nodes and the statistical behaviour of traffic sources are not fully considered. Beyond the previous work, chapter 6 introduces a new family of robust CFDAMA-based protocols. CFDAMA-SRR and CFDAMA-NoClock are the current family members. The former is proposed for large-scale and widely-spread UASNs, whereas the latter is proposed for networks facing particular challenges in attaining synchronisation amongst node clocks. They are examined analytically and empirically. The novelty of this family of protocols is embodied in the systematic way of sharing the CFDAMA request channel by considering the spatial distribution of nodes with respect to the gateway node. Both protocols allow the sensor nodes to make their capacity requests one after another in round-robin turns going in the outbound direction of the gateway. CFDAMA-NoClock has an additional novel aspect which is a new synchronisation algorithm that achieves CFDAMA-like packet reception at the gateway without the need for a synchronised clock in every node. Both analytical and simulation approaches of a network deployed on the sea bed show that CFDAMA-SRR can outperform its underlying scheme, CFDAMA-RR, especially when sensor nodes are widely spread. The CFDAMA-NoClock scheme is shown to be able to closely match its underlying scheme CFDAMA-PB despite the absence of synchronised node clocks. The protocol demonstrates a high level of practicality and simplicity. The elimination of synchronised clocks increases its practicality. The MAC operations required to be processed on the sensor nodes are minimal, as all the complexity associated with the MAC functionality is implemented at the gateway node.

7.1.2 Hypothesis Revisited

Chapter 1 states the hypothesis driving the work presented in the thesis, and it is reiterated here:

Medium access control protocols incorporating a hybrid capacity assignment strategy can provide centralised wireless networks featuring time-variant channel and traffic characteristics with the necessary adaptability for excellent delay/utilisation performance.

The primary contributions detailed in the previous section can be summarised from the perspective put by the above hypothesis as follows:

- CFDAMA, which is a combined capacity assignment scheme, is examined in the context of UASNs, and simulated in a way that demonstrates its time-variant channel and traffic characteristics. It is shown to offer excellent delay/utilisation performance over the full range of channel capacity with two distinct traffic models and various node population sizes. It is shown to adapt very well to the changes in the traffic statistical behaviour owing to the responsive transitions from free to demand assignment, or vice versa, based on the level of the offered traffic. Fairness is demonstrated as a key feature of the scheme as it is implemented with round robin capacity request strategy. The key drawback is the performance limitation to the demand assignment delay boundary of 1.5 gateway hops.

- CFDAMA-IS, which is a newly proposed form of CFDAMA, is examined through similar underwater scenarios as standard CFDAMA. The scheme is shown to offer superior performance to CFDAMA in dealing with the trade-off between end-to-end delay and channel utilisation. The major advantage of the CFDAMA-IS scheme is the presence of an intermediate CFDAMA scheduler, reducing the minimum demand assignment delay boundary of 1.5 gateway hops significantly. The scheme would perform better if the spatial distribution of nodes and the statistical behaviour of traffic sources were factored in when distributing request slots among sensor nodes via the round robin algorithm.

- CFDAMA-SRR, which is a newly proposed robust scheme based on CFDAMA, is examined through more realistic underwater scenarios. In addition to the incorporation of well-known underwater propagation and ambient noise models, actual sound prorogation speed values are used, provided by the BELLHOP acoustic field computation program. Due to the long propagation delay underwater and the fact that sensor nodes can be widely spread, implementing CFDAMA with one of the conventional request strategies and without considering the location of nodes results in poorer efficiency than the level of which the scheme is capable. CFDAMA-SRR systematise the round robin algorithm that is used to distribute the request slots among sensor nodes. The scheme is shown to offer a superior delay/utilisation performance than any other request strategy, with consistent throughput and stable end-to-end delay performance for a wide range of underwater scenarios. Like any other scheduling-based scheme, CFDAMA-SRR may have difficulties in attaining synchronisation among nodes in the presence of extreme underwater conditions.

- CFDAMA-NoClock, which is a newly proposed underwater-specific scheme based on CFDAMA, is examined for the same underwater scenarios through which CFDAMA-

SRR was examined. The novel scheme incorporates an original synchronisation algorithm eliminating the use of synchronised clocks, which increases the practicality of this CFDAMA variant even in extreme underwater conditions. The simple algorithm is processed mainly at the gateway node keeping the complexity associated with the functionality of the scheme at minimal. The scheme is shown to exhibit excellent delay/utilisation performance very close to the performance achieved by CFDAMA-PAR. The new scheduling features make this scheme a feasible networking solution for robust and efficient deployments in the real world.

These original contributions are empirically, and in some cases analytically, shown to provide significant improvements in the adaptability and fairness of combined capacity assignment schemes; hence, upholding the hypothesis of the thesis.

7.2 Recommendations for Further Work

7.2.1 Practical Consideration and Improvement to CFDAMA-NoClock

Practical implementation of the CFDAMA-NoClock scheme in a real sea trial is encouraged. The scheme demonstrates simplicity suiting data gathering in UASNs composed of low cost, low power acoustic nano-modems, such as those developed at the University of Newcastle, UK [121]. Despite the fact that our study has covered most of the theoretical aspects of the new scheme using both analytical and numerical event-driven simulations, several practical issues posing additional challenges are still expected. A further investigation is required through real trials to highlight these issues. Strategies to get around them and required modifications would also be a useful follow-up on this study. The cost associated with such real trails is a fundamental issue, necessitating the need for well-designed, specific and economic trails. To reinforce beneficial outcomes of any further studies of real UASN deployment involving CFDAMA-NoClock, examples of potential issues and suggest solutions are given as follows:

- In the setup stage required prior to the actual data transmission stage, the gateway blindly attempts to estimate all link propagation delays across the network by transmitting a ping packet to every sensor node. This operation has a time-variant chance of success. Additional robustness mechanism is required to overcome any potential ping packet loss, such as incorporating multiple attempts until at least one ping packet is reciprocated by each sensor node.

- The actual format of the ACK-REQ packet needs investigating based on application requirements, network size and acoustic modem capabilities. The packet is used to inform every node the number of allocated data slots and the amount of time the node has to wait before it can start a run of successive packet transmissions as allocated. The new study should aim for short transmission time of this packet with respect to its propagation delays to achieve excellent delay/utilisation performance. The original CFDAMA-NoClock is designed based on one universal ACK-REQ packet to be broadcast to all sensor nodes for every data transmission cycle. If the number of nodes is substantially large and the data rate of the acoustic modem is very low, then the universal packet could be replaced with a train of short ACK-REQ packets streamlined to individual nodes as appropriate.

- The guard interval between successive packets is a key design factor. A large number of practical deployment aspects may result in timing errors in packet arrivals, leading to collisions if the timing error is greater than the guard interval. The causes of packet collisions require further investigation examining the impact of reading delay of sensors, signal processing delay of acoustic modems, software crashes and hardware incompatibilities among different sensor nodes and nodes unpredictable motion.

These issues are just examples and many others may occur during real employment, and hence, further modifications to the CFDAMA-NoClock protocol may be required.

7.2.2 Comparison between CFDAMA-NoClock and TDA-MAC

The CFDAMA-NoClock scheme enables back-to-back packet reception at the gateway node without the use of global timing, but rather the use of a method of relative timing instructed on a frame-by-frame basis. This mirrors TDA-MAC [2] where TDMA-like packet arrivals are achieved while nodes are timely independent of each other and each node is regularly instructed how to track appropriate transmission timing but not on a frame-by-frame basis.

The two schemes differ in their approach to achieving collision-free packet arrivals and achievable delay/utilisation performance. In TDA-MAC, every sensor node transmits a single data packet; and this transmission is timed to happen at a certain instructed time referenced to the reception of a packet that is broadcast by the gateway. The achievable channel utilisation is based on the duration of those single transmitted data packets with respect to their propagation time. The protocol is critical to the duration of data packets, the population density and the spatial distribution of nodes. In certain cases depending on packet inter-arrival time at the traffic source capacity gaps may occur amongst the successive data packet arrivals at the gateway. In the CFDAMA-NoClock scheme, the CFDAMA forward

frame is replaced by a packet acting similarly to the broadcast reference packet of TDA-MAC, but with extra payloads. A packet is broadcast to inform every node the number of successive slots allocated to it and how long the node must delay the transmission of a run of successive packets equal to the number of allocated slots. This delay is calculated using a different way from that which is used in TDA-MAC. Transmitting a train of packets instead of a single packet gives superior performance for CFDAMA-NoClock over TDA-MAC. It allows instantaneous adaptation to any changes in the statistical behaviour of data traffic sources in terms of the duration of a specific burst, inter-burst gaps, the duty cycle of bursts and the channel load level.

It would be interesting to conduct a new study comparing the performance of these two TDMA-like protocols, one of which can be classified as adaptive TDMA, while the other as fixed TDMA protocols.

7.2.3 Applying Reinforcement Learning to Control Access to CFDAMA Request Channel

ALOHA-Q [122] is a well-known MAC protocol incorporating reinforcement learning. The protocol demonstrates simplicity, and yet it is capable of providing channel utilisation far superior to the conventional ALOHA protocol. CFDAMA requires a sub-MAC protocol to control access to the capacity request channel, i.e. a request strategy. This opens up opportunities for performance enhancement. In chapter 2, it is shown that Slotted ALOHA can provide rapid channel access but with poor channel utilisation. In this respect, it would be a worthwhile contribution to investigate the possibility of involving reinforcement learning, in the form of ALOHA-Q, to coordinate access to the request channel.

In [122], simulation results indicate that in the context of underwater acoustic networks, ALOHA-Q can achieve up to 30% performance enhancement over the traditional ALOHA protocol. ALOHA-Q initially starts to work as slotted ALOHA; before it begins to gradually attain a TDMA style of scheduling by implementing reinforcement learning enabling nodes to learn and decide upon transmission turns. To what extent this can improve the performance of CFDAMA has yet to be explored, but it should help especially in applications where traditional request strategies may be inefficient, i.e. very large-scale networks comprising a very large number of nodes.

7.2.4 Improvement to The Performance of The Free Assignment Scheme Underlying CFDAMA

By combining of two capacity assignment schemes as well as a capacity request strategy, CFDAMA has several aspects of which further investigations can be useful. In addition to the request strategies, the free assignment scheme is a CFDAMA aspect in which reinforcement learning is worth trying. The typical algorithm used to freely assign data slots is round robin as it is simple and maintains fairness between nodes. Given the independence of data traffic sources, nodes differ in their exploitation of the freely assigned slots. Based on the statistical behaviour of individual data traffic sources, some nodes will have greater exploitation of the freely assigned slots than others. This is also dependent on the nature of a given application. A new technique is required to replace the round-robin free assignment algorithm underlying the CFDAMA scheduler. Reinforcement learning can be implemented at the gateway to learn about every node's utilisation of the freely assigned slots. The new technique may start initially assigning the free slots based on a round robin approach, but it should gradually transit to a new stage where the free slots are assigned based on the predicted requirements that need to be learnt about every node. The new technique needs to keep a track of every freely assigned slot and whether or not the corresponding node has used it for useful data transmission. After a number of CFDAMA frames, the new technique should be able to predict the number of free slots required in the following CFDAMA frame and which nodes will need them. This should boost the effectiveness of CFDAMA and help to achieve enhanced channel utilisation.

7.2.5 Dependency of CFDAMA Performance on Source Traffic

In simulation-based studies of MAC protocols, selecting an appropriate data traffic model to evaluate the network performance is a fundamental factor. To reflect on the wide-ranging UASN applications, this thesis is one of few evaluating the performance of its proposed MAC protocols under distinct data traffic models. More specifically, MAC schemes proposed in this thesis are examined with exponentially random burst traffic type (based on Poisson data traffic) and periodic ON/OFF traffic type of periodic data gathering conditions (based on Pareto ON/OFF data traffic). These two types of source traffic can represent a wide range of underwater sensing tasks, i.e water pollution assessment, fish tracking and seismic monitoring. However, in order to design a MAC protocol that can effectively serve a given application in practice, more specific data traffic types representing individual resource requirements and sensitivity to delay are required to be involved in the design and examination process.

CFDAMA, in general, is able to adapt to the traffic variations as the results in chapter 5 and chapter 6 show. Wider investigation into the traffic characteristic of UASNs is required; however, further experiments on the dependency of MAC protocol performance on different UASN traffic characteristics is also required. New insights into this area could help stimulate ideas and generate new techniques to further enhance CFDAMA performance.

7.2.6 Effect of Upper Layers on MAC Layer Protocols

MAC protocols are traditionally studied independently from the protocols operating at upper layers of the network architecture. Focussing purely on the MAC layer enables deep knowledge to be gained about MAC issues, but may lead to sort of misleading observations and results due to the exclusion of other factors related to upper layers. Higher layers such as routing, transportation and application layers must have an impact on the operation and performance of a MAC scheme. Provided that the entire end-to-end connection includes at least a gateway hop, the higher layer protocols will definitely impact the flow of data traffic across the gateway link to a certain extent. Involvement of higher layer protocols should create more realistic underwater scenarios for the evaluation of MAC protocol performance. It is encouraged to develop the full understanding about the interactions and influences of the upper layers, once a thorough knowledge of the MAC layer issues and techniques is gained; theretofore, it would be a useful area of further work.

Taking the application layer as an example, the resulting effect includes the time required by a sensor from the moment it detects, measures and records a physical property to the moment it responds. Some applications can timeout; if the sensor readings required within specified time limits have not been made available, they can terminate the task and in some instances, a crash may be caused. The sensor's software and hardware can, therefore, potentially change the packet arrival process as well as the end to end packet delay at the gateway. Another example is the transportation layer, reliable transportation layer protocols typically incorporate window-based flow control techniques to regulate end to end flow of packets across a network. Based on certain factors, this can also affect the packet inter-arrival time at the gateway.

7.2.7 Security at The MAC Layer

At this layer, cyber attacks can be carried out; for example, traffic jamming attacks. All it takes to perform such an attack is to identify some information about the packet formats and the MAC protocol being used. The saboteur can use fake control or data packets in order to content for the channel and cause packet collisions. Such attacks, as well as spoofing

attacks, can be very serious, especially for homeland security applications. In this regard, the gateway node needs to know if a packet comes from a legitimate sensor node or it is injected in the link by a malicious sensor node. How this authentication should be performed is an interesting future topic for underwater acoustic networks in general and UASNs in particular.

References

[1] M. Stojanovic, "On the relationship between capacity and distance in an underwater acoustic communication channel," *ACM SIGMOBILE Mobile Computing and Communications Review*, vol. 11, no. 4, pp. 34–43, 2007.

[2] N. Morozs, P. Mitchell, and Y. V. Zakharov, "Tda-mac: Tdma without clock synchronization in underwater acoustic networks," *IEEE Access*, vol. 6, pp. 1091–1108, 2018.

[3] A. F. Harris III, M. Stojanovic, and M. Zorzi, "When underwater acoustic nodes should sleep with one eye open: idle-time power management in underwater sensor networks," in *Proceedings of the 1st ACM international workshop on Underwater networks*. ACM, 2006, pp. 105–108.

[4] I. F. Akyildiz, D. Pompili, and T. Melodia, "Underwater acoustic sensor networks: research challenges," *Ad hoc networks*, vol. 3, no. 3, pp. 257–279, 2005.

[5] J. Lloret, "Underwater sensor nodes and networks," pp. 11 782–11 796, 2013. [Online]. Available: http://www.mdpi.com/1424-8220/13/9/11782

[6] C.-C. Kao, Y.-S. Lin, G.-D. Wu, and C.-J. Huang, "A comprehensive study on the internet of underwater things: applications, challenges, and channel models," *Sensors*, vol. 17, no. 7, p. 1477, 2017.

[7] E. Felemban, F. K. Shaikh, U. M. Qureshi, A. A. Sheikh, and S. B. Qaisar, "Underwater sensor network applications: A comprehensive survey," *International Journal of Distributed Sensor Networks*, vol. 11, no. 11, p. 896832, 2015.

[8] A. Faustine, A. N. Mvuma, H. J. Mongi, M. C. Gabriel, A. J. Tenge, and S. B. Kucel, "Wireless sensor networks for water quality monitoring and control within lake victoria basin: prototype development," *Wireless Sensor Network*, vol. 6, no. 12, p. 281, 2014.

[9] G. Acar and A. Adams, "Acmenet: an underwater acoustic sensor network protocol for real-time environmental monitoring in coastal areas," *IEE Proceedings-Radar, Sonar and Navigation*, vol. 153, no. 4, pp. 365–380, 2006.

[10] C. Alippi, R. Camplani, C. Galperti, and M. Roveri, "A robust, adaptive, solar-powered wsn framework for aquatic environmental monitoring," *IEEE Sensors Journal*, vol. 11, no. 1, pp. 45–55, 2011.

[11] C. A. Pérez, M. Jimenez, F. Soto, R. Torres, J. López, and A. Iborra, "A system for monitoring marine environments based on wireless sensor networks," in *OCEANS, 2011 IEEE-Spain*. IEEE, 2011, pp. 1–6.

[12] S. Zhang, J. Yu, A. Zhang, L. Yang, and Y. Shu, "Marine vehicle sensor network architecture and protocol designs for ocean observation," *Sensors*, vol. 12, no. 1, pp. 373–390, 2012.

[13] H. Yang, H. Wu, and Y. He, "Architecture of wireless sensor network for monitoring aquatic environment of marine shellfish," in *Asian Control Conference, 2009. ASCC 2009. 7th*. IEEE, 2009, pp. 1147–1151.

[14] N. Nasser, A. Zaman, L. Karim, and N. Khan, "Cpws: An efficient routing protocol for rgb sensor-based fish pond monitoring system," in *2012 IEEE 8th International Conference on Wireless and Mobile Computing, Networking and Communications (WiMob)*. IEEE, 2012, pp. 7–11.

[15] A. Pirisi, F. Grimaccia, M. Mussetta, R. E. Zich, R. Johnstone, M. Palaniswami, and S. Rajasegarar, "Optimization of an energy harvesting buoy for coral reef monitoring," in *Evolutionary Computation (CEC), 2013 IEEE Congress on*. IEEE, 2013, pp. 629–634.

[16] S. Bainbridge, D. Eggeling, and G. Page, "Lessons from the field—two years of deploying operational wireless sensor networks on the great barrier reef," *Sensors*, vol. 11, no. 7, pp. 6842–6855, 2011.

[17] S. Srinivas, P. Ranjitha, R. Ramya, and G. K. Narendra, "Investigation of oceanic environment using large-scale uwsn and uanets," in *Wireless Communications, Networking and Mobile Computing (WiCOM), 2012 8th International Conference on*. IEEE, 2012, pp. 1–5.

[18] I. Jawhar, N. Mohamed, and K. Shuaib, "A framework for pipeline infrastructure monitoring using wireless sensor networks," in *Wireless telecommunications symposium, 2007. WTS 2007*. IEEE, 2007, pp. 1–7.

[19] S. Tyan, S.-H. Oh, M. Domingo, and A. Caiti, "Auv-rm: underwater sensor network scheme for auv based river monitoring," *Research Trend in Computer and Applications, SERCE*, vol. 24, pp. 53–55, 2013.

[20] P. Kumar, P. Kumar, P. Priyadarshini, and Srija, "Underwater acoustic sensor network for early warning generation," in *2012 Oceans*, Oct 2012, pp. 1–6.

[21] A. Khan and L. Jenkins, "Undersea wireless sensor network for ocean pollution prevention," in *Communication Systems Software and Middleware and Workshops, 2008. COMSWARE 2008. 3rd International Conference on*. IEEE, 2008, pp. 2–8.

[22] D. P. Williams, "On optimal auv track-spacing for underwater mine detection," in *Robotics and Automation (ICRA), 2010 IEEE International Conference on*. IEEE, 2010, pp. 4755–4762.

[23] S. Kumar, A. Perry, C. Moeller, D. Skvoretz, M. Ebbert, R. Ostrom, S. Bennett, and P. Czipott, "Real-time tracking magnetic gradiometer for underwater mine detection," in *OCEANS'04. MTTS/IEEE TECHNO-OCEAN'04*, vol. 2. IEEE, 2004, pp. 874–878.

[24] C. Rao, K. Mukherjee, S. Gupta, A. Ray, and S. Phoha, "Underwater mine detection using symbolic pattern analysis of sidescan sonar images," in *American Control Conference, 2009. ACC'09.* IEEE, 2009, pp. 5416–5421.

[25] S. Khaledi, H. Mann, J. Perkovich, and S. Zayed, "Design of an underwater mine detection system," in *Proceedings of the IEEE Systems and Information Engineering Design Symposium (SIEDS), Charlottesville, VA, USA*, vol. 25, 2014.

[26] M. J. Hamilton, S. Kemna, and D. Hughes, "Antisubmarine warfare applications for autonomous underwater vehicles: the glint09 sea trial results," *Journal of Field Robotics*, vol. 27, no. 6, pp. 890–902, 2010.

[27] R. Manjula and S. S. Manvi, "Coverage optimization based sensor deployment by using pso for anti-submarine detection in uwasns," in *Ocean Electronics (SYMPOL), 2013*. IEEE, 2013, pp. 15–22.

[28] S. Kemna, M. J. Hamilton, D. T. Hughes, and K. D. LePage, "Adaptive autonomous underwater vehicles for littoral surveillance," *Intelligent service robotics*, vol. 4, no. 4, p. 245, 2011.

[29] A. Caiti, V. Calabro, A. Munafo, G. Dini, and A. Lo Duca, "Mobile underwater sensor networks for protection and security: field experience at the uan11 experiment," *Journal of Field Robotics*, vol. 30, no. 2, pp. 237–253, 2013.

[30] M. Waldmeyer, H.-P. Tan, and W. K. Seah, "Multi-stage auv-aided localization for underwater wireless sensor networks," in *Advanced Information Networking and Applications (WAINA), 2011 IEEE Workshops of International Conference on*. IEEE, 2011, pp. 908–913.

[31] Y. Guo and Y. Liu, "Localization for anchor-free underwater sensor networks," *Computers & Electrical Engineering*, vol. 39, no. 6, pp. 1812–1821, 2013.

[32] P. Carroll, S. Zhou, K. Mahmood, H. Zhou, X. Xu, and J.-H. Cui, "On-demand asynchronous localization for underwater sensor networks," in *Oceans, 2012*. IEEE, 2012, pp. 1–4.

[33] T. Le Sage, A. Bindel, P. Conway, S. Slawson, and A. West, "Development of a wireless sensor network for embedded monitoring of human motion in a harsh environment," in *Communication Software and Networks (ICCSN), 2011 IEEE 3rd International Conference on*. IEEE, 2011, pp. 112–115.

[34] T. Le Sage, P. Conway, L. Justham, S. Slawson, A. Bindel, and A. West, "A component based integrated system for signal processing of swimming performance," in *Signal Processing and Multimedia Applications (SIGMAP), Proceedings of the 2010 International Conference on*. IEEE, 2010, pp. 73–79.

[35] W. D. Wilson, "Speed of sound in sea water as a function of temperature, pressure, and salinity," *The Journal of the Acoustical Society of America*, vol. 32, no. 6, pp. 641–644, 1960.

[36] F. Guerra, P. Casari, and M. Zorzi, "World ocean simulation system (woss): A simulation tool for underwater networks with realistic propagation modeling," in *Proceedings of the Fourth ACM International Workshop on UnderWater Networks*, ser. WUWNet '09. ACM, 2009, pp. 4:1–4:8.

[37] A. Sehgal, *Analysis & Simulation of the Deep Sea Acoustic Channel for Sensor Networks*. Lulu. com, 2013.

[38] W. H. Thorp, "Deep-ocean sound attenuation in the sub-and low-kilocycle-per-second region," *The Journal of the Acoustical Society of America*, vol. 38, no. 4, pp. 648–654, 1965.

[39] F. Fisher and V. Simmons, "Sound absorption in sea water," *The Journal of the Acoustical Society of America*, vol. 62, no. 3, pp. 558–564, 1977.

[40] M. A. Ainslie and J. G. McColm, "A simplified formula for viscous and chemical absorption in sea water," *The Journal of the Acoustical Society of America*, vol. 103, no. 3, pp. 1671–1672, 1998.

[41] V. S. Frost and B. Melamed, "Traffic modeling for telecommunications networks," *IEEE Communications Magazine*, vol. 32, no. 3, pp. 70–80, 1994.

[42] V. Paxson and S. Floyd, "Wide area traffic: the failure of poisson modeling," *IEEE/ACM Transactions on Networking (ToN)*, vol. 3, no. 3, pp. 226–244, 1995.

[43] W. E. Leland, M. S. Taqqu, W. Willinger, and D. V. Wilson, "On the self-similar nature of ethernet traffic (extended version)," *IEEE/ACM Transactions on Networking (ToN)*, vol. 2, no. 1, pp. 1–15, 1994.

[44] A. A. Syed, W. Ye, and J. Heidemann, "Comparison and evaluation of the t-lohi mac for underwater acoustic sensor networks," *IEEE Journal on Selected Areas in Communications*, vol. 26, no. 9, 2008.

[45] W.-H. Liao and C.-C. Huang, "Sf-mac: A spatially fair mac protocol for underwater acoustic sensor networks," *IEEE Sensors Journal*, vol. 12, no. 6, pp. 1686–1694, 2012.

[46] C. Li, Y. Xu, C. Xu, Z. An, B. Diao, and X. Li, "Dtmac: A delay tolerant mac protocol for underwater wireless sensor networks," *IEEE Sensors Journal*, vol. 16, no. 11, pp. 4137–4146, 2016.

[47] A. Mainwaring, D. Culler, J. Polastre, R. Szewczyk, and J. Anderson, "Wireless sensor networks for habitat monitoring," in *Proceedings of the 1st ACM international workshop on Wireless sensor networks and applications*. Acm, 2002, pp. 88–97.

[48] Q. Wang, "Traffic analysis & modeling in wireless sensor networks and their applications on network optimization and anomaly detection," *Network Protocols and Algorithms*, vol. 2, no. 1, pp. 74–92, 2010.

[49] I. Hammoodi, B. Stewart, A. Kocian, and S. McMeekin, "A comprehensive performance study of opnet modeler for zigbee wireless sensor networks," in *Next Generation Mobile Applications. NGMAST'09. 3rd Intern. Conf*, 2009, pp. 357–362.

[50] W. Willinger, M. S. Taqqu, R. Sherman, and D. V. Wilson, "Self-similarity through high-variability: statistical analysis of ethernet lan traffic at the source level," *IEEE/ACM Transactions on Networking (ToN)*, vol. 5, no. 1, pp. 71–86, 1997.

[51] H. Zimmermann, "Osi reference model–the iso model of architecture for open systems interconnection," *IEEE Transactions on communications*, vol. 28, no. 4, pp. 425–432, 1980.

[52] A. Porto and M. Stojanovic, "Optimizing the transmission range in an underwater acoustic network," in *OCEANS 2007*. IEEE, 2007, pp. 1–5.

[53] W. Ye and J. Heidemann, "Medium access control in wireless sensor networks," in *Wireless sensor networks*. Springer, 2004, pp. 73–91.

[54] C. L. Fullmer and J. Garcia-Luna-Aceves, "Floor acquisition multiple access (fama) for packet-radio networks," in *ACM SIGCOMM computer communication review*, vol. 25, no. 4. ACM, 1995, pp. 262–273.

[55] C.-C. Hsu, K. C.-J. Lin, Y.-R. Lai, and C.-F. Chou, "On exploiting spatial-temporal uncertainty in max-min fairness in underwater sensor networks," *IEEE Communications Letters*, vol. 14, no. 12, pp. 1098–1100, 2010.

[56] J. Rice, B. Creber, C. Fletcher, P. Baxley, K. Rogers, K. McDonald, D. Rees, M. Wolf, S. Merriam, R. Mehio *et al.*, "Evolution of seaweb underwater acoustic networking," in *Oceans 2000 MTS/IEEE Conference and Exhibition*, vol. 3. IEEE, 2000, pp. 2007–2017.

[57] E. M. Sozer, M. Stojanovic, and J. G. Proakis, "Underwater acoustic networks," *IEEE journal of oceanic engineering*, vol. 25, no. 1, pp. 72–83, 2000.

[58] L. T. Tracy and S. Roy, "A reservation mac protocol for ad-hoc underwater acoustic sensor networks," in *Proceedings of the third ACM international workshop on Underwater Networks*. ACM, 2008, pp. 95–98.

[59] D. Pompili, T. Melodia, and I. F. Akyildiz, "A cdma-based medium access control for underwater acoustic sensor networks," *IEEE Transactions on Wireless Communications*, vol. 8, no. 4, 2009.

[60] M. K. Watfa, S. Selman, and H. Denkilkian, "Uw-mac: An underwater sensor network mac protocol," *International journal of communication systems*, vol. 23, no. 4, pp. 485–506, 2010.

[61] S. Climent, J. V. Capella, N. Meratnia, and J. J. Serrano, "Underwater sensor networks: A new energy efficient and robust architecture," *Sensors*, vol. 12, no. 1, pp. 704–731, 2012.

[62] A. Jayasuriya, S. Perreau, A. Dadej, S. Gordon *et al.*, "Hidden vs exposed terminal problem in ad hoc networks," Ph.D. dissertation, ATNAC 2004, 2004.

[63] J. Partan, J. Kurose, and B. N. Levine, "A survey of practical issues in underwater networks," *ACM SIGMOBILE Mobile Computing and Communications Review*, vol. 11, no. 4, pp. 23–33, 2007.

[64] A. A. Syed, W. Ye, J. Heidemann, and B. Krishnamachari, "Understanding spatio-temporal uncertainty in medium access with aloha protocols," in *Proceedings of the second workshop on Underwater networks*. ACM, 2007, pp. 41–48.

[65] N. Chirdchoo, W.-S. Soh, and K. C. Chua, "Aloha-based mac protocols with collision avoidance for underwater acoustic networks," in *INFOCOM 2007. 26th IEEE International Conference on Computer Communications. IEEE*. IEEE, 2007, pp. 2271–2275.

[66] Y.-J. Chen and H.-L. Wang, "Ordered csma: a collision-free mac protocol for underwater acoustic networks," in *OCEANS 2007*. IEEE, 2007, pp. 1–6.

[67] X. Guo, M. R. Frater, and M. J. Ryan, "A propagation-delay-tolerant collision avoidance protocol for underwater acoustic sensor networks," in *OCEANS 2006-Asia Pacific*. IEEE, 2007, pp. 1–6.

[68] P. Xie and J.-H. Cui, "R-mac: An energy-efficient mac protocol for underwater sensor networks," in *2007 International Conference on Wireless Algorithms, Systems and Applications*. IEEE, 2007, pp. 187–198.

[69] V. Rodoplu and M. K. Park, "An energy-efficient mac protocol for underwater wireless acoustic networks," in *OCEANS, 2005. Proceedings of MTS/IEEE*. IEEE, 2005, pp. 1198–1203.

[70] M. K. Park and V. Rodoplu, "Uwan-mac: An energy-efficient mac protocol for underwater acoustic wireless sensor networks," *IEEE journal of oceanic engineering*, vol. 32, no. 3, pp. 710–720, 2007.

[71] I. F. Akyildiz, D. Pompili, and T. Melodia, "State-of-the-art in protocol research for underwater acoustic sensor networks," in *Proceedings of the 1st ACM international workshop on Underwater networks*. ACM, 2006, pp. 7–16.

[72] P. E. Milling, "Carrier sense multiple access with collision avoidance utilizing rotating time staggered access windows," Dec. 9 1986, uS Patent 4,628,311.

[73] R. Creber, J. Rice, P. Baxley, and C. Fletcher, "Performance of undersea acoustic networking using rts/cts handshaking and arq retransmission," in *OCEANS, 2001. MTS/IEEE Conference and Exhibition*, vol. 4. IEEE, 2001, pp. 2083–2086.

[74] V. Rodoplu and A. A. Gohari, "Mac protocol design for underwater networks: challenges and new directions," *Ladislao*, vol. 1, pp. 23–26, 2008.

[75] W. Ye, J. Heidemann, and D. Estrin, "Medium access control with coordinated adaptive sleeping for wireless sensor networks," *IEEE/ACM Trans. Netw.*, vol. 12, no. 3, pp. 493–506, Jun. 2004. [Online]. Available: http://dx.doi.org/10.1109/TNET.2004.828953

[76] A. F. Harris, III, M. Stojanovic, and M. Zorzi, "When underwater acoustic nodes should sleep with one eye open: Idle-time power management in underwater sensor networks," in *Proceedings of the 1st ACM International Workshop on Underwater Networks*, ser. WUWNet '06. ACM, 2006, pp. 105–108.

[77] J.-Y. Lee, N.-Y. Yun, S. Muminov, S.-Y. Shin, Y.-S. Ryuh, and S.-H. Park, "A focus on practical assessment of mac protocols for underwater acoustic communication with regard to network architecture," *IETE Technical Review*, vol. 30, no. 5, pp. 375–381, 2013.

[78] P. Xie and J.-H. Cui, "Exploring random access and handshaking techniques in large-scale underwater wireless acoustic sensor networks," in *OCEANS 2006*. IEEE, 2006, pp. 1–6.

[79] A. Roy and N. Sarma, "Effects of various factors on performance of mac protocols for underwater wireless sensor networks," *Materials Today: Proceedings*, vol. 5, no. 1, pp. 2263–2274, 2018.

[80] A. Roy and N. Sarma, "Performance analysis of energy-efficient mac protocols for underwater sensor networks," in *2015 2nd International Conference on Computing for Sustainable Global Development (INDIACom)*, March 2015, pp. 297–303.

[81] D. D. Perkins, H. D. Hughes, and C. B. Owen, "Factors affecting the performance of ad hoc networks," in *Communications, 2002. ICC 2002. IEEE International Conference on*, vol. 4. IEEE, 2002, pp. 2048–2052.

[82] S. Basagni, C. Petrioli, R. Petroccia, and M. Stojanovic, "Choosing the packet size in multi-hop underwater networks," in *OCEANS 2010 IEEE-Sydney*. IEEE, 2010, pp. 1–9.

[83] Y. E. Sagduyu and A. Ephremides, "The problem of medium access control in wireless sensor networks," *IEEE Wireless communications*, vol. 11, no. 6, pp. 44–53, 2004.

[84] C.-C. Hsu, K.-F. Lai, C.-F. Chou, and K.-J. Lin, "St-mac: Spatial-temporal mac scheduling for underwater sensor networks," in *INFOCOM 2009, IEEE*. IEEE, 2009, pp. 1827–1835.

[85] K. Kredo II, P. Djukic, and P. Mohapatra, "Stump: Exploiting position diversity in the staggered tdma underwater mac protocol," in *INFOCOM 2009, IEEE*. IEEE, 2009, pp. 2961–2965.

[86] D. Cavendish and M. Gerla, "Internet qos routing using the bellman-ford algorithm," in *High Performance Networking*. Springer, 1998, pp. 627–646.

[87] K. Kredo II and P. Mohapatra, "Distributed scheduling and routing in underwater wireless networks," in *Global Telecommunications Conference (GLOBECOM 2010), 2010 IEEE*. IEEE, 2010, pp. 1–6.

[88] W. Van Kleunen, N. Meratnia, and P. J. Havinga, "Mds-mac: a scheduled mac for localization, time-synchronisation and communication in underwater acoustic networks," in *2012 IEEE 15th International Conference on Computational Science and Engineering*. IEEE, 2012, pp. 666–672.

[89] W. van Kleunen, N. Meratnia, and P. J. Havinga, "Mac scheduling in large-scale underwater acoustic networks," in *Proceedings of the International Conference on Wireless Information Networks and Systems*. IEEE, 2011, pp. 27–34.

[90] J. Ahn, A. Syed, B. Krishnamachari, and J. Heidemann, "Design and analysis of a propagation delay tolerant aloha protocol for underwater networks," *Ad Hoc Networks*, vol. 9, no. 5, pp. 752–766, 2011.

[91] M. Molins and M. Stojanovic, "Slotted fama: a mac protocol for underwater acoustic networks," in *OCEANS 2006-Asia Pacific*. IEEE, 2007, pp. 1–7.

[92] R. Diamant and L. Lampe, "Spatial reuse time-division multiple access for broadcast ad hoc underwater acoustic communication networks," *IEEE Journal of Oceanic Engineering*, vol. 36, no. 2, pp. 172–185, 2011.

[93] Y. Zhu, Z. Peng, J.-H. Cui, and H. Chen, "Toward practical mac design for underwater acoustic networks," *IEEE Transactions on Mobile Computing*, vol. 14, no. 4, pp. 872–886, 2015.

[94] L. Hong, F. Hong, Z.-W. Guo, and X. Yang, "A tdma-based mac protocol in underwater sensor networks," in *Wireless Communications, Networking and Mobile Computing, 2008. WiCOM'08. 4th International Conference on*. IEEE, 2008, pp. 1–4.

[95] S.-Y. Shin, J.-I. Namgung, and S.-H. Park, "Sbmac: Smart blocking mac mechanism for variable uw-asn (underwater acoustic sensor network) environment," *Sensors*, vol. 10, no. 1, pp. 501–525, 2010.

[96] Y. Xiao, Y. Zhang, J. H. Gibson, G. G. Xie, and H. Chen, "Performance analysis of aloha and p-persistent aloha for multi-hop underwater acoustic sensor networks," *Cluster Computing*, vol. 14, no. 1, pp. 65–80, 2011.

[97] P. Karn *et al.*, "Maca-a new channel access method for packet radio," in *ARRL/CRRL Amateur radio 9th computer networking conference*, vol. 140. London, Canada, 1990, pp. 134–140.

[98] B. Peleato and M. Stojanovic, "Distance aware collision avoidance protocol for ad-hoc underwater acoustic sensor networks," *IEEE Communications Letters*, vol. 11, no. 12, 2007.

[99] Z. Peng, Y. Zhu, Z. Zhou, Z. Guo, and J.-H. Cui, "Cope-mac: A contention-based medium access control protocol with parallel reservation for underwater acoustic networks," in *OCEANS 2010 IEEE-Sydney*. IEEE, 2010, pp. 1–10.

[100] N. Chirdchoo, W.-s. Soh, and K. C. Chua, "Ript: A receiver-initiated reservation-based protocol for underwater acoustic networks," *IEEE Journal on Selected Areas in Communications*, vol. 26, no. 9, pp. 1744–1753, 2008.

[101] A. A. Syed, W. Ye, and J. Heidemann, "T-lohi: A new class of mac protocols for underwater acoustic sensor networks," in *INFOCOM 2008. The 27th Conference on Computer Communications. IEEE*. IEEE, 2008, pp. 231–235.

[102] J. Heidemann, M. Stojanovic, and M. Zorzi, "Underwater sensor networks: applications, advances and challenges," *Phil. Trans. R. Soc. A*, vol. 370, no. 1958, pp. 158–175, 2012.

[103] A. Hung, M.-J. Montpetit, G. Kesidis, and P. Takats, "A framework for atm via satellite," in *Proceedings of GLOBECOM'96. 1996 IEEE Global Telecommunications Conference*, vol. 2. IEEE, 1996, pp. 1020–1025.

[104] M. Mobasseri and V. C. Leung, "Bandwidth assignment for vbr traffic in broadband satellite networks," in *2000 Canadian Conference on Electrical and Computer Engineering. Conference Proceedings. Navigating to a New Era (Cat. No. 00TH8492)*, vol. 2. IEEE, 2000, pp. 654–658.

[105] W. M. Gorma and P. D. Mitchell, "Performance of the combined free/demand assignment multiple access protocol via underwater networks," in *Proceedings of the International Conference on Underwater Networks & Systems*, ser. WUWNET'17. New York, NY, USA: ACM, 2017, pp. 5:1–5:2.

[106] N. Abramson, "The throughput of packet broadcasting channels," *IEEE Transactions on Communications*, vol. 25, no. 1, pp. 117–128, 1977.

[107] L. Kleinrock and S. Lam, "Packet switching in a multiaccess broadcast channel: Performance evaluation," *IEEE transactions on Communications*, vol. 23, no. 4, pp. 410–423, 1975.

[108] W. D. Wilson, "Speed of sound in sea water as a function of temperature, pressure, and salinity," *The Journal of the Acoustical Society of America*, vol. 32, no. 6, pp. 641–644, 1960.

[109] M. Stojanovic and J. Preisig, "Underwater acoustic communication channels: Propagation models and statistical characterization," *IEEE Communications Magazine*, vol. 47, no. 1, pp. 84–89, 2009.

[110] A. K. Mohapatra, N. Gautam, and R. L. Gibson, "Combined routing and node replacement in energy-efficient underwater sensor networks for seismic monitoring," *IEEE Journal of Oceanic Engineering*, vol. 38, no. 1, pp. 80–90, 2013.

[111] C. Petrioli, R. Petroccia, J. Shusta, and L. Freitag, "From underwater simulation to at-sea testing using the ns-2 network simulator," in *IEEE OCEANS 2011*. IEEE, 2011, pp. 1–9.

[112] W. Gorma, P. Mitchell, and Y. Zakharov, "Cfdama-is: Mac protocol for underwater acoustic sensor networks," in *International Conference on Broadband Communications, Networks and Systems*. Springer, 2018, pp. 191–200.

[113] T. Le-Ngoc and J. I. Mohammed, "Combined free/demand assignment multiple access (cfdama) protocols for packet satellite communications," in *Universal Personal Communications, 1993. Personal Communications: Gateway to the 21st Century. Conference Record., 2nd International Conference on*, vol. 2. IEEE, 1993, pp. 824–828.

[114] P. D. Mitchell, D. Grace, and T. C. Tozer, "Performance of the combined free/demand assignment multiple access protocol with combined request strategies via satellite," in *12th IEEE International Symposium on Personal, Indoor and Mobile Radio Communications. PIMRC 2001. Proceedings (Cat. No.01TH8598)*, vol. 2, Oct 2001, pp. 90–94.

[115] P. D. Mitchell, D. Grace, and T. C. Tozer, "Comparative performance of the cfdama protocol via satellite with various terminal request strategies," in *GLOBECOM'01. IEEE Global Telecommunications Conference (Cat. No. 01CH37270)*, vol. 4. IEEE, 2001, pp. 2720–2724.

[116] T. LE-NGOC and S. Krishnamurthy, "Performance of combined free/demand assignment multiple-access schemes in satellite communications," *International Journal of Satellite Communications*, vol. 14, no. 1, pp. 11–21, 1996.

[117] T. Le-Ngoc and I. M. Jahangir, "Performance analysis of cfdama-pb protocol for packet satellite communications," *IEEE Transactions on Communications*, vol. 46, no. 9, pp. 1206–1214, 1998.

[118] W. Gorma, P. D. Mitchell, N. Morozs, and Y. V. Zakharov, "Cfdama-srr: A mac protocol for underwater acoustic sensor networks," *IEEE Access*, vol. 7, pp. 60 721–60 735, 2019.

[119] W. Chan, T.-C. Lu, and R.-J. Chen, "Pollaczek-khinchin formula for the m/g/1 queue in discrete time with vacations," *IEE Proceedings-Computers and Digital Techniques*, vol. 144, no. 4, pp. 222–226, 1997.

[120] B. Dushaw., "Worldwide sound speed, temperature, salinity, and buoyancy from the noaa world ocean atlas." *Available: http://staff.washington.edu/dushaw/WOA/*, 2009.

[121] J. A. Neasham, G. Goodfellow, and R. Sharphouse, "Development of the "seatrac" miniature acoustic modem and usbl positioning units for subsea robotics and diver applications," in *OCEANS 2015-Genova*. IEEE, 2015, pp. 1–8.

[122] S. H. Park, P. D. Mitchell, and D. Grace, "Performance of the aloha-q mac protocol for underwater acoustic networks," in *2018 International Conference on Computing, Electronics & Communications Engineering (iCCECE)*. IEEE, 2018, pp. 189–194.